Analyzing the mechanisms of LMO2-induced T-cell leukemia and the functional dissection of the role of the LMO2 target HHEX in adult hematopoiesis

By

Charnise Amoré Goodings

Dissertation

Submitted to the Faculty of the

Graduate School of Vanderbilt University

in partial fulfillment of the requirements

for the degree of

DOCTOR OF PHILOSOPHY

in

Cancer Biology

May 2015

Nashville, Tennessee

Approved:

Stephen Brandt, M.D.

Sandra Zinkel, M.D., Ph.D.

Scott Hiebert, Ph.D.

Utpal Davé, M.D

Dedication

This thesis is dedicated to

my beloved father, Charles A. Goodings Sr.,

my loving brother, Jermaine A. Brown and

my amazing grandmother, Manulita Turnbull.

Although you guys are not here to live in this moment with me, I know I have done nothing less than make you all proud of me. Thank you for being big supporters of me when you were alive.

Acknowledgments

"Trust in the LORD with all your heart and lean not on your own understanding" – Proverbs 3:5. If it is one thing that has kept me going in graduate school it is my faith in God. Not only has my faith in God kept me strong through the graduate school process but also a wonderful support system.

I would like to thank my mentor Utpal Davé for the useful comments, remarks and engagement throughout my graduate school process. I would like to thank you for encouraging my research and for allowing me to grow as a research scientist. Furthermore, I would like to thank Drs. Stephen Brandt, Sandra Zinkel and Scott Hiebert for serving on my committee and motivating me to be a rigorous scientist.

The work presented in this thesis would not have been possible without funding from the Initiative for Maximizing Student Diversity (R25GM062459), the Microenvironmental Influences in Cancer training grant (T32CA009592), and an F31 award F31HL117624 from the NIH.

During this process I have been able to work with some of the most wonderful individuals. To Susan Cleveland, thank you so much for being a mentor to me, a second mother, and a wonderful friend. I thank you so much for being there to motivate me and also providing me with a wonderful support system and fun times inside and outside of the lab. To Natalina Elliot, thank you for providing me with great advice and moral support throughout this process. To Elizabeth Mathias, thank you for giving me so many reasons to smile. You were always a ray of sunshine on gloomy days. To Elizabeth Smith, words cannot

begin to describe how much I appreciate all that you have done for me during your time in the lab. You have been the reason for many of my smiles, the motivation behind so many of my achievements and the reason why I think someday I would love to mentor wonderful people like you. To Stephen Smith, Justin Layer and Rati Tripathi, thank you for your advice and collaborations throughout my time with you.

Outside of the lab special thanks to Patrice Wagner for being my friend, breakfast buddy, confidant, shoulder to cry on and so much more. Without your wonderful support I would not have been able to make it through some days. To Celestial Jones-Paris and Andrea Hill thank you so much for all that you have done for me. Without you my transition to Nashville would not have been so warm. To those who I may not mention, I would like to thank you for any support and/or guidance you provided during this process. I would also like to thank the members of the Schrader Lane Church of Christ for their unwavering support and for becoming a second family. Special thanks to my 6th grade teacher Ms. Ava Brathwaite. You have been such a wonderful supporter from the first day I stepped into your 6th grade class and have never stopped supporting and encouraging me even through my graduate school studies.

A special thanks to my best friend, J'Quahnia Tyson. You have been there through everything. Thank you for staying at my side through my best times and never abandoning me at my lowest points. To my siblings Yla and Chaz Goodings and my whole entire family I thank you all for all the support and love. I would like to thank my grandfather Samuel Turnbull for supporting me every

single step of the way. To my Aunt Jacqueline Turnbull, thank you for all your sound advice and motivation.

Finally I would like to thank my biggest cheerleader, my one woman army, the main reason for my success, the best mother ever, my mother Denise Turnbull-Goodings. Ma, without you this degree would have never been possible. Thank you for letting me cry on your shoulders, thanks for listening to me whine and complain and thanks for never allowing me to quit. There are not enough words in this world to describe the love and appreciation I have for you. You believed in me even when I did not believe in myself and for that I will forever be proud to be your one and only daughter.

Table of Contents

List of Figures

List of Tables

List of Abbreviations

7AAD	7-Aminoactinomycin D
AKT	Protein kinase B
AML	Acute myeloid leukemia
ATM	ataxia telangiectasia-mutated gene
B220	CD45R/B220 B cell antigen
B6	black 6
bHLH	basic helix-loop-helix
Blk	B lymphocyte kinase
Bmi-1	B cell-specific Moloney murine leukemia virus integration site 1
BMT	Bone marrow transplant
BrdU	Bromodeoxyuridine
BTG	B-cell translocation gene
CAFC	colony area forming cell
Ccnd1	Cyclin D1
Ccnd2	Cyclin D2
Ccnd3	Cyclin D3
Ccne1	Cyclin E1
CD	cluster of differentiation
CD127	interleukin-7 receptor
CD135	receptor for the cytokine Flt3 ligand
CD150	Signaling lymphocytic activation molecule
CD19	B-lymphocyte antigen

CD2	T-cell surface antigen
CD21/CD35	Complement receptor type 2
CD23	"low-affinity" receptor for IgE
CD24a	Signal transducer CD24
CD25	interleukin-2 receptor α chain
CD3	T-cell co-receptor
CD34	Hematopoietic progenitor cell antigen CD34
CD4	T-cell marker
CD44	T-cell marker
CD48	B-lymphocyte activation marker
Cdk6	Cyclin-dependent kinase 6
Cdkn1a	Cyclin-dependent kinase inhibitor 1
Cdkn1b	Cyclin-dependent kinase inhibitor 1B
Cdkn2c	Cyclin-dependent kinase inhibitor 2C
CFA	competitive repopulation assay
CFC	colony forming cells
CFU-S	colony forming unit-S
c-Kit	CD117 antigen, stem cell factor receptor
cKO	conditional knockout
Clec7a	C-type lectin domain family 7 member A
CLP	common lymphoid progenitor
CMP	common myeloid progenitor
DL1	Delta ligand 1

DNA	Deoxyribonucleic acid
DP	double positive
E2A	Transcription factor 3 (E12/E47)
E2F4	E2F transcription factor 4
Ebf1	early B-cell factor 1
eIF-4E	Eukaryotic translation initiation factor 4E
ER	estrogen receptor
ES	embryonic stem cells
ETP	early thy
ETP-ALL	early T-cell precursor acute lymphoblastic leukemia
FACS	Fluorescence activated cell sorting
FITC	Fluorescein isothiocyanate
Flt3	Fms-related tyrosine kinase 3
GADD45	Growth Arrest and DNA Damage family
Gata 1	GATA binding protein 1
Gata 2	GATA binding protein 2
Gata 3	GATA binding protein 3
GFP	green fluorescent protein
GMP	Granulocyte-Monocyte Progenitor
Gr1	Myeloid differentiation antigen Gr-1
GUSB	Beta-glucuronidase
HAART	Highly Active Antiretroviral Therapy
Heb	Transcription factor 12

HER-2	Receptor tyrosine-protein kinase erbB-2
Hhex	Hematopoietically-expressed homeobox
Hoxa9	Homeobox A9
Hoxb4	Homeobox B4
HSC	Hematopoietic stem cell
HSPC	Hematopoietic stem and progenitor cells
IgH	Immunoglobulin H
IgM	Immunoglobulin M
Igκ	immunoglobulin light chain kappa
IL2Rα	interleukin-2 receptor alpha
IL7Rα	interleukin-7 receptor alpha
ILK	Integrin-linked kinase
IMDM	Iscove's Modified Dulbecco's Media
IRES	Internal ribosome entry site
ISP	immature single-positive
LDB1	LIM domain-binding protein 1
LMO	LIM domain only
LMO2	LIM domain only 2
LMPP	lymphoid-primed multipotent progenitor
LSK	Lineage Negative/Sca-1+/c-Kit+
LTC-IC	Long-Term Culture-Initiating Cell
LT-HSC	Long-term hematopoietic stem cell
LYL1	Lymphoblastic leukemia associated hematopoiesis regulator 1

Mac1	Macrophage-1 antigen
MAPK	Mitogen-activated protein kinase
MEP	Megakaryocyte-erythrocyte progenitors
MIG	Murine Stem Cell Virus Internal ribosome entry site green fluorescent protein
MPP	multipotent progenitor
mRNA	messenger RNA
MSCV	Murine Stem Cell Virus
MZ	marginal zone
NK	natural killer
OLIG2	Oligodendrocyte transcription factor
p16	Cyclin-dependent kinase inhibitor 2A
p19	ARF tumor suppressor
p21	CDK-interacting protein 1
p27	Cyclin-dependent kinase inhibitor 1B
PEDF	Pigment epithelium-derived factor
PI3K	phosphatidylinositide 3-kinase
Pi3kcd	phosphatidylinositide 3-kinase delta
Pik3cg	phosphatidylinositide 3-kinase gamma
PRH	proline-rich homeodomain
PTEN	Phosphatase and tensin homolog
Rag1	recombination-activating gene 1
Rag2	recombination-activating gene 2

Rb	retinoblastoma protein
RNA	Ribonucleic acid
RT-PCR	real-time PCR
S16	16S ribosomal RNA
Sca1	Stem cell antigen 1 (Ly6a)
SCL/TAL1	T-cell acute lymphocytic leukemia protein 1
Shh	Sonic hedgehog
ST-HSC	Short-term hematopoietic stem cell
T1	Transitional B cells T1
T2	Transitional B cells T2
TBP	TATA-binding protein
TCF12	Transcription factor 12
TCF3	Transcription factor 3
TCR	T cell receptor
Ter 119	erythroid antigen
Tgf1	Transforming growth factor beta 1
Thy1.1	thymocyte antigen 1
TLE	Transducin-like enhancer protein 1
Tp53	Tumor protein p53
VDJ	**V**ariable, **D**iverse, and **J**oining gene segments
Vpreb	Pre-B lymphocyte 1
Wnt	Wingless-type MMTV integration site family
WT	wild type

X-SCID	X-linked severe combined immunodeficiency
αMEM	Minimum Essential Medium Eagle - Alpha

CHAPTER I

Introduction

Hematopoiesis

Hematopoiesis is a hierarchal system that originates with the hematopoietic stem cell (HSC) (Figure 1). The multipotent compartment consists of cells with decreasing levels of self-renewal ability and increasing levels of mitosis[1]. The stem and progenitor compartment is comprised of long-term HSCs (LT-HSCs), short-term HSCs (ST-HSCs), and multipotent progenitors (MPPs). The myeloid and lymphoid branch of development each consist of a common progenitor; the common myeloid progenitor (CMP) and the common lymphoid progenitor (CLP)[2,3]. The CLP gives rise to committed precursors that later differentiates into B-, T- and NK cells of the lymphoid system while the CMP differentiates into the granulocyte-monocyte progenitor (GMP) which is the common progenitor for granulocytes, monocytes and the megakaryocyte-erythrocyte progenitor (MEP)[3]. Recently, a common progenitor, known as the lymphoid-primed multipotent progenitor (LMPP), that gives rise to CLP and the GMP, has been identified[4].

The maintenance of the hematopoietic system depends on the ability of hematopoietic stem cells (HSCs) to self-renew and differentiate into all blood cell lineages. These blood cells originate and mature in the bone marrow where they exist as a heterogeneous population of less differentiated and mature blood types. Amongst these varying cell types are hematopoietic stem cells. The idea that a hematopoietic stem cell existed was proposed when a cell with colony

forming unit – spleen (CFU-S) action was identified[5]. Since this discovery, further research has led to the development of *in vitro* and *in vivo* assays that evaluate the differentiation and self-renewal abilities

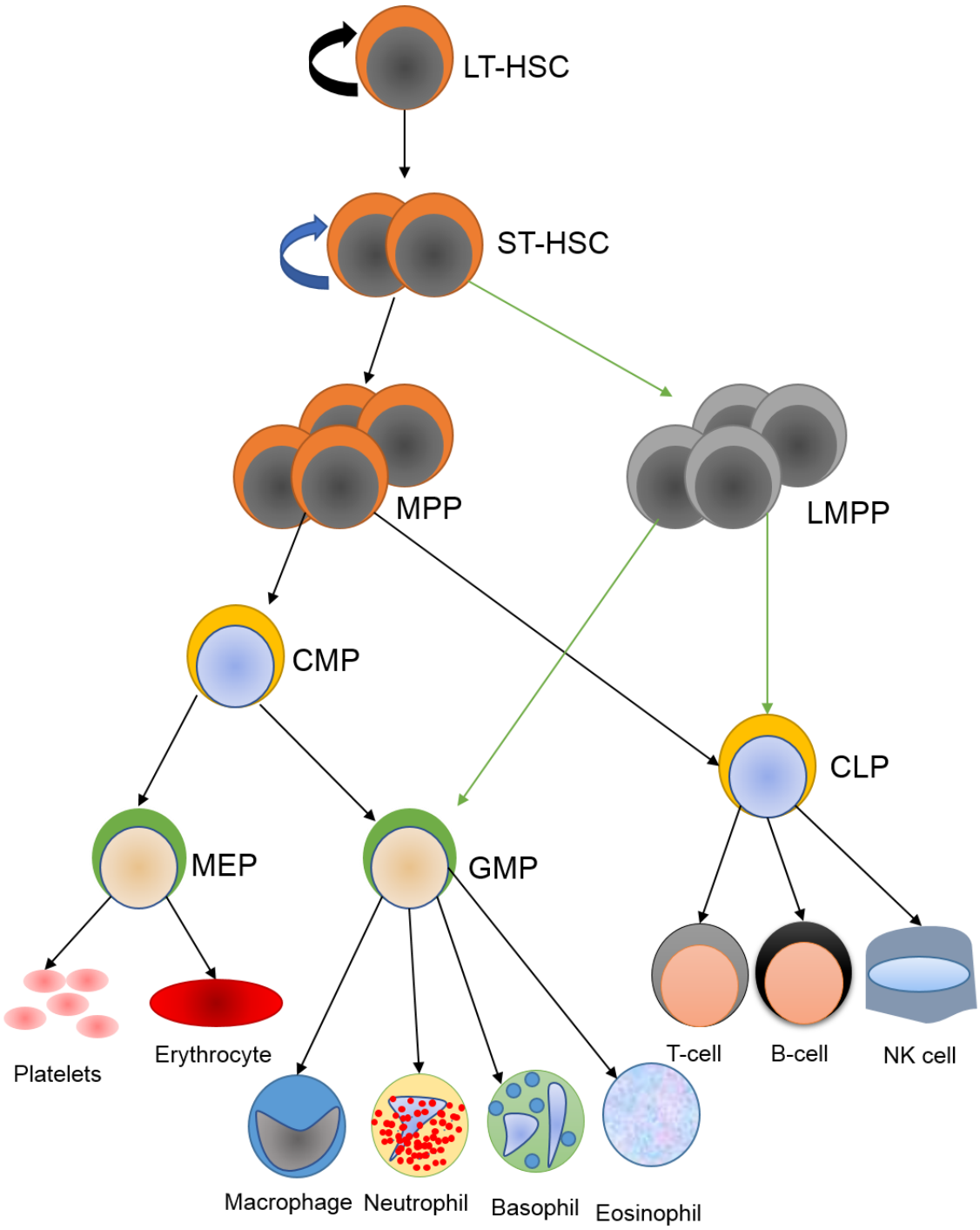
LT-HSC
ST-HSC
MPP
LMPP
CMP
CLP
MEP
GMP
Platelets
Erythrocyte
T-cell
B-cell
NK cell
Macrophage
Neutrophil
Basophil
Eosinophil

Figure 1. Cellular hierarchy of the hematopoietic system.

Hematopoietic cells originate from hematopoietic stem cells (HSCs). HSCs have self-renewal capacity as well as the ability to give rise to multipotent progenitor cells. Multi-potent progenitors have lost their self-renewal ability but still have the ability to give rise to multi-lineage committed progenitors such as MEPs, CLPs and GMPs. Committed progenitors further differentiate into lineage restricted precursors which differentiate into mature lineages

of HSCs and the identification of cell surface markers used to purify populations of HSCs.

Identification and characterization of HSCs

Hematopoietic cells can be identified based on specific cell surface markers. No particular antigen can be used to specifically detect HSCs. While HSCs do not express lineage specific cell surface markers, HSCs can be enriched 20-500 fold by using antibodies against lineage markers to exclude more mature cells[6]. HSCs also express the cell surface markers c-Kit and Sca1, these cells are referred to as Lineage- Sca1+ c-Kit+ (LSKs)[7-10]. Although, HSCs are known to have this LSK phenotype only 3-10% of LSKs are actually long-term hematopoietic stem cells (LT-HSCs)[11,12]. Additional markers such as Thy1.1, CD34, Flt3, IL7Rα, CD150 and CD48 are used to delineate other progenitor populations[2,13-18]. In the last few years, many immunophenotyping schemes have been established to identify hematopoietic stem and progenitor cells (HSPCs) population (Table 1,Table 2 and Table 3). While stem cells can be purified by cell surface markers, there are also functional assays that are used to identify purified HSCs.

Multiple i*n vitro* and *vivo* assays have been developed to test the functionality of hematopoietic stem and progenitor cells (HSPCs) by measuring two fundamental properties of these cells; 1) their ability to differentiate and 2) their ability to self-renew. These assays include the long-term colony-initiating cell (LTC-IC) assay, colony-forming cell (CFC) assay, cobblestone area-forming cells (CAFCs) assay and the colony- forming unit-spleen (CFU-S) assay[7,9].

Table 1. Cell surface markers used to distinguish HSPC populations.

Marker Phenotype	Populations
Lineage-Sca1+c-kit+ (LSK)	Hematopoietic stem and progenitor cells (HSPCs)
LSK Flt3-	Long-term HSCs (LT-HSCs)
LSK Flt3int	Short-term HSCs (ST-HSCs)
LSK Flt3hi	Multipotent Progenitors (MPPs)
LSK lL7Rα+	Common Lymphoid Progenitors (CLPs)

Table 2. Cell surface markers used to distinguish HSPC populations.

Marker Phenotype	Populations
Lineage-Sca1+c-kit+ (LSK)	Hematopoietic stem and progenitor cells (HSPCs)
LSK CD34- CD48- CD150+ flt3-	Hematopoietic stem cells (HSCs)
LSK CD34+ CD48- CD150+ flt3-	Multipotent progenitor 1 (MPP1)
LSK CD34+ CD48+ CD150+ flt3-	Multipotent progenitor 2 (MPP2)
LSK CD34+ CD48+ CD150- flt3-	Multipotent progenitor 3 (MPP3)
LSK CD34+ CD48+ CD150- flt3+	Multipotent progenitor 4 (MPP4)

Table 3. Option 3: Cell surface markers used to distinguish HSPC populations.

Marker Phenotype	Populations
Lineage-Sca1+c-kit+ (LSK)	Hematopoietic stem and progenitor cells (HSPCs)
LSK flt3-CD34-	Long-term HSCs (LT-HSCs)
LSK flt3-CD34-CD48-CD150+	Long-term HSCs SLAM (SLAM)
LSK flt3-CD34+	Short-term HSCs (ST-HSCs)
LSK flt3+CD34+	Multipotent Progenitors (MPPs)
LSK IL7Rα+	Common Lymphoid Progenitors (CLPs)
Lin-sca1-c-kit+	Myeloid Progenitors
Lin-sca1-a-kitCD34+FcγRint	Common myeloid progenitors (CMPs)
Lin-sca1-a-kitCD34+FcγR-	Megakaryocyte-erythrocyte progenitors (MEPs)
Lin-sca1-a-kitCD34+FcγR+	Granulocyte-macrophage progenitors (GMPs)

The CFC assay is a short term assay (less than 3 weeks) in which bone marrow cells are grown in semisolid media, usually a methylcellulose-based media, with cytokines. Since the resulting colonies have single cell origins, different lineage specific progenitors can be identified and quantified based on output colonies. Both the LTC-IC and the CAFCs assays are long-term co-culture assays that are used to predict the frequency of HSCs. The LTC-IC assay is defined by its ability to produce daughter CFCs after co-culture within 5-12 weeks. The CAFCs assay is defined by its ability to produce “cobblestone”-like colonies in culture. Although the LTC-IC and CAFC assays overlap they are not identical as the LTC-ICs represents more of an immature cell type[19,20]. While these assays may be useful in limiting dilution format to quantify HSC number, their reliability has been controversial because of variable culture conditions and the use of different feeder layers[9]. The CFU-S assay is a short term (1-3 weeks) *in vivo* assay that measures cells that home to the spleen, rapidly proliferate and form macroscopic colonies after being injected into irradiated recipient mice. The CAFC, LTC-IC and CFU-S assays reveal cells that are more mature than HSCs but are more primitive than CFCs.

In vivo transplantation is the benchmark for LT-HSC function[7,9,12]. These assays are readily performed in mice, by transplanting test cells (e.g.. knockout cells) from a donor mouse to a congenic recipient (e.g. expression of a different isotype of a commonly expressed cell surface antigen such as the pan hematopoietic marker CD45, the two isotypes are CD45.1 and CD45.2). This competitive repopulation assay (CRA) assesses the ability of test cells to sustain

long-term engraftment in the presence of control congenic cells. The competitive repopulating unit (CRU) can be calculated by co-transplanting decreasing numbers of test cells together with a fixed number of control cells into a lethally irradiated recipient[21]. In order to demonstrate long-term reconstitution, donor cells should be able to contribute to multiple lineages 16 weeks post-transplant. Moreover, serial transplantation can be used to determine the self-renewal ability of the LT-HSC.

Fate and commitment

At any given moment, HSCs face several possible cell fate decisions such as self-renewal, differentiation, quiescence and apoptosis (Figure 2). Whether fate decision is stochastic or deterministic is controversial[5,22-24].

Quiescence

Most cells tend to remain quiescent, which seems to be essential for adult HSCs. One hypothesis for choosing to remain quiescent is suggests that quiescence limits the chances of mutation to occur and allows cells time to repair DNA damage[25]. There are two competing models used to describe the mechanisms that lead to the notion of quiescence as a stem cell fate choice. The clonal succession model suggests that quiescent HSCs are recruited to divide and differentiate, and when exhausted are replaced from a new set of HSCs activated from a quiescent state[26]. Today the preferred model is the clonal maintenance model, which suggests that after an initial flux of clones following HSC transplantation, engraftment is maintained by a few stable clones throughout the individual's life[27-29].

Self-renewal

A stem cell has the ability to self-renew by two different cell divisions; symmetrical or asymmetrical division. Symmetrical division is when both daughter cells are stem cells, while asymmetrical division is when one daughter is a stem cell and the other undergoes differentiation. Regardless of the mode of cell division chosen, stem cells can preserve themselves and serve their host during a lifetime. Various signaling pathways have been implicated in the influencing of HSC self-renewal. These pathways include Wnt, Notch, Hoxb4, Bmi-1, sonic hedgehog (Shh), thrombopoietin, and Lnk[30-37].

Apoptosis

The death of unwanted cells by apoptosis is vital for the development and maintenance of all life. Apoptosis controls our immune system by eliminating B and T cells producing dangerous self-reactive receptors or failing to produce useful antigen-specific receptors[38]. Whenever apoptosis is deregulated it can result in a wide range of disorders such as autoimmunity, cancer and neurodegenerative diseases. Apoptosis has been implicated as an important alternative fate for HSCs[24,39]. For example, overexpression of the anti-apoptotic gene *Bcl-2* led to an increase in HSC pools, which indicates that apoptosis plays a role in the regulation of HSC pool size[40].

Differentiation

Humans produce approximately $1X10^{12}$ new blood cells daily. This requires a massive expansion somewhere between the mainly quiescent HSC and the mature, non-dividing blood cells. Cytokines and transcription factors

usually govern lineage specification[41]. When a HSC is fated for differentiation, it will upregulate lineage-specific genes and abolish the transcriptional program of the unselected lineages[42,43]. This suggests that key lineage-specific factors must promote their own lineage differentiation, while simultaneously shutting off factors that are specific for other lineages. When hematopoiesis is blocked in differentiation or has deregulated self-renewal, leukemia or lymphoma can result [44]. Two transcription factors important for normal hematopoiesis are E2A and Hhex.

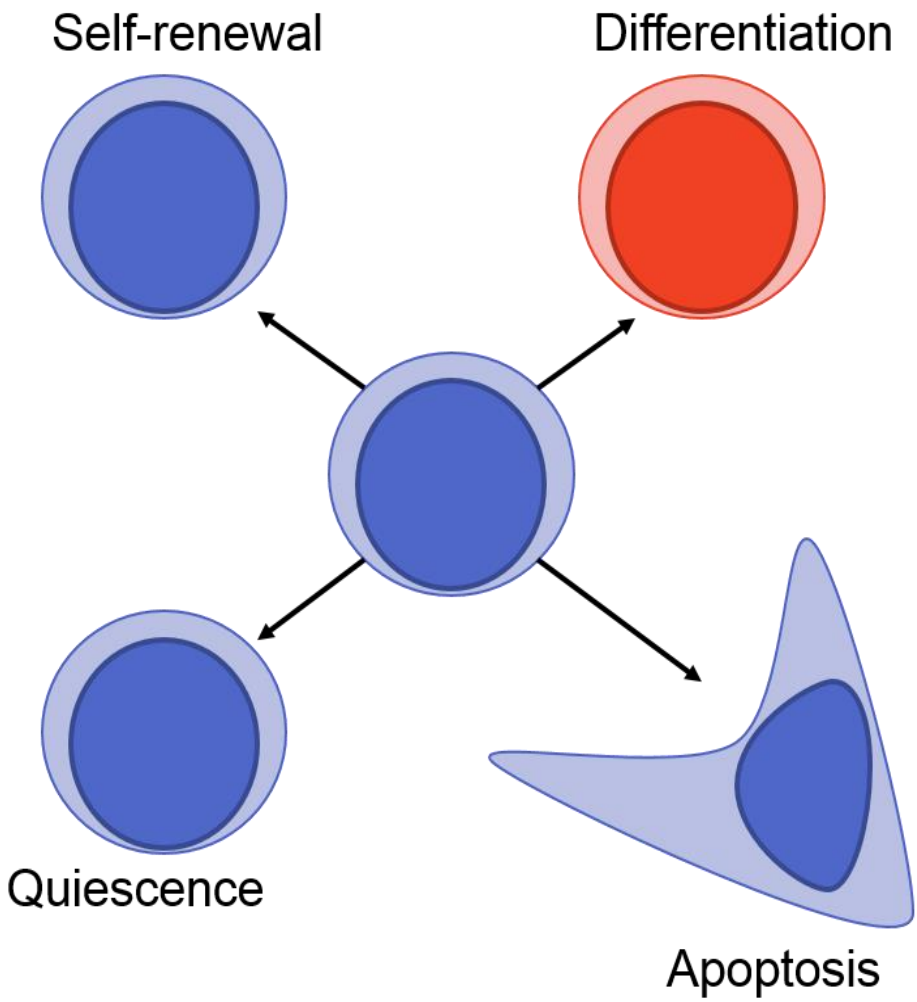

Figure 2. HSC fate options.

During cell division HSCs face different fate decisions. These decisions include the decision to remain a HSC via self-renewal, to differentiate into a more mature lineage, to undergo apoptosis or to remain quiescent.

E proteins

Identification and function

E proteins are transcription factors that contain a DNA-binding domain known as the basic helix-loop-helix (bHLH) domain[45]. Class I bHLH E proteins, E47, E12, E2-2, and Heb can heterodimerize with class II bHLH proteins such as TAL1[46]. The heterodimers function as transcription activators and repressors by recruiting co-activator or co-repressor complexes[47]. Class I bHLH proteins can also form homodimers, which act as transcriptional activators. E47 and E12 are encoded by the E2A gene (*TCF3*) and are identical except for residues at the carboxyl-terminus that result from alternative splicing[48]. Heb is encoded by the TCF12 gene and also has multiple isoforms from alternative splicing and promoter usage[49]. E proteins are widely expressed in various hematopoietic lineages and play important roles in cell fate decisions, differentiation and proliferation[50].

E protein function has been studied extensively in B-cell development. E proteins were first identified by their ability to bind to E-box sequences in the enhancer regions of both *Igκ* and *IgH*[46,50]. *E2A* null mice are unable to develop pro-B cells, and do not express most B-cell-lineage-associated genes. The fetal liver and bone marrow of *E2A* null mice did not show VDJ recombination. Along with the direct role of E2A proteins during recombination at the Igκ and IgH loci, E proteins are responsible for regulating the transcription of both *Rag1* and *Rag2*. The knockout of the *E2A* gene results in a high incidence of T-ALL

development[51]. This finding suggests that E2A is not only important for B-cell development but also acts as a tumor suppressor.

Hematopoietically expressed homeobox (Hhex)

Structure and function

Hematopoietically expressed homeobox protein (Hex or Hhex), also known as proline- rich homeodomain (PRH) protein is a transcription factor that contains three main domains: a proline-rich N-terminal domain, a homeodomain and an acidic C-terminal domain[52]. Crosslinking studies have shown that the HHEX protein is able to form oligomers within cells[53-55]. The N terminal of Hhex contains two regions that allow for the protein to associate with itself. Both the homeodomain and the C-terminal domain are important for the activation functions of Hhex[56,57].

Hhex has both repressive and activation effects on transcription via direct and indirect mechanisms[53,54,58-66]. Hhex can directly bind to the promoter sites and intronic regions of genes and cause transcriptional repression by recruitment of Groucho/TLE family co-repressor proteins[54]. Hhex may also repress transcription by competing with TATA Binding Protein (TBP) at TATA boxes[64]. Hhex can activate transcription by directly binding to promoters and forming complexes with other DNA binding proteins to activate transcription such as at the Na+-dependent bile acid co-transporter (NTCP) promoter[56,57]. Hhex also acts as cell proliferation inhibitor by repressing the transport of mRNA important for proliferation.

Role in hematopoiesis

Hhex is a transcription factor that has an important role in embryonic development and hematopoiesis[54,64,26]. Hhex regulates embryonic development transcriptionally and post transcriptionally[64] and is important for cell proliferation. Knockout of *Hhex* resulted in embryonic lethality at embryonic stage E10.5[67,68]. During the early stages of embryonic development, *Hhex* is expressed in tissues that contribute to hematopoiesis. In mice, *Hhex* is expressed in the blood islands of the yolk sak[69,70]. Later in embryonic development, *Hhex* is expressed in fetal liver.

Role in Leukemia

Hhex has been implicated in many human leukemias. *Hhex* is a common integration site in retroviral insertional mutagenesis studies and it induces T-ALL in bone marrow transduction and transplantation mouse models[71]. Transgenic mouse models show that overexpression of Hhex results in aberrant T-cell proliferation[72]. HHEX is hypothesized to be a tumor suppressor gene in acute myeloid leukemia (AML) based on an unusual post-transcriptional regulation by repressing mRNA transport and translation of CCND1 by disrupting the activity of the eukaryotic initiation factor 4E (eIF-4E)[73]. Hhex is down-regulated and mis-localized in some subsets of human leukemias, as loss of nuclear Hhex resulted in the loss of proliferation inhibition by Hhex[54,73-76].

T-cell Acute Lymphoblastic Leukemia (T-ALL)

Description of disease

T-cell acute lymphoblastic leukemia (T-ALL) is an aggressive leukemia that is characterized by elevated levels of bone marrow and circulating blasts, enlarged lymph nodes and often involves the central nervous system[77,78]. Similar to other forms of leukemia, T-ALL is caused by genetic alterations in hematopoietic precursors. These genetic changes can result in various abnormalities such as loss of cell cycle control, unlimited self-renewal capacity, impaired differentiation, hyper proliferation and resistance to death signals[78]. T-ALL accounts for about 15% of childhood leukemias and 25% of adult leukemias.

Historically, T-ALL in children has an overall poor prognosis when compared to all other subtypes of childhood leukemias and lymphomas[79]. With all the research done on pediatric T-ALL, the 5-year event-free survival is approximately 75%. Unfortunately, the biology and outcome of adult T-ALL is not well understood[80]. This may be due to the rarity of adult T-ALL which makes the clinical and biological factors that may determine disease outcome in adults difficult to study.

A common theme in acute leukemias is transcriptional deregulation. In the case of T-ALL, the transcriptional deregulation of normal transcription factor proteins results in their ability to exert oncogenic potential by altering various gene regulation programs important for hematopoietic differentiation[78]. Two genes frequently deregulated in T-ALL are LIM-domain only proteins, LMO1 and LMO2[81-83].

Lim-domain only proteins

Identification and function

The LIM domain Only-2 (LMO2) gene is frequently deregulated in human acute T-cell lymphoblastic leukemias (T-ALL). The first member of the LMO (Lim-domain only) family was *LMO1*[82,84]. *LMO2* was later discovered due to its association with the t(11;14) (p13;q11) and t(7;11) (q35;p13) chromosomal translocations[81,83]. LMO2 was first cloned from T-ALLs with chromosomal translocation breakpoints at 11p13[85] but, LMO2 and its paralog, LMO1, are deregulated by diverse mechanisms[86]. Fifty percent of all acute T cell leukemias that carry one frequent reciprocal translocation involving LMO2 and TAL1/SCL are the most prevalent[87]. The LMO2-associated chromosomal translocations occur by abnormal activity of the RAG recombinase. Since RAG recombinase mediates normal V-J and VDJ rearrangement of the T-cell receptor (*TCR*) genes, irregular function results in interchromosomal translocation rather than normal intrachromosomal rearrangement[88].

Lmo2 was also activated by retroviral insertion in a gene therapy trial for X-linked severe combined immunodeficiency (X-SCID)[89-91]. Patients with X-SCID received gene therapy treatment using retrovirally expressed IL2RG, which resulted in five (5) out of twenty (20) patients developing a T-ALL like syndrome due to an integration into the *LMO2* gene.

Lmo2 is necessary for early stages of hematopoiesis[92]. A study of *Lmo2* knockout mice found that *Lmo2* null mice are unable to undergo yolk sac erythropoiesis; leading to death around E10.5[93]. In addition, *Xenopus* and

zebrafish embryos that Lmo2 was important for primitive erythropoiesis[94,95]. Using *Lmo2*$^{-/-}$ embryonic stem (ES) cells injected into C57BL/6 blastocysts, failed to contribute to the hematopoiesis of adult mice[96]. Null mutations of the *Lmo2* gene revealed there was no obligatory role for Lmo2 in lymphopoiesis. These findings suggest Lmo2 has a crucial role in hematopoietic development.

Molecular Binding Partners

The LMO2 protein serves as a bridging protein in a multiprotein DNA-binding complex[97-100]. LMO2, the best characterized member of the LMO gene family, encodes an 18 kilo Dalton (kDa) protein that has two Zinc-binding domains called LIM domains that serve as interfaces for interactions with class II basic helix-loop-helix (bHLH) proteins, GATA (1-3) proteins, and the scaffolding protein, LIM domain binding 1 (LDB1)[101-103]. In erythroid cells, this Lmo2 complex is able to bind to DNA through the GATA-1 Zinc fingers and the bHLH motifs of TAL1 and E47 (Figure 3A). This complex recognizes a unique bipartite DNA sequence that is comprised of an E-box separated by about one helix turn from a GATA 1 site.

An Lmo2 multiprotein complex, analogous to the complex found in erythroid cells, was found in Lmo2-induced T-ALLs taken from CD2-Lmo2 transgenic mice. In T-ALL, the LMO2-associated complex may differ in content from the complex described in erythroid cells and may occupy sites other than E box-GATA motifs[97,104,105]. For example, the Lmo2 complex found in leukemias were only comprised of LMO2, TAL1, E47 and LDB1 and was bound to a bipartite E box-E box motif[97] (Figure 3B). There are two E box binding sites in the bipartite DNA binding elements, in CD4 and CD8 double negative immature thymocytes. This

finding corresponds with the observed increase in double negative thymocytes in Lmo2 transgenic mice.

Role in leukemogenesis

Gene expression studies of human and murine T-ALL show remarkable correlation between gene expression of LMO2 (and LMO1) and class II bHLH genes, TAL1, LYL1, or OLIG2, implying that LMO2 and the bHLH proteins cooperate in T-ALL pathogenesis [106,107]. Indeed, Tal1/Scl transgenes are weak tumor initiators but the co-expression of LMO genes can accelerate T-ALL onset and increase penetrance in these mouse models[108-110].

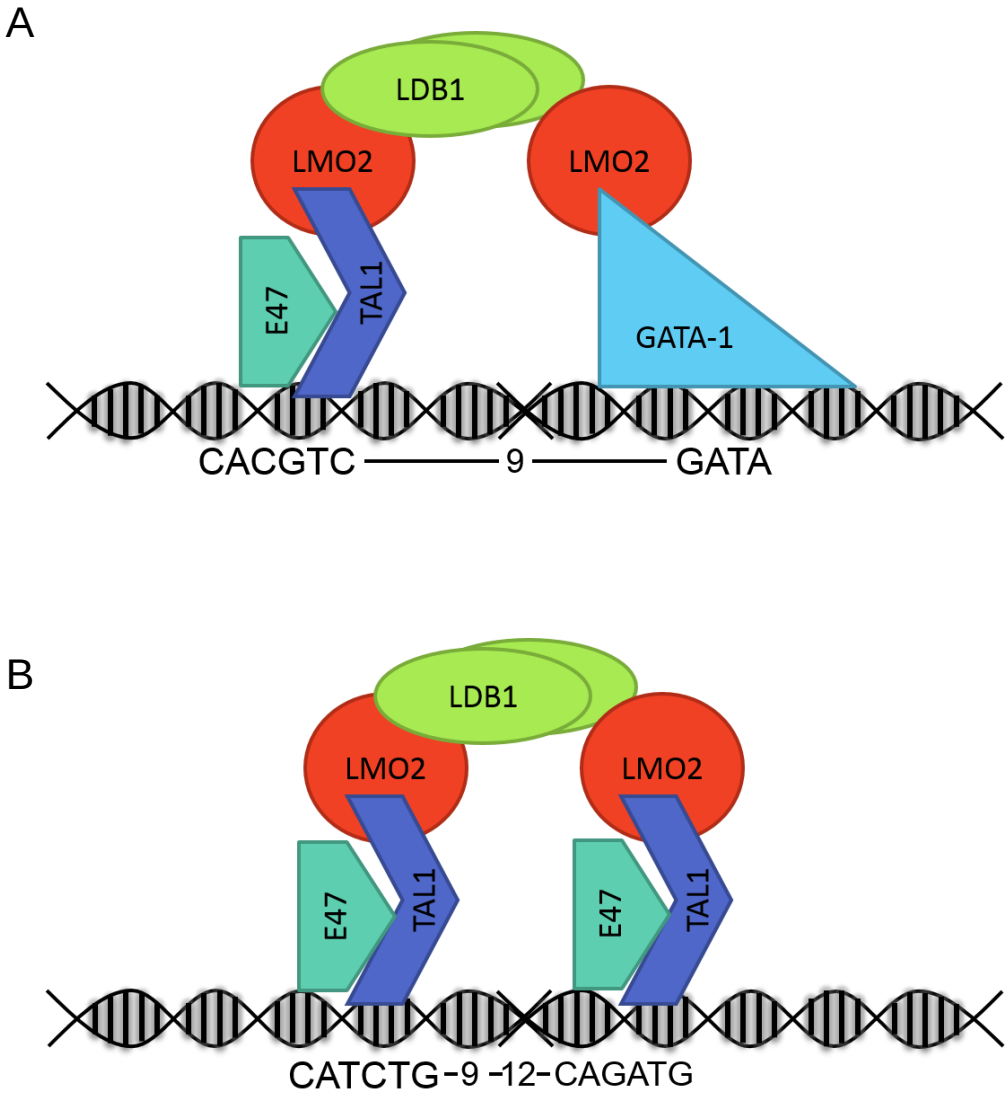

Figure 3. LMO2 is a bridging molecule in multiprotein complexes.

(A) In normal erythroid cells LMO2 is found associated with the proteins TAL1, E47, LDB1 and GATA1 in a DNA binding complex that acts as a transcription factor. (B) In T cell leukemia cells Lmo2 is found to be associated with the proteins Tal1, E47 and Ldb1 on different DNA binding sequences.

Lmo2 and E2A

Studies show *Lmo2* Tg and *E2A*$^{-/-}$ mice spontaneously develop T-ALL. *E2A*$^{-/-}$ and Lmo2 overexpressing thymocytes undergo a differentiation arrest at the same double negative stage (DN2-3) prior to expression of CD4 and CD8[111,112]. McCormack and colleagues found that Lmo2 also requires class II bHLH for the induction of T-ALL[113].

Lmo2 and Hhex

Lmo2-associate complexes occupy the promoter and enhancer of Hhex[104]. Gene expression analysis of both human T-ALL and CD2-Lmo2 transgenic mouse models revealed that Lmo2 is expressed in two mutually exclusive profiles, one of which includes Hhex[104]. Hhex is a direct target of Lmo2 in which Lmo2 occupied the Hhex promoter. Lmo2, Lyl1 and Hhex were all upregulated in a very difficult to treat subset of T-ALL known as ETP-ALL. T-ALL patients with Hhex overexpression have a significantly worse prognosis.

Hypotheses

Two major hypotheses have been put forward to explain the role of Lmo2 containing complexes in T-ALL induction (Figure 4): 1) Lmo2 containing complexes may result in the inhibition of other partners and their normal function. One such possibility is the Lmo2-containing complex may be inhibiting the normal function of E2A homo/heterodimers. 2) Recognition of the dual E-box motif by the Lmo2-containing complexes may result in the abnormal regulation of target genes. Lmo2-associatied complexes in hematopoietic cells can bind DNA

and either activate or repress gene expression. The Lmo2 complex may be able to activate genes involved in leukemogenesis such as *Hhex*.

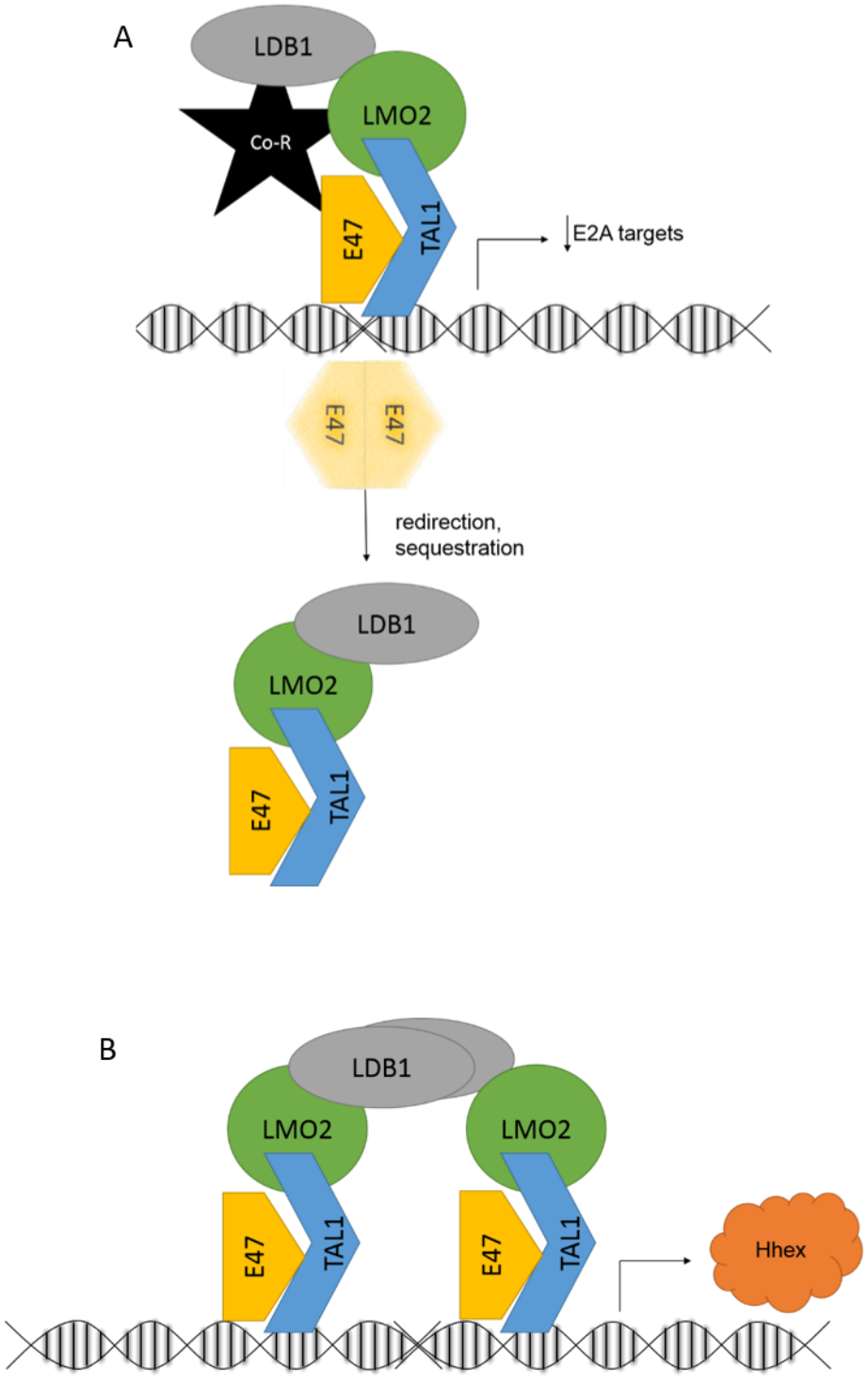
A
LDB1
LMO2
Co-R
E47
TAL1
E2A targets
E47
E47
redirection,
sequestration
LDB1
LMO2
E47
TAL1
B
LDB1
LMO2
LMO2
E47
TAL1
E47
TAL1
Hhex

Figure 4. Models of Lmo2 induced T-ALL.

In T cell leukemia cells Lmo2 is found to be associated with the proteins Tal1, E47 and Ldb1. (A) It has been hypothesized that Tal1 sequesters E47 which results in the redirection of E47 and the downregulation of E47 targets. (B) The binding of Lmo2 associated complexes to GATA sites have been hypothesized to upregulate oncogenes such as Hhex.

CHAPTER II

Materials and Methods

Mice

Floxed Hhex mice were created at NCI Frederick. Briefly, the murine *Hhex* gene was cloned from a 129 BAC by retrieval methods previously described[114]. A single *lox* and a *loxP* plus *Frt*-flanked neo cassette were targeted to the resulting construct in two steps in EL350 cells through recombineering. First, to insert the single 5′ *loxP* site, a targeting cassette containing *Pgk-em7-neo* flanked by homology arms to 1st intron of *Hhex* was constructed in PL400. The homology arms are PCR amplified using the following primers:

5′-arm sense, 5′- CGC GAA GCT TGC AGA ACA TGA GTG TGA CCG-3′

5′-arm antisense, 5′- CGC GGA ATT CAT GAG AGC ACT TCC CAA GGC-3′;

3′-arm sense, 5′- CGC GCT CGA GAA AGA GCG CAC CCT GAG TCT -3′;

3′-arm antisense, 5′- CGC GGG ATC CCC AGA ACG CAA CCA TGT TCC -3′.

The homology arms were sequence verified, restriction digested, and cloned into PL400 via four-way ligation. The targeting cassette was released by a *BamH*I/*Hin*dIII double digest and targeted through co-electroporation into heat shock-induced EL350 cells. The *Pgk-em7-neo* sequence was then removed by electroporation into arabinose-induced Cre-expressing EL350 cells, leaving behind a single *loxP* site. To insert the second *loxP* site after exon 4 of *Hhex*, a targeting cassette containing *frt-Pgk-Em7-neo-frt-loxP* flanked by homology arms to targeting site was constructed in PL451. Homology arms were amplified using the following primers:

5′-arm sense, 5′- CGC GAA GCT TCC TAA ACA TGA CAC CTA AAG -3′;

5′-arm antisense, 5′- CGC GGA ATT CCA CCC TGC TTG GTC CTC TTC-3′;

3′-arm sense, 5′- CGC GGG ATC CGA TTG GAG CTG CCA CTG AGT -3′;

3′-arm antisense, 5′- CGC GGC GGC CGC AGC AGC TGG AAC CTG ACA AC -3′.

The targeting cassette was released by *Not*I/*Hin*dIII double digest and targeted similarly as described above. The conditional targeting vector was then linearized by *Not*I digestion and electroporated into 129-derived CJ7 embryonic stem (ES) cells, using standard procedures. G418 (180 μg/ml) and ganciclovir (2 μM) double-resistant clones were analyzed by Southern blotting hybridization, using both 5′ and 3′ external probes. External probes were PCR amplified using the following primers:

5′ probe, sense, 5′- CCC CAC TAC ACC TGG CTA AC -3′

5′ probe, antisense, 5′- ACG TGG ATG GTA TCA AAG CC -3′

3′-probe, sense, 5′- GGG ATT TGT TGT TGC TGT GC-3′

3′-probe, antisense, 5′- CTG GAT GCT GGT GAC TCA GA -3′

Correctly targeted clones were then injected into C57BL/6 blastocysts using standard procedures, and resulting chimeras were mated with C57BL/6 females to obtain germline transmission of the targeted allele. The Neo cassette was removed by crossing to the *Flp* recombinase strain. The floxed *Hhex* mice were generated by backcrossing *Hhex*$^{lox/+}$ to B6 for 10 generations followed by intercrossing to create homozygous floxed mice, *Hhex*$^{lox/lox}$. Control littermates were of equivalent genetic backgrounds. B6.Vav-iCre transgenic mice were

purchased from Jackson Laboratories and were crossed with the floxed mice to create *Hhex* conditional knockout mice (*Hhex cKO*). Both $Hhex^{lox/lox}$ and cKO mice were used for *in vitro* and *in vivo* studies with the former called WT.

B6.SJL (CD45.1) mice were purchased from Charles River and used as host mice for transplantation. All mice were kept in a specific-pathogen-free animal facility at Vanderbilt University with approved protocols from the IACUC.

Genotyping

Genomic DNA was isolated from mouse bone marrow, spleen and thymus using Qiagen DNeasy Blood and Tissue kit per manufacturer's instructions (cat#69504). Primer sequences for PCR amplification of the *Hhex* floxed and cKO allele were 5'-GCTCTCCAGCCACTTTGGAG-3', 5'-GCACACCTGTGGCTAAATGCA-3' and 5'-CATCAGGGTATGAGGAGAAG-3'. Primer sequences for PCR amplification of the *Lmo2* transgene were 5'-ATGTCCTCGGCCATCGAAAGGAAGAGCC-3' and 5'-CCCATTGATCTTGGTCCACT-3'.

Plasmid constructs

The E47/estrogen receptor (E47-ER) [115,116] plasmid was graciously provided by Dr. Cornelis Murre (UC San Diego, California). This vector expresses a chimeric protein contain amino acids 1-651 of human E47 fused to amino acid 251-599 of the murine estrogen receptor (Figure 5). The E47-ER plasmid also encodes the human CD25 (hCD25) which allows for rapid selection of transduced cells.

Retroviruses

To produce virus, the E47-ER and pCL-Eco plasmids were co-transfected into the Phoenix packaging cell line (ATCC) using calcium phosphate precipitation as described[117,118]. Viral supernatant was collected 48 hours after transfection from transfected Phoenix cells and titered on 3T3 cells by FACS and detection hCD25. The T-ALL cell lines were transduced by spinfection; cells were pelleted at 2000 rpm with 8 µg/mL of polybrene for 1 hour at 4°C. On average, 50-90% of cells expressed hCD25 at the cell surface which were sorted and maintained in culture.

Cell culture

Four B6 T-ALL cell lines; 007,020, 027, and 080 were maintained in IMDM medium containing 10% fetal bovine serum and 1% penicillin and streptomycin. For E47-ER stably expressing lines, 007,020, 027, and 080 cells were transduced with E47-ER using spinfection and then selected with hCD25. We analyzed growth by counting cells directly by hemacytometer and by CyQuant Cell Proliferation Assay kit (Life Technologies, Grand Island, New York).

OP9 assay

OP9-DL1 and OP9-GFP cells were maintained in culture as described[119]. Cells were cultured in α-MEM media with 20% fetal calf serum and 1% penicillin/streptomycin. Stem cells from the bone marrow of 6-8 week old mice were harvested and sorted using flow cytometry and Lineage- Sca1+ c-Kit+ (LSK) cells were collected. LSK cells were cultured in 24 well plates containing 75% confluent irradiated OP9-GFP cells with 6ng/mL murine IL-7 and murine Flt-

3 ligand. Cells were collected seven days post plating. Double negative thymocytes from the thymi of 8 week old mice were harvested by depleting CD8 and CD4 positive cells. DN cells were then cultured in 24 well plates containing 75% confluent irradiated OP9-DL1 cells with 6ng/mL murine IL-7 and murine flt-3 ligand. Cells were collected, washed and plated on fresh OP9-DL1 cultures every 7 days.

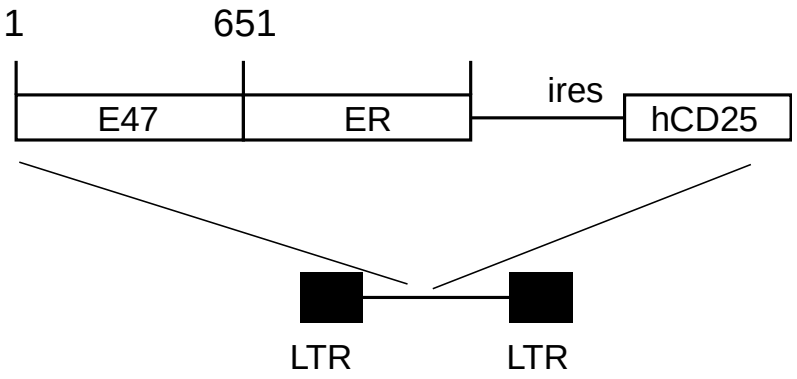

Figure 5. A schematic showing retroviral vector used in experiments.

An E47-ER fusion encoding cDNA followed by an internal ribosomal entry site followed by human CD25 cDNA driven by the LTR of a gamma retrovirus.

Histology and peripheral blood analysis

For complete blood counts, peripheral blood was collected retro orbitally and analyzed by Hemavet (Drew Scientific Inc., Dallas, Texas).

Flow cytometry analysis

FACS analysis was done using anti-CD4 (FITC-conjugated Rat anti-mouse, 553650, BD Pharmingen) and anti-CD8 (PE Rat anti-mouse, 55032, BD Pharmingen). Sorting was done using FITC-conjugated anti-hCD25 (347643, BD Biosciences).

Mononuclear cells were purified by lysis of erythrocytes. For analysis and sorting, antibodies (BD Pharmingen and eBiosciences) directed against B220(RA3-6B2), CD19(1D3), CD4(GK1.5), CD8a(53-6.7), Mac1(M1/70), Gr1(RB6-8C5), c-kit (ACK2), Sca1(D7), Ter 119(TER-119), CD135(A2F10), CD48(C7), CD150(9D1), CD21/CD35(7G6), IgM(R6-60.2), CD23(B3B4), CD127(SB/199), CD44(IM7), and CD25 (PC61) were used. To distinguish donor from host cells in transplanted mice, cells were stained with anti-CD45.1 (A20) and CD45.2 (104). FacsARIA, LSRFortessa, LSRIII, and FACS Canto II flow cytometers were used for sorting and analysis.

Apoptosis

Cleaved caspase 3 was analyzed by FACS using antibody 9661 per manufacturer's instructions (Cell Signaling Technology).

Table 4. Antibodies used in experiments. Marker column shows the cell surface antigen; 1 denotes BD Pharmingen as the source; 2 denotes eBiosciences. The clone numbers are shown.

Marker	Clone
CD45R/B220 [1,2]	RA3-6B2
CD19 [1]	1D3
CD4 [1]	GK1.5
CD8a [1]	53-6.7
Mac1 [1,2]	M1/70
Gr1 [1,2]	RB6-8C5
c-kit [1,2]	ACK2
Sca1 [1]	D7
Ter 119 [1,2]	TER-119
CD135 [2]	A2F10
CD48 [1]	C7
CD150 [2]	9D1
CD21/CD35 [1]	7G6
IgM [1]	R6-60.2
CD23 [1]	B3B4
CD127 [1,2]	SB/199
CD44 [1]	IM7
CD25 [1]	PC61
CD3e [1]	145-2C11
CD45.1 [1]	A20
CD45.2 [1]	104

Cell cycle

In vitro

FACS data was imported into Flojo for further analysis. Bromodeoxyuridine (BrdU) incorporation was analyzed per manufacturer's instructions (BD Biosciences, San Jose, California). Briefly, cells were incubated with 1 mM of BrdU for 1 hour then collected and analyzed by FACS using anti-BrdU and 7-aminoactinomycin D (7-AAD) incorporation. Intracellular cleaved caspase 3 staining was performed using the BD Cytoperm/ Cytofix kit (BD Biosciences, San Jose, California). Statistical analyses were done using GraphPad Prism 6.0.

In vivo

Mice were injected with 1 mg of BrdU in 150 uL PBS via intraperitoneal injections. Two hours post injection mice were sacrificed and bone marrow was harvested to quantify the stem and progenitor populations via flow cytometry. Bromodeoxyuridine (BrdU) incorporation was analyzed per manufacturer's instructions (BD Biosciences, San Jose, California).

IgH rearrangement PCR

PCR analysis of IgH rearrangement was used to determine the ability of Hhex cKO B cells to undergo normal gene arrangement. Genomic DNA from $B220^{+}$ cells from Hhex cKO and WT spleens were subjected to nested PCR analysis. Primers were designed to amplify four possible junctions between D-Q52 and JH regions[120]. The first round of PCR was completed using the following primers and PCR conditions: DH1 Q52-1 5'- CACAGACCTTTCTCCATAGTTGATAACTCAG-3' and JH4-1 5'- AGGCTCTGAGATCCCTAGACAG-3'; denaturing at 95C for 1

min, annealing at 60C for 1 min, extension at 72C for 2.5 min (28 cycles). The second round of PCR was completed using 4% of the reaction from round one with the following primers and PCR conditions: DH Q52-2 5'-GCCTCAGAGTCCCTGTGGTCTCTGACTGGT-3' and JH4-2 5'-GGGTCTAGACTCTCAGCCGGCTCCCTCAGGG-3'; denaturing at 95C for 20 sec, annealing at 60C for 1 min, extension at 72C for 2 min (35 cycles).

Cell fractionation and western blotting

Western blot analysis was done with anti-E47 (sc-763, Santa Cruz Biotechnology), anti-Lmo2 (monoclonal antibody provided by Dr. Ron Levy, Stanford), and anti-tubulin (sc-55529, Santa Cruz Biotechnology) antibodies. Cell fractionation was done as previously described. Quantification of proteins by Western blotting was done using 680nm and 800nm infrared dye-conjugated secondary antibodies (LI-COR) on the Odyssey machine.

Gene expression analysis

Total RNA was purified by TRIzol (Life Technologies, Grand Island, New York) per manufacturer's instructions. First strand cDNA was synthesized using oligo-dT primers, random hexamers and reverse transcriptase enzyme (Omniscript, Qiagen, Valencia, California). Quantitative PCR was performed on cDNA using Sybr green (Bio-Rad, Hercules, California) and the MyIQ (Biorad) with the following primers:

Table 5. Primers used for qRT-PCR .

	Forward	Reverse
CD4	AGTTCTCTCCATGTCCAACCTAAGGGTTCA	TCCGCTGACTCTCCCTCACTCTTATAGGC
p21	TTCCGCACAGGAGCAAAGT	CGGCGCAACTGCTCACT
Cdk6	GGCGTACCCACAGAAACCATA	AGGTAAGGGCCATCTGAAAACT
Cyclin E1	GCAGCGAGCAGGAGACAGA	GCTGCTTCCACACCACTGTCTT
Cyclin E2	CGCAGCCGTTTACAAGCTAAG	TGGGTTTCTTGCGGAGAGTCT
Rb	TCTACCTCCCTTGCCCTGTTT	CAGAAGGCGTGCACAGAGTGT
E2F4	AAGCTGGCAGCCGACACT	AGCACGTTGGTGATGTCGTAGAT
P19	CGGTATCCACTATGCTTCTGGAA	CCGCTGCGCCACTCAA
P16	GGGTTTCGCCCAACGCCCCGA	TGCAGCACCACCAGCGTGTCC
Cyclin D3	TGCCAAAACGCCCCAGTAC	CGGGATGCCCGAAGGA
P57	CAGCGGACGATGGAAGAAC	CTCCGGTTCCTGCTACATGAA
P27	GGCCCGGTCAATCATGAA	TTGCGCTGACTCGCTTCTTC
S16	AGGAGCGATTTGCTGGTGTG	GCTACCAGGGCCTTTGAGAT
Hex	CTGGTTTCAGAATCGCCGAGCT	ATGTCCACCTCCTGGTCGGAATCC
HHEX	CCTCTGCATAAAAGGAAAGGCGG	TCTGATCACAGGAACTGTCCAAACTTTC
GUSB	CTCATTTGGAATTTTGCCGATTTCATGACTGA	CTCTCTCGCAAAAGGAACGCTGCACTTTTT

RNA-seq was performed as previously described[121]. Briefly, whole RNA was isolated by RNeasy kit (Qiagen) using established protocols. For RNA isolated from the LSK-OP9 co-culture, no amplification was performed. RNA was checked for quality on the Bioanalyzer. For RNA isolated from sorted LSK; $Flt3^{lo}$ and LSK; $Flt3^{hi}$ sorted cells, we had low input RNA (range 4.8ng-11.9ng) and was therefore subjected to cDNA amplification using the SMARTer Ultra Low RNA Kit (Clontech, Catalog # 634936). The cDNA was sheared using the Covaris S2 instrument with the following parameters: duty 10%, Intensity 5, 200 Cycles/Burst Time 5 minutes, and mode frequency sweeping. Once the cDNA was sheared, the entire volume was used as input into the Illumina TruSeq ChIP Sample Prep Kit (Catalog #IP-202-1012) and the Illumina protocol was primarily used. However, instead of the Illumina PCR ChIP master mix, the KAPA Hot Start PCR Kit (Kapa Biosystems) was used with only 15 cycles PCR to minimize duplication. The samples were then quality controlled, normalized, clustered, and sequenced according to Illumina's best practices. Multiple stage of quality control (QC) of sequencing data was carried out [122]. Raw data and alignment QC were performed using QC3 [123], expression analysis were carried out using MultiRankSeq [124]. All data passed QC. Raw data were aligned with TopHat 2 [125] and gene expression levels were quantified using Cufflinks [126]. RPKM (reads per kilobase per million reads) based approaches (Cuffdiff) were used to detect differentially expressed genes. False discovery rate (FDR < 0.05) was used to correct for multiple testing. To identify lincRNA, we performed gene annotation using lincRNA reference Gencode v19 released by the ENCODE project [127].

In vivo stem and progenitor assays

Competitive Bone Marrow Transplant Assays

Competitive bone marrow transplantation assays were performed by intravenous injection of mixed CD45.2 donor whole bone marrow cells with CD45.1 competitor bone marrow. Hhex$^{lox/lox}$ and *Hhex cKO* carried the CD45.2 allele. Recipient mice were lethally irradiated with 9.5 Gy.

Sublethal Irradiation Assay

Hhex $^{lox/lox}$ and *Hhex cKO* littermates were sublethally irradiated with a dose of 6.5 Gy and allowed 3, 6 and 9 weeks to recover post irradiation.

Homing and Engraftment Assays

To analyze homing, bone marrow from WT and Hhex cKO mice were harvested and used for transplantation. BM cells (80,000) were first plated in methylcellulose culture media for the CFU-C assay to quantify the input number of HSPCs. Ten million donor cells were retro-orbitally injected into lethally irradiated CD45.1^{+} host mice; 16 hours post-transplant, bone marrow from recipient mice were collected and cultured in triplicate for CFU-C assay. Homing was calculated using the following equation:

$$\text{Homing (\%)} = \frac{number\ of\ output\ colonies/dish}{number\ of\ input\ colonies} \times 2 \times 4 \times \frac{100}{18} * 100$$

To analyze engraftment, recipient CD45.1 mice were lethally irradiated and injected with donor bone marrow from either WT or *Hhex* cKO CD45.2 mice. 7 days post injection mice were sacrificed and flow cytometry was used to assess the presence of both CD45.1 and CD45.2 in bone marrow, spleen, thymus and peripheral blood.

CHAPTER III

Enforced E47 expression has differential effects on Lmo2 induced T-ALLs

Background and Significance

The LIM domain only (LMO2) gene and its paralogue LMO1 are frequently deregulated in T-cell acute lymphoblastic leukemia (T-ALL) via various mechanisms[78,86,92]. LMO2 interacts with class II bHLH proteins, GATA proteins and LIM domain binding 1 protein (LDB1)[86,92,103,128,129]. It forms macromolecular complexes at E-boxes and GATA sites in the promoter and enhancer regions of genes[99,100,130,131]. The LMO2 complex may occupy other sites besides E-box/GATA sites and have different binding partners in T-ALL versus erythroid cells[97,104,105].

Class II bHLH proteins heterodimerize with class I bHLH proteins such as E proteins E47, E12, E2.2 and Heb[46]. Both E proteins E47 and E12 are encoded by the same gene, E2A. Knockout of *E2A* results in profound defects in the development of T- and B-cells and the spontaneous development of T-ALL[51,111,132,133]. *E2A*$^{-/-}$ thymocytes have a differentiation block similar to one observed in *Lmo2* transgenic thymocytes. These findings have played an important role in the paradigm in understanding the oncogenic function of Lmo2. One hypothesis is that the Lmo2/Tal1-associated complex binds to E proteins and directs them away from their normal targets (Figure 4A). By understanding the role of E47 in Lmo2-induced T-ALL we hoped to better understand the mechanism of Lmo2 oncogenesis.

Results

Enforced E47-ER homodimerization causes attenuated growth in some Lmo2-induced T-ALL cell lines

E47-ER expression was enforced in four previously described Lmo2-induced T-ALL cell lines[134] (03007, 03020, 03027, 32080 abbreviated 007, 020, 027 and 080) using a retroviral vector that expresses E47-ER-ires human CD25 (referred to as E47-ER) (Figure 5). Cells expressing the E47-ER ires-hCD25 vector were selected by flow cytometry using an anti-hCD25 antibody (Figure 6). Western blot analysis was performed to analyze the protein levels of E47-ER, endogenous E47, and Lmo2 (Figure 7). All cell lines except 027 (lane 10),which had less, had comparable expression of E47-ER. Upon enforced E47-ER homodimerization, using 300nM 4HT, all four cell lines showed marked increases in E47-ER expression (lanes 4,8,12 and 16). Stable expression of E47-ER had no effect on growth of the T-ALL cell lines; however, enforced homodimerization resulted in attenuated growth in both 020-E47 and 080-E47 cell lines (Figure 8).

Lmo2-induced T-ALL cell lines sensitive to E47-ER homodimerization undergo G1 growth arrest

In order to understand the mechanism for attenuated growth observed post E47 homodimerization in 020-E47 and 080-E47, we assessed proliferation using BrdU and 7AAD. Lines 007-E47, 020-E47, 027-E47 and 080-E47 showed comparable numbers of BrdU positive cells to their parental counterparts (Figure 9). Enforced homodimerization via 4HT treatment showed a marked decrease in

BrdU positive cells and a reciprocal increase in G0/G1 populations in both 020 and 080 cell lines (Figure 9 and Figure 10).

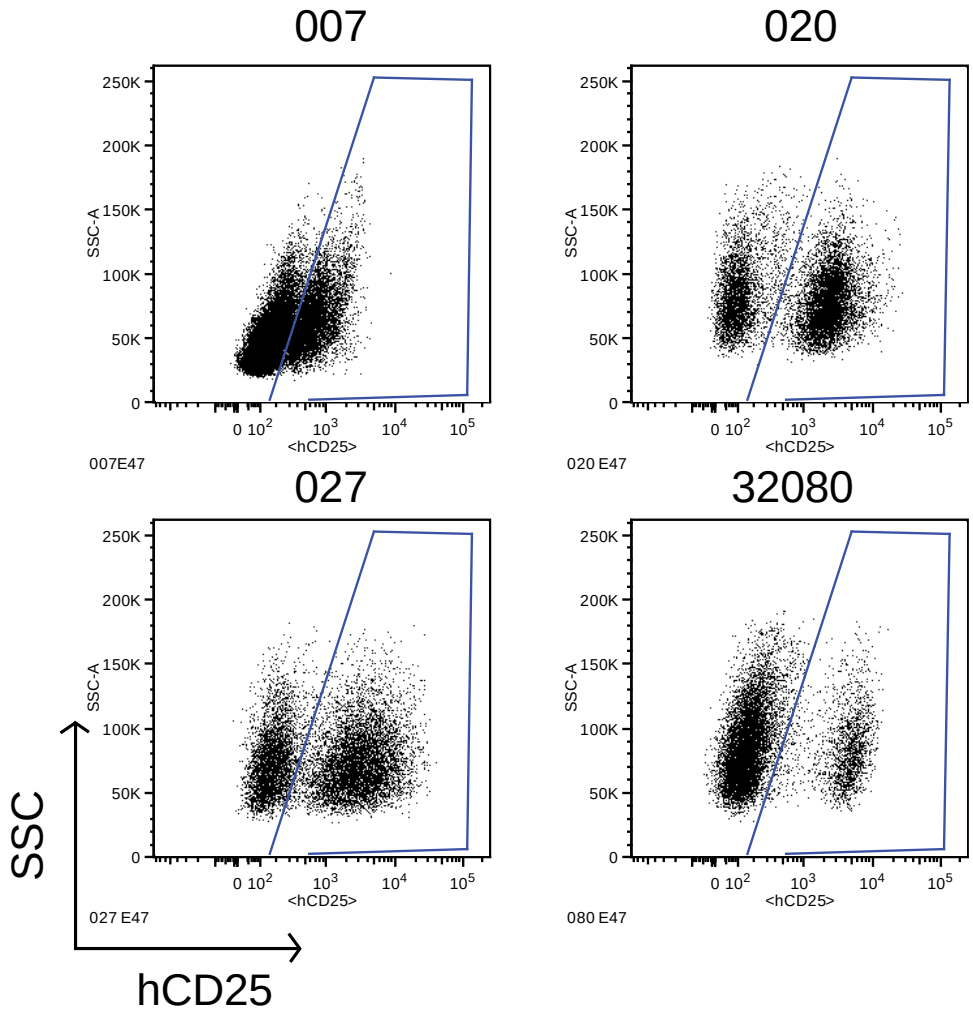

Figure 6. E47-ER expressing cells sorted using hCD25.

FACS plots of four Lmo2-induced T-ALL cell lines 007, 020, 027, and 080 after being transduced with the E47-ER retrovirus. The x-axis shows expression of human CD25 and the y-axis shows side scatter. Cells selected as CD25 positive shown in blue boxes.

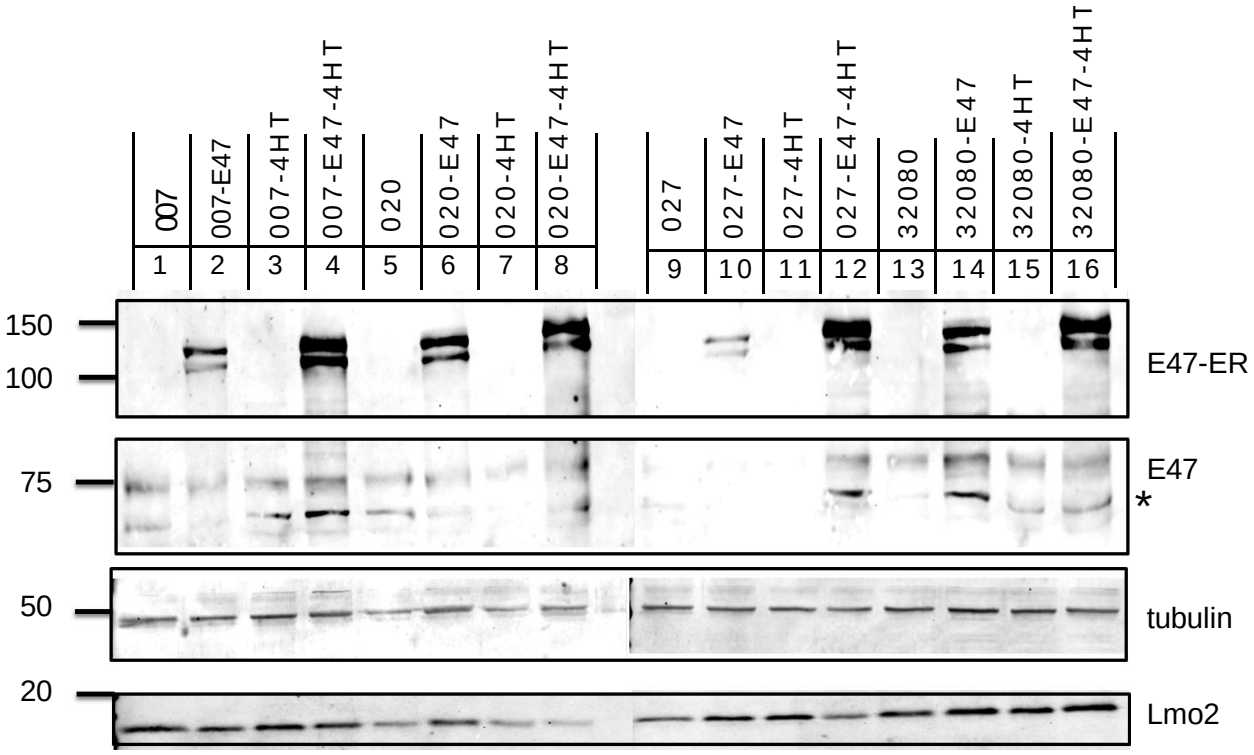

Figure 7. Western blot analysis of T-ALL cell lines.

Whole cells lysates were subjected to SDS-PAGE and analyzed by western for E47, tubulin and Lmo2. The E47-ER fusion protein had a slower migration than endogenous E47. Lysates from cells with enforced homodimerization via 4HT treatment showed greater E47-ER protein.

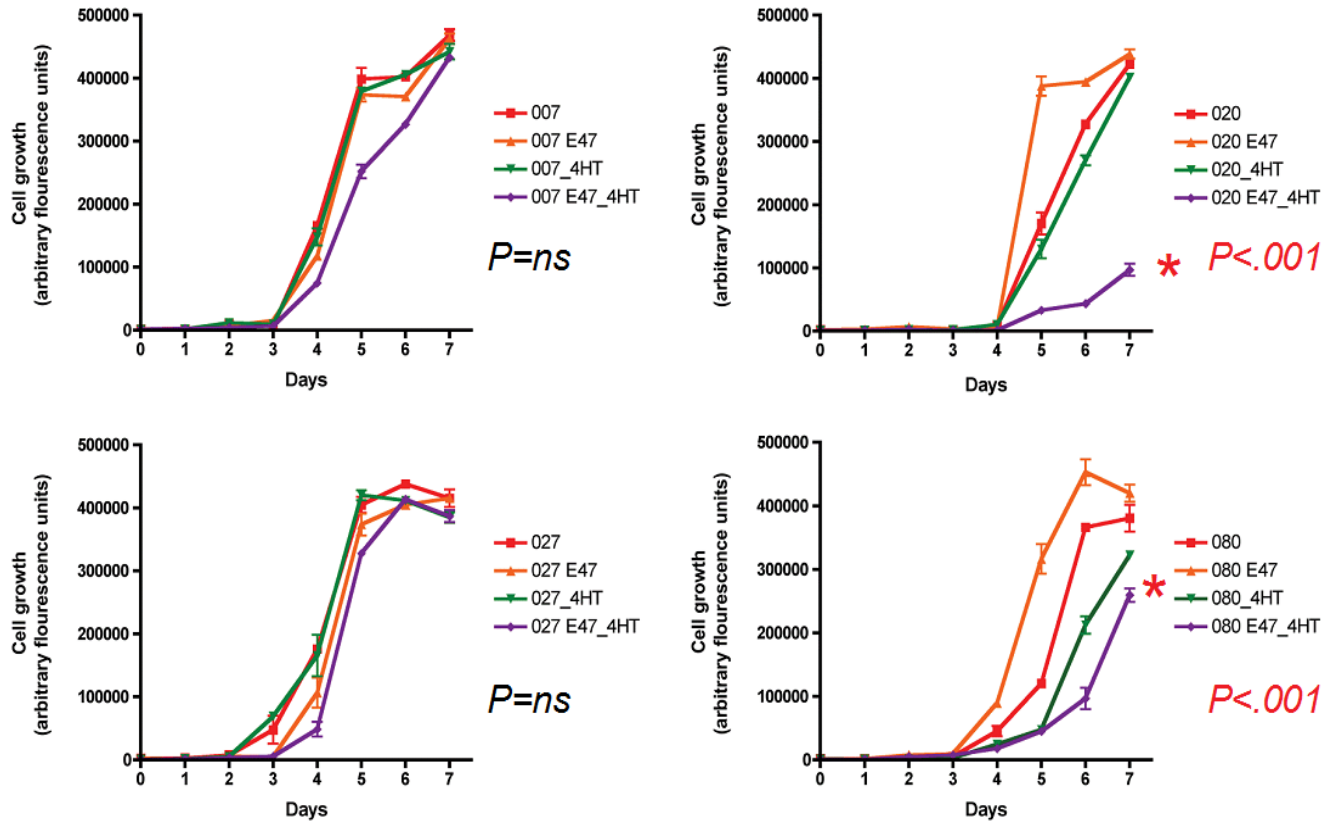

Figure 8. Enforced E47 homodimerization results in growth arrest in 2 T-ALL cell lines.

The four Lmo2-induced T-ALL cell lines and those expressing E47-ER were analyzed for growth with or without 4HT treatment. The x-axis shows days and the y-axis shows arbitrary fluorescence units. Each point of the growth curve was compared by 2-way ANOVA. Cell lines 007 and 027 showed no statistically significant difference in growth upon 4HT treatment

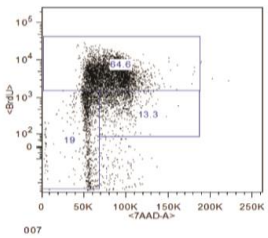

007
(65)

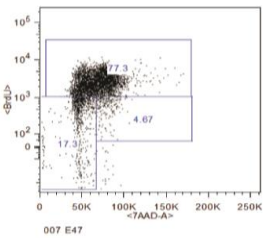

007-E47
(77)

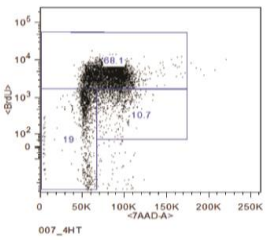

007-4HT
(68)

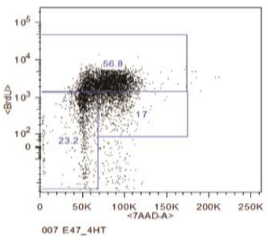

007-E47-4HT
(57)

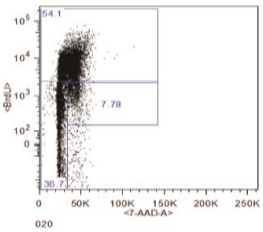

020
(54)

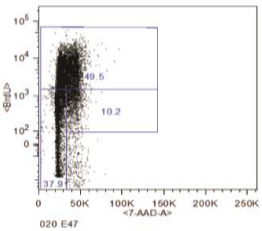

020-E47
(50)

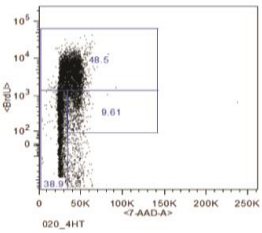

020-4HT
(48)

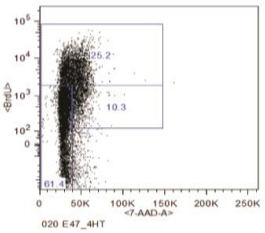

020-E47-4HT
(25)

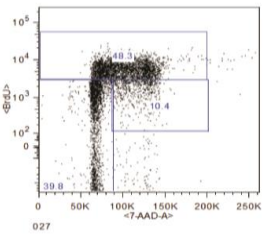

027
(48)

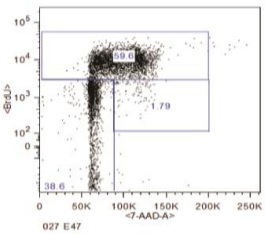

027-E47
(60)

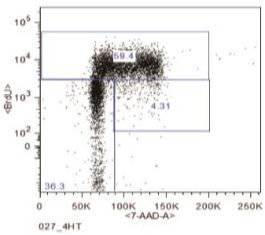

027-4HT
(59)

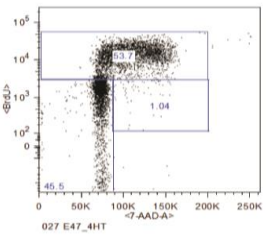

027-E47-4HT
(54)

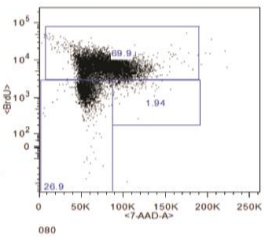

080
(70)

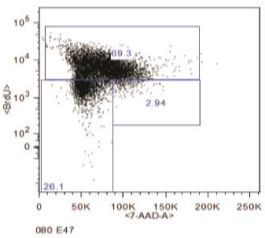

080-E47
(69)

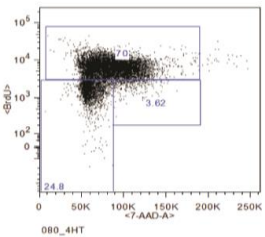

080-4HT
(70)

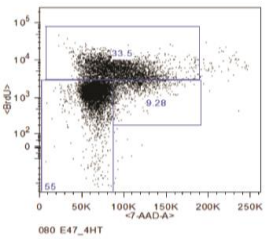

080-E47-4HT
(33)

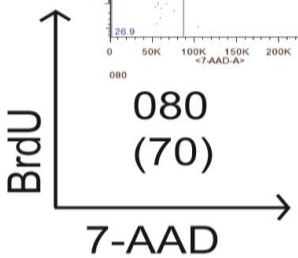

Figure 9. Representative flow plots for BrdU and 7-ADD.

Cell lines, either parental or stably expressing E47-ER, were treated with 4HT for 24 hours, then pulsed for 45 minutes with BrdU. Percentage of S phase cells are shown in parentheses.

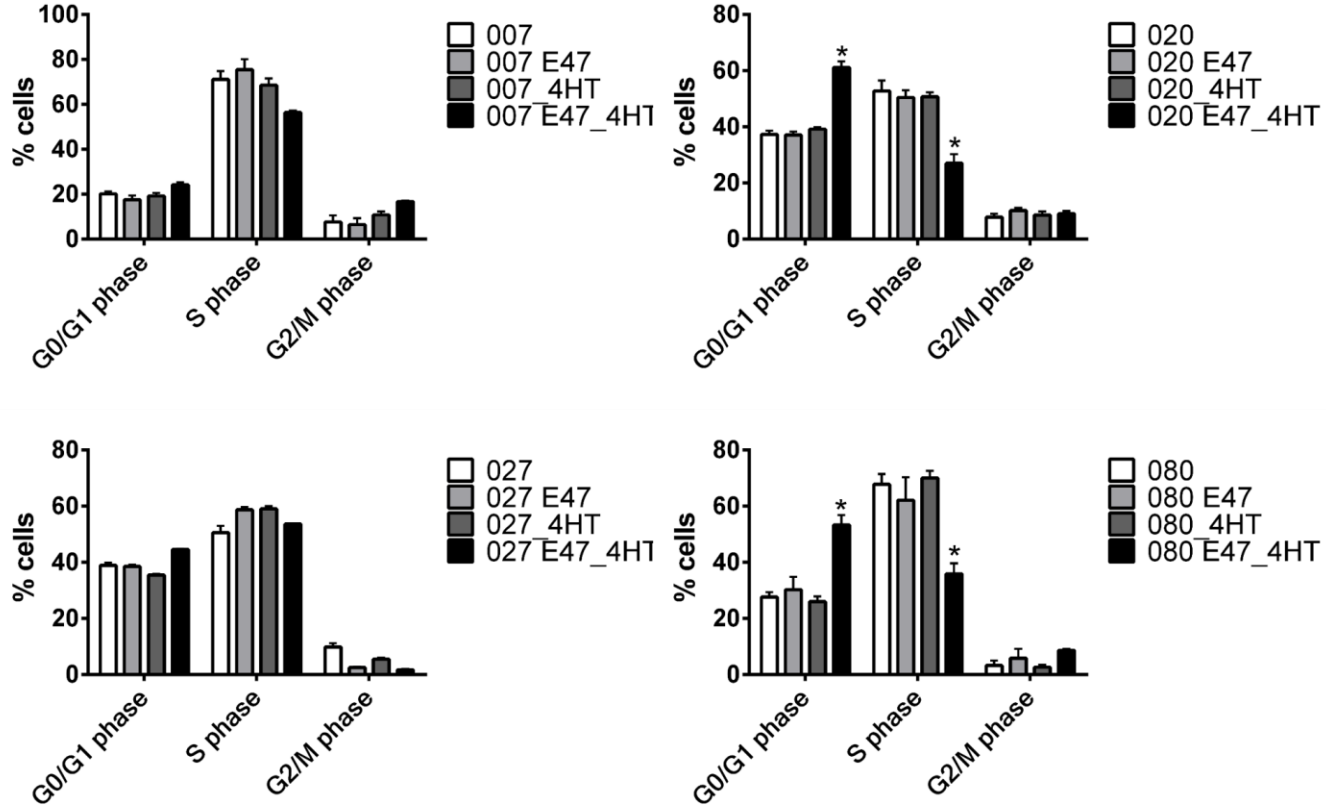

Figure 10. Cell cycle profiles of Lmo2-induced T-ALL cell lines.

Bar graphs show the mean and the standard error of the mean for three independent cell cycle analyses. Pairwise comparisons of the proportion of cells in each phase of the cell cycle was done using student's t-test. Asterisks denote statistically significant comparisons: P=.002 for G1phase and P=.002 for cells in G1 and S phase comparisons of 080-E47-4HT versus 080-4HT; P=.0007 for G1 phase and P=.003 for S phase comparisons of 020-E47-4HTversus 020-4HT.

We also analyzed the proportion of cells undergoing apoptosis using intracellular staining for cleaved caspase 3 (Figure 11). Cell line 007 showed a reduction in apoptosis in E47-ER stably expressing lines and 020-E47 showed a decrease in apoptosis upon E47 homodimerization (Figure 11). There was no change in apoptosis in 027 cell lines. The 080-E47 showed an increase in apoptosis upon E47 homodimerization. These data show that cell lines sensitive to E47 homodimerization (020 and 080) underwent G1 arrest and decreased S phase entry but did not show a consistent pattern of apoptosis as a result of E47 homodimerization.

Enforced E47-ER homodimerization activated CD4 expression

Based on their CD4 and CD8 expression, the four Lmo2- induced T-ALL cell lines bear resemblance to various stages of T-cell development[134] (Figure 12). The cell lines 007 and 080 have a mixture of CD8 intermediate single positive (ISP)-like and CD4 and CD8 double positive (DP)-like cells. The 007 line has fewer DP-like (18%) and more ISP-like (82%) cells than the 080 (50% ISP-like and 50% DP-like). The 020 cell line expresses both CD4 and CD8; resembling DP-like cells. The 027 cell line does not express CD4 or CD8 and resembles double negative (DN) cells. Stable expression of E47-ER increased CD4 protein expression in the 007 cell line, and was markedly increased upon enforced homodimerization (Figure 12). There was no difference in CD4 and CD8 protein expression in 020-E47 lines even after enforced homodimerization. The 027-E47 cell line showed an increase in CD8 ISP-like and DP-like cells.

The increased abundance of CD4 protein shown by flow cytometry correlated with increased CD4 mRNA expression (Figure 13). Interestingly, transcriptional profiling revealed genes such as IL2ra (-2 fold compared to 027-E47, -6.2 compared to 080-E47) and CD24a (-1.2 fold compared to 027-E47 and 080-E47) were repressed upon E47-ER

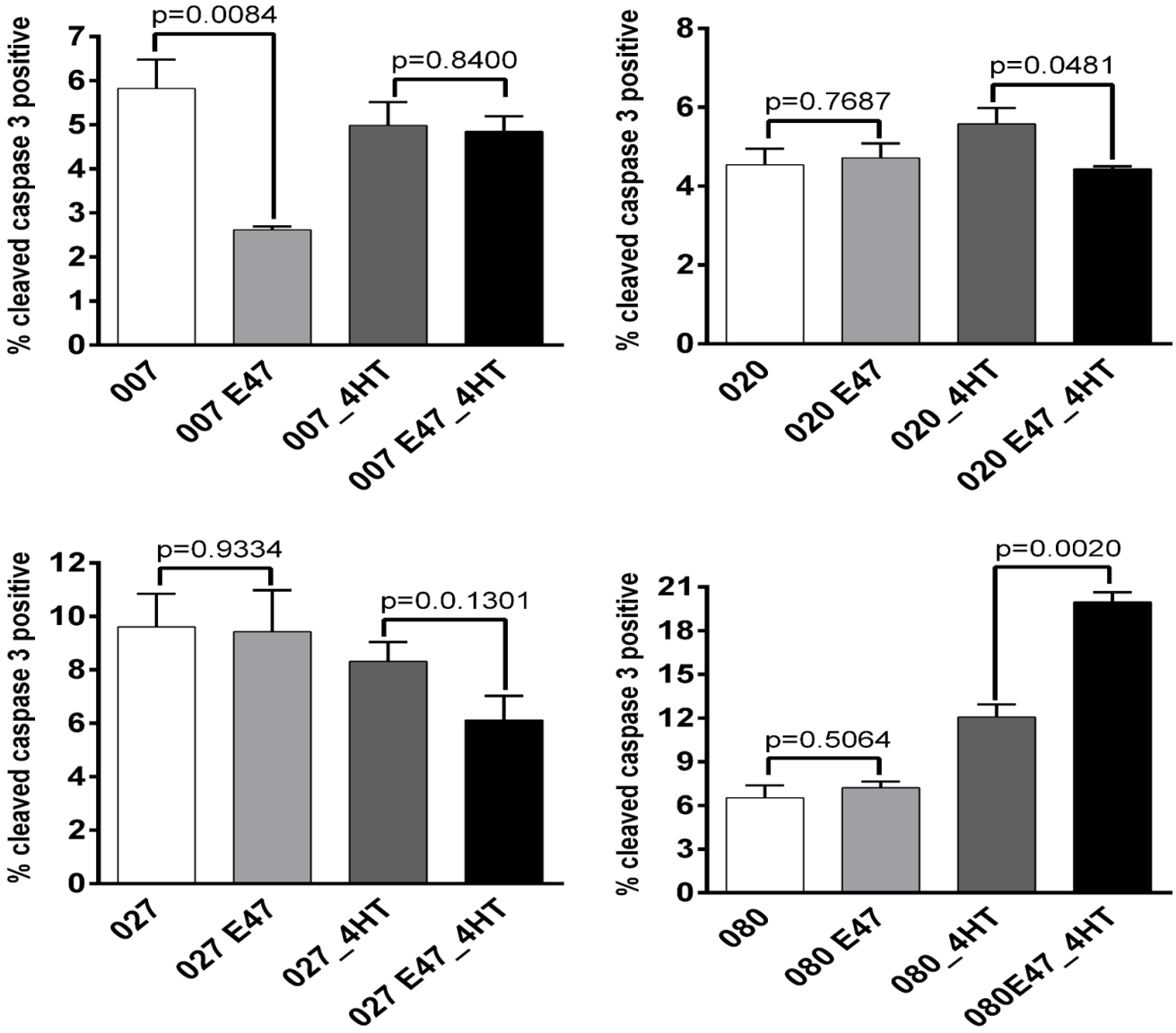

Figure 11. Apoptosis analysis using intracellular staining for cleaved caspase 3.

Parental cell lines and those stably expressing E47-ER, were treated with 4HT and then analyzed for intracellular cleaved caspase 3 by flow cytometry. The bar graphs show the mean and standard error for triplicate analyses. P-values were generated by pairwise comparison by Student's t-test.

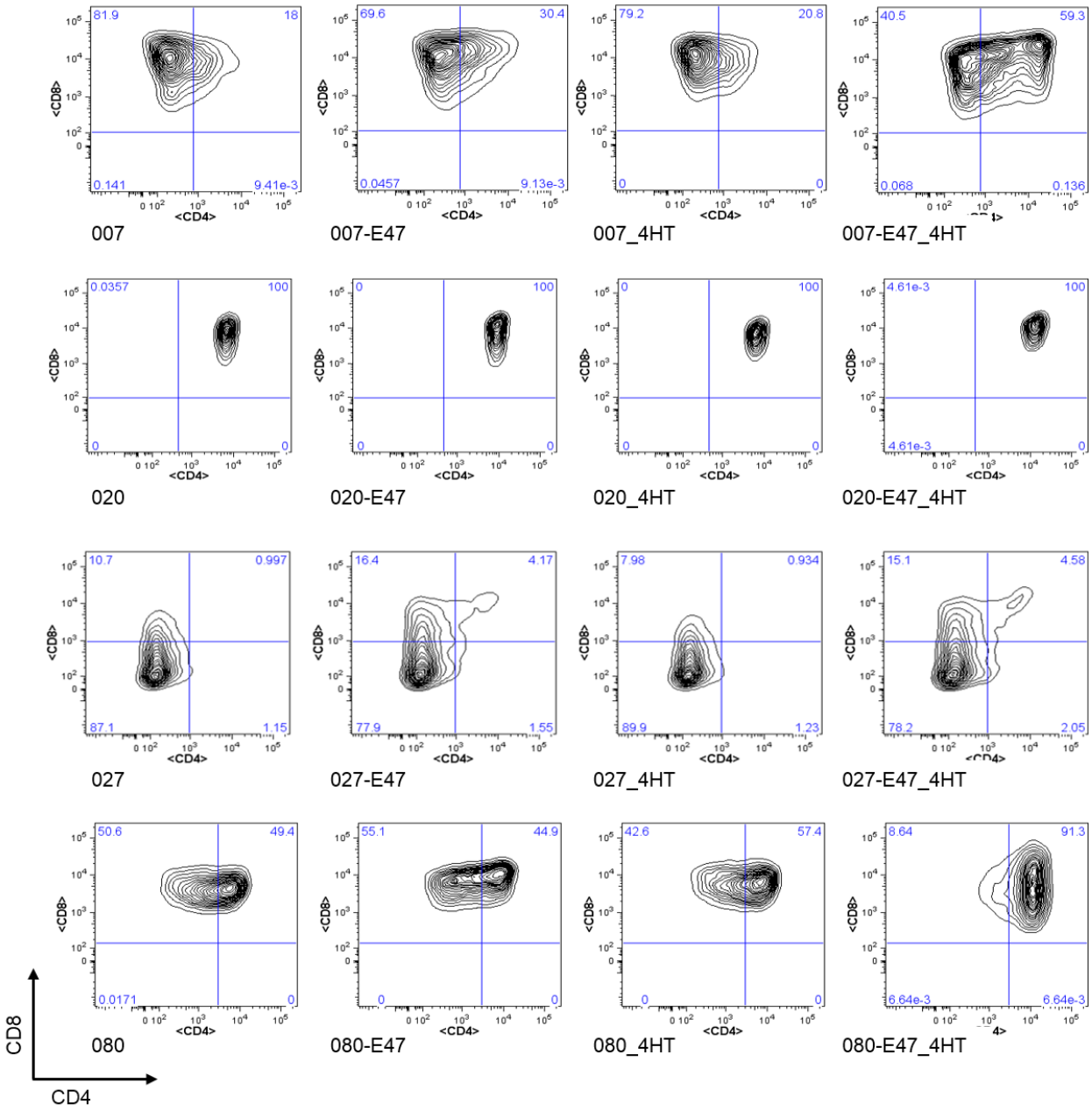

Figure 12. Enforced E47 expression activates CD4 protein.

Parental cell lines and those stably expressing E47-ER, with and without 4HT treatment, were analyzed for CD4 and CD8 expression using flow cytometry. The x-axis shows CD4 and the y-axis shows CD8, 24 hours after 4HT treatment.

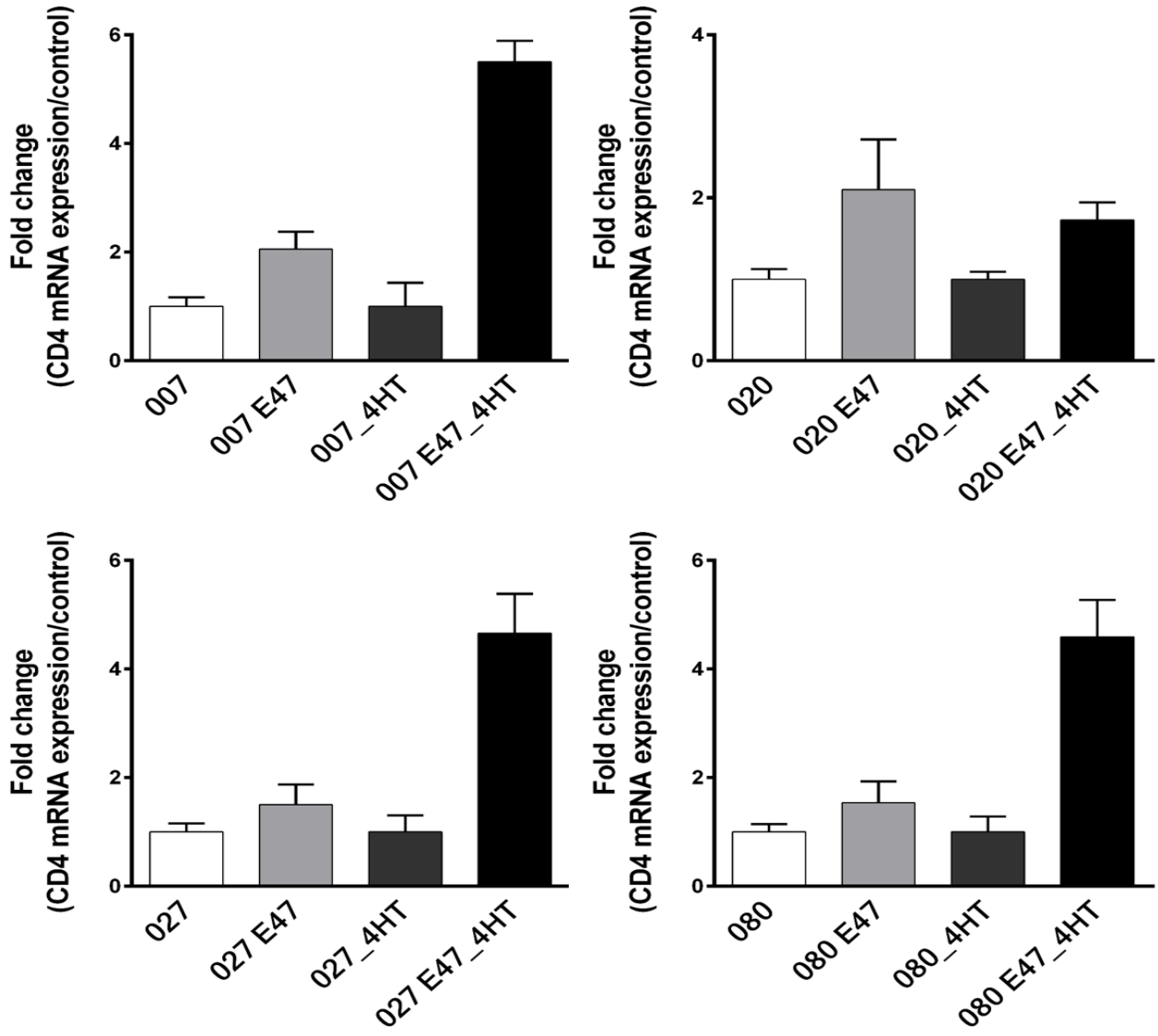

Figure 13. CD4 mRNA expression.

Parental cell lines and those stably expressing E47-ER, with and without 4HT treatment, were analyzed for CD4 mRNA expression using quantitative RT-PCR analysis. The y-axis represents fold change from baseline which is the mRNA present in the parental line. The mean and standard error of mean are shown for triplicate analyses.

homodimerization while genes such as CD8a (1.93-fold in 080-E47-4HT v. 080-E47) were activated upon E47-ER homodimerization. These findings suggest that enforced E47 homodimerization promoted differentiation in Lmo2-induced T-ALLs.

Enforced E47 homodimerization has no effect on E47 localization

Our CD4 transcription data suggests that E47-ER is able to enter the nucleus of cells and activate transcription. Also, we were able to determine that enforced E47-ER homodimerization was able to increase transcriptional activation. To confirm our findings, we fractionated all cell lines into nuclear and cytosolic fractions and blotted for E47 (Figure 14). We observed that absolute E47-ER protein levels in the nucleus and cytosol did not correlate with sensitivity or resistance to the growth inhibition observed upon E47-ER homodimerization (Figure 15). We also assessed endogenous E47 protein levels and did not discern a correlation between sensitive or resistant cell lines and the amount of nuclear or cytosolic protein and nuclear to cytosolic ratio of protein (Figure 16). We did observe that E47-ER and E47 protein levels were more concentrated in the cytosol versus the nucleus in all cell lines.

Differential gene regulation by E47-ER in sensitive vs resistant cell lines

In order to analyze the transcriptional effects of enforced homodimerization of E47-ER, we performed RNA-seq on 027, 027-E47 and 027-E47_4HT and compared it to 080, 080-E47 and 080-E47_4HT (Table 6). This also allowed us to identify E47 targets that may be associated with sensitivity and/or resistance to enforced E47-ER homodimerization. RNA-seq data analysis

revealed 830 genes were differentially expressed between 027-E47 and 027-E47_4HT and 820 genes were differentially expressed between 080-E47 and 080-E47_4HT with a corrected P-value less than 0.05.

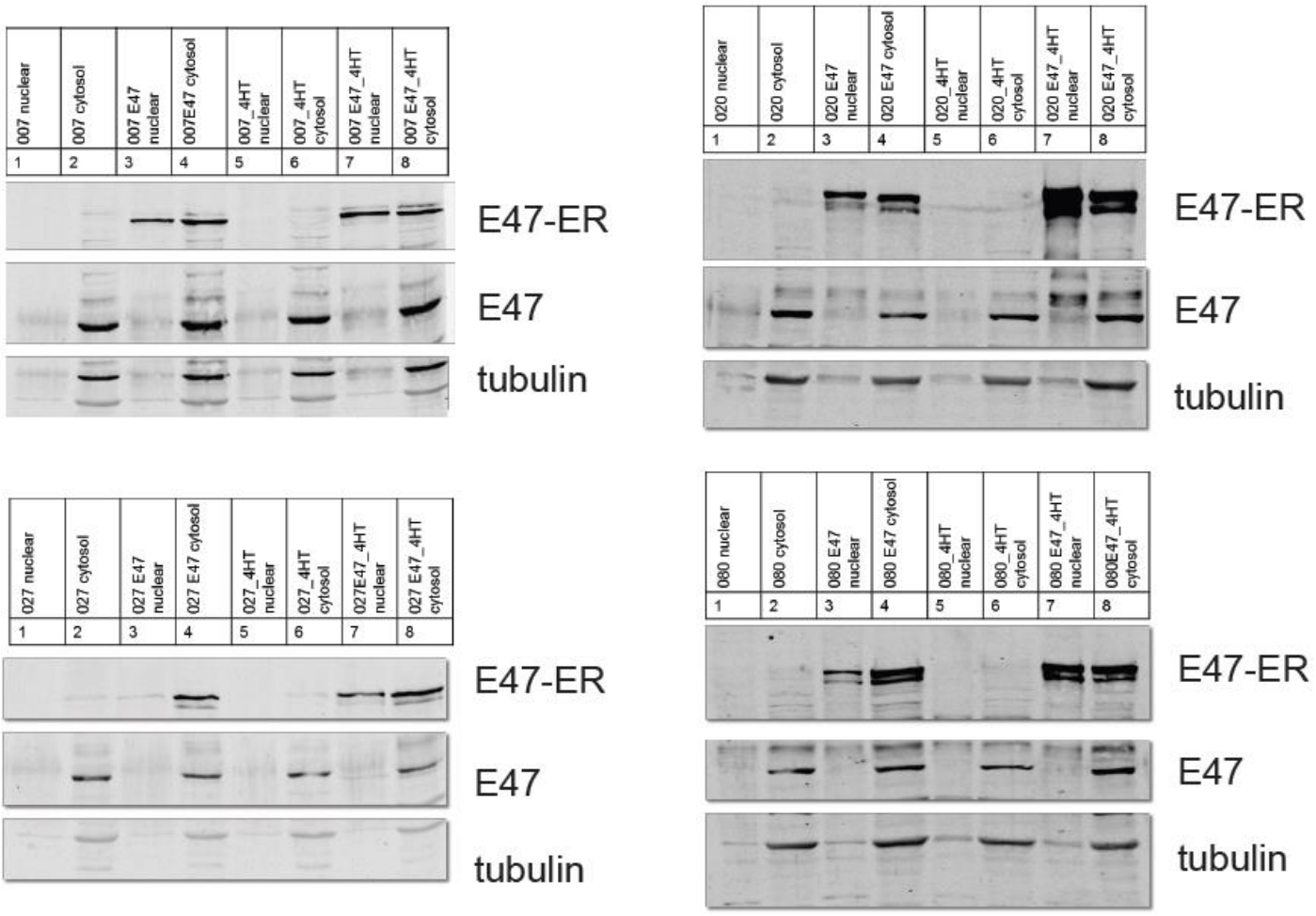

Figure 14. Fractionation of E47 expressing T-ALL cell lines.

Each Lmo2-induced T-ALL line was fractionated into cytoplasmic and nuclear fractions. The proteins were then separated by SDS-PAGE and blotted for either E47 or tubulin.

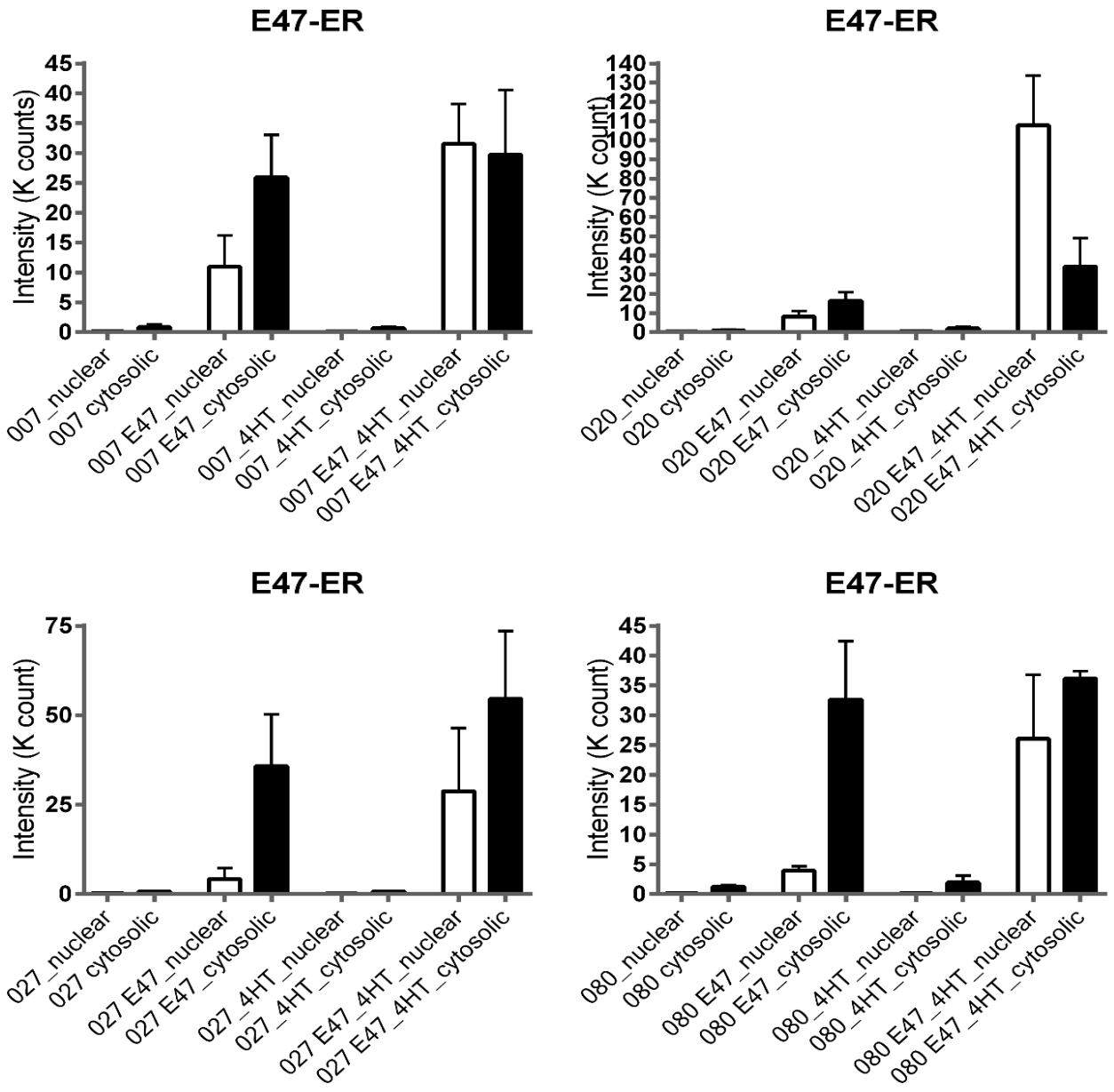

Figure 15. E47-ER protein levels.

SDS-PAGE gels were blotted and labeled with infrared-dye labeled secondary antibodies for quantification using the Odyssey instrument. Graphs show quantification of E47-ER protein and standard error of mean for parental lines (007, 020, 027, 080) and stable lines (with E47-ER) with and without 4HT. The y-axis shows the intensity of infrared dye in K count.

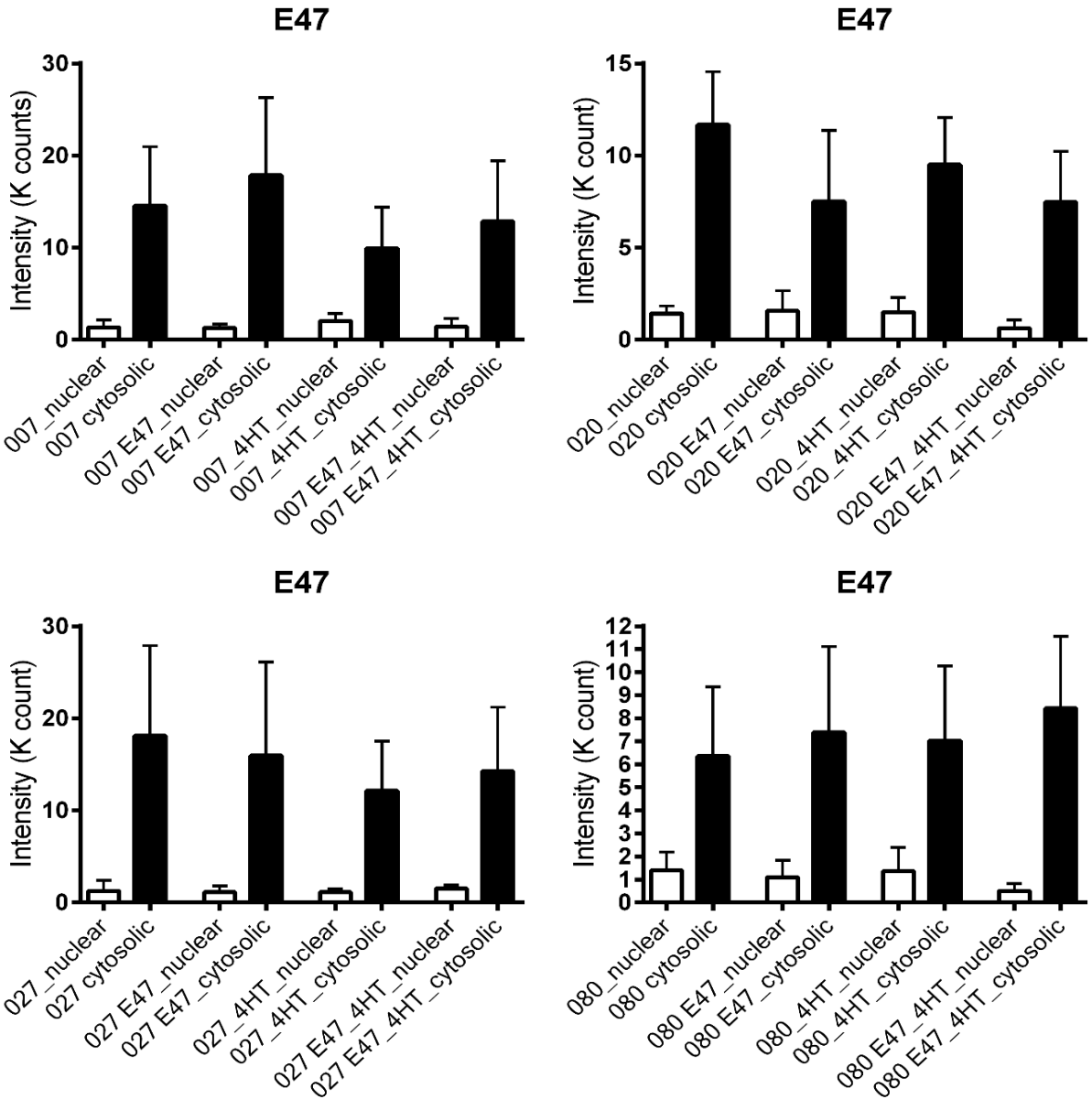

Figure 16. E47 protein levels.

SDS-PAGE gels were blotted and labeled with infrared-dye labeled secondary antibodies for quantification using the Odyssey instrument. Graphs show quantification of endogenous E47 protein and standard error of mean for parental lines (007, 020, 027, 080) and stable lines (with E47-ER) with and without 4HT. The y-axis shows the intensity of infrared dye in K count.

Table 6. RNA-seq analysis of cell lines sensitive (080) and resistant (027) to E47-ER homodimerization.

Values shown are reads per kilobase of gene per million reads (RPKMs). Fold change is the RPKM in E47_4HT divided by RPKM in the parental lines. The RPKMs of 027-E47_4HT And 080-E47_4HT were compared to generate P values which were corrected for multiple hypothesis testing.

Gene	**027**	**027 +E47**	**027 +E47 +4HT**	**080**	**080 +E47**	**080 +E47 +4HT**	**027 Fold**	**080 Fold**	***P***
Rorc	8.83	10.47	46.83	67.96	137.47	296.75	5.30	4.37	0
Gpr56	4.00	2.34	19.17	46.41	59.10	232.03	4.79	5.00	0
Dhrs3	0.17	0.16	0.34	6.93	10.60	33.41	1.98	4.82	0
Ptpre	3.69	2.97	15.21	1.94	2.07	8.72	4.13	4.49	ns
Socs3	3.60	6.80	14.13	5.91	10.85	28.05	3.93	4.75	ns
Hes1	68.13	84.25	89.60	86.98	79.80	99.06	1.32	1.14	ns
Xbp1	63.19	51.87	114.16	20.14	23.59	89.72	1.81	4.45	ns
Sell	146.66	58.62	23.07	37.84	8.61	1.71	0.16	0.05	3.17E-05
Cdk6	8.30	10.39	4.83	40.91	34.75	20.25	0.58	0.49	0.000202
Jund1	5.48	9.77	12.48	4.92	4.50	5.45	2.28	1.11	ns
E2F4	106.34	106.85	169.67	66.65	76.60	142.67	1.60	2.14	ns
Myc	93.28	113.12	68.88	141.58	142.05	104.76	0.74	0.74	ns
Axin2	12.51	12.82	8.75	22.58	22.03	15.04	0.70	0.67	ns
Casp3	49.44	48.61	46.91	75.02	42.59	33.55	0.95	0.45	ns
Casp6	22.14	20.14	21.17	18.13	18.71	24.72	0.96	1.36	ns
Bid	25.21	36.76	38.04	63.15	64.15	75.51	1.51	1.20	0.022
Gadd45a	47.14	50.36	98.81	23.31	14.65	11.85	2.10	0.51	5.10E-11
Gadd45b	0.86	0.97	2.80	0.16	0.12	0.18	3.27	1.13	0.0003
Cdkn1a	6.36	14.27	25.26	25.42	9.27	34.82	3.97	1.37	ns
Ccne1	20.20	21.76	48.01	12.47	3.26	9.39	2.38	0.75	1.38E-05
Rb1	8.40	8.37	4.77	14.06	10.32	5.42	0.57	0.39	0.057
Cyp11a	0.00	0.05	0.36	0.05	0.00	0.43	n/c	8.17	ns
Plcg2	9.03	9.93	10.69	0.04	0.04	0.03	1.18	0.68	0
Dgke	10.69	10.55	10.43	11.65	11.54	10.29	0.98	0.88	ns
Cerk	8.47	10.34	12.98	10.22	20.97	36.83	1.53	3.60	1.40E-05
Ets2	42.79	48.63	65.48	11.08	12.53	32.64	1.53	2.95	0.021
Cd3e	196.58	181.08	210.60	158.37	170.44	243.32	1.07	1.54	ns
Gfi1b	0.80	1.03	16.05	0.03	0.06	3.01	19.96	107.53	0.001965
Gfi1	46.91	46.10	59.53	41.81	43.80	69.94	1.27	1.67	ns
Gata3	60.01	62.01	33.15	147.97	124.04	43.43	0.55	0.29	ns
Foxo1	31.54	33.88	29.69	11.60	13.10	17.68	0.94	1.52	ns
Cd1d1	14.51	14.54	9.78	14.37	11.59	9.40	0.67	0.65	ns
Id2	83.67	85.46	492.49	19.57	27.32	248.41	5.89	12.69	ns
Rag2	27.48	22.95	21.51	27.35	33.94	57.96	0.78	2.12	0.027
Rag1	91.24	83.49	95.22	89.96	96.59	250.49	1.04	2.78	0.005
Id1	30.47	36.62	171.36	10.80	25.35	284.40	5.62	26.33	0
Cd4	1.68	8.37	30.05	27.49	67.63	257.12	17.91	9.35	4.43E-12

In the 027-E47 cell line, 486 genes were downregulated upon enforced homodimerization with 4HT, while 334 genes were upregulated (Figure 17). This trend was different in the 080-E47 cell line where there were 377 upregulated genes and 453 downregulated genes upon enforced homodimerization. Between the 027-E47_4HT and 080-E47_4HT cell lines, there were 268 genes in common. We found that there were 561 genes differentially expressed in 080-E47_4HT and not in 027-E47_4HT. This led us to hypothesize that of those 561 genes, some may account for the growth arrest phenotype seen in 080-E47_4HT cells.

To test this hypothesis, we narrowed down the list of genes using pathway analysis by Ingenuity on the genes differentially expressed between 027-E47 and 027-E47_4HT and 080-E47 and 080-E47_4HT. The key upstream regulators for the 027 cells were Tp53, IL2, Tgfb1, Myc and E47 (Tcf3), while the key regulators in 080 cells were TCR, IL2, Tp53 and E47. E47 was identified as the upstream driver of gene expression in both cell lines; confirming that our pathway analysis was accurate. Pathway analysis revealed that the top canonical pathways in 027 cells were Molecular Mechanisms of Cancer (P=1.19E-9), and GADD45 signaling (P=1.98E-8) and more (Table 7). The top canonical pathways in 080 cells were Glioblastoma multiforme signaling (P=3.01E-6), Granzyme A signaling (P-3.68E-6), PTEN signaling (P=8.68E-6) and more (Table 8).

The Glioblastoma multiforme signaling pathway contains many of the same genes that are also present in the PI3K/AKT pathway. These genes include but are not limited to *PIK3CG* and *PIK3CD* (Table 9) which are also in the

PTEN pathway (Table 10). Previous studies have not shown these two genes as targets of E47; however, the mRNAs for both genes were repressed upon enforced homodimerization of E47 in 080

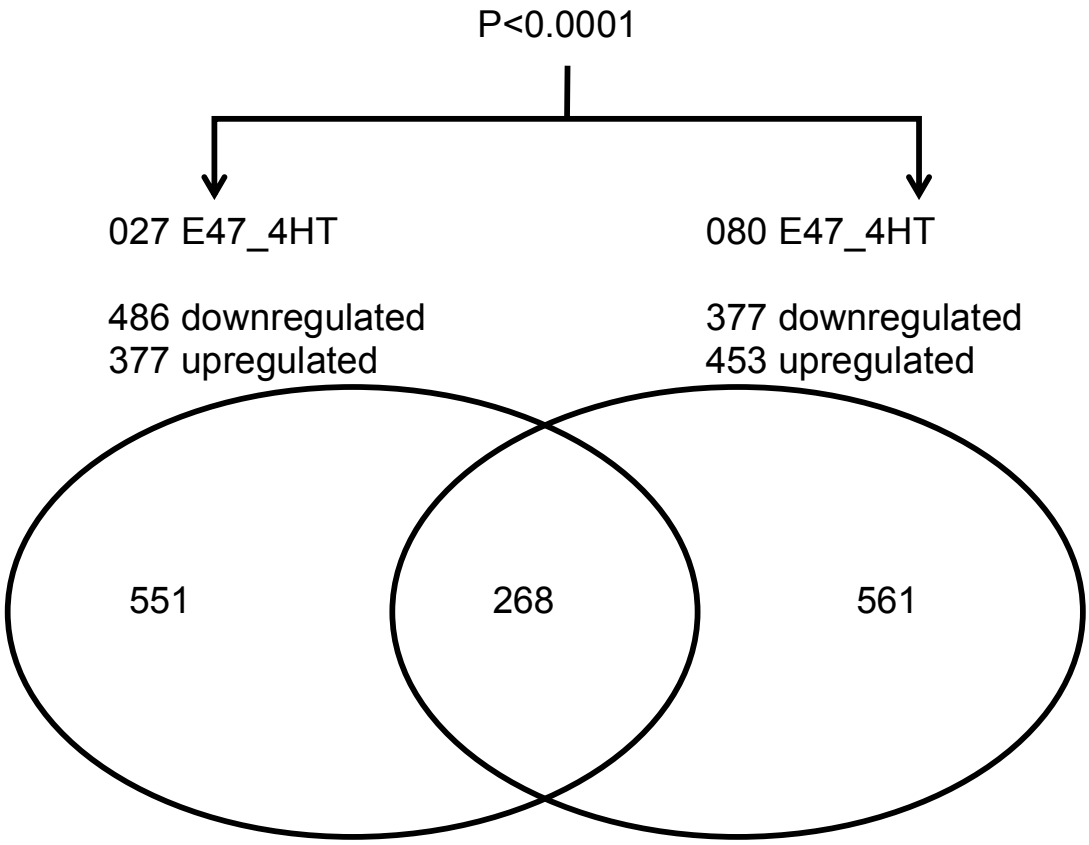

Figure 17. Venn diagram of global gene expression changes in Lmo2-induced T-ALLs resistant and sensitive to E47-ER's effects.

Gene expression was compared in 027-E47 and 080-E47 cell lines after treatment with 4HT. The Venn diagram shows the number of genes statistically upregulated or downregulated after 4HT treatment. The distribution of genes was compared between parental lines by Chi-square analysis generating a P-value less than 0.0001. The Venn diagram also shows the number of genes differentially and similarly expressed between 027-E47_4HT and 080-E47_4HT cell lines.

Table 7. Top canonical pathways for 027 cell line.

Ingenuity Canonical Pathways for 027	-log(p-value)	Ratio
Molecular Mechanisms of Cancer	8.93E+00	1.01E-01
GADD45 Signaling	7.71E+00	3.75E-01
Estrogen-mediated S-phase Entry	6.88E+00	3.21E-01
Cell Cycle: G1/S Checkpoint Regulation	6.81E+00	1.94E-01
Antiproliferative Role of TOB in T Cell Signaling	5.43E+00	3.08E-01
Factors Promoting Cardiogenesis in Vertebrates	5.17E+00	1.41E-01
Cyclins and Cell Cycle Regulation	5.00E+00	1.35E-01
Protein Kinase A Signaling	4.91E+00	8.07E-02
Chronic Myeloid Leukemia Signaling	4.88E+00	1.32E-01
Glioma Signaling	4.18E+00	1.15E-01
Aryl Hydrocarbon Receptor Signaling	4.03E+00	9.36E-02
HER-2 Signaling in Breast Cancer	3.85E+00	1.34E-01
Breast Cancer Regulation by Stathmin1	3.79E+00	8.88E-02
Glioblastoma Multiforme Signaling	3.78E+00	9.52E-02
Cell Cycle: G2/M DNA Damage Checkpoint Regulation	3.64E+00	1.63E-01
NF-Îºß Activation by Viruses	3.30E+00	1.20E-01
Phospholipase C Signaling	3.15E+00	7.55E-02
Pancreatic Adenocarcinoma Signaling	3.09E+00	9.38E-02
Mouse Embryonic Stem Cell Pluripotency	3.00E+00	1.11E-01
T Helper Cell Differentiation	2.91E+00	1.25E-01
PEDF Signaling	2.82E+00	1.14E-01
Regulation of the Epithelial-Mesenchymal Transition Pathway	2.79E+00	8.16E-02
TGF-Î² Signaling	2.75E+00	1.06E-01
LPS-stimulated MAPK Signaling	2.74E+00	1.08E-01
Cell Cycle Regulation by BTG Family Proteins	2.71E+00	1.54E-01
ATM Signaling	2.71E+00	1.21E-01
Acute Myeloid Leukemia Signaling	2.58E+00	1.07E-01

Table 8. Top canonical pathways for 080 cell line.

Ingenuity Canonical Pathways for 32080	-log(p-value)	Ratio
Glioblastoma Multiforme Signaling	5.52E+00	1.13E-01
Granzyme A Signaling	5.43E+00	3.50E-01
Cell Cycle: G1/S Checkpoint Regulation	5.22E+00	1.67E-01
PTEN Signaling	5.06E+00	1.16E-01
T Helper Cell Differentiation	5.01E+00	1.67E-01
Chronic Myeloid Leukemia Signaling	4.93E+00	1.32E-01
Small Cell Lung Cancer Signaling	4.88E+00	1.28E-01
Estrogen-mediated S-phase Entry	4.67E+00	2.50E-01
HER-2 Signaling in Breast Cancer	4.57E+00	1.46E-01
Lymphotoxin Î² Receptor Signaling	4.52E+00	1.61E-01
UVA-Induced MAPK Signaling	4.43E+00	1.33E-01
Thrombin Signaling	4.40E+00	9.48E-02
Breast Cancer Regulation by Stathmin1	4.33E+00	9.35E-02
Glioma Signaling	4.23E+00	1.15E-01
Protein Kinase A Signaling	4.22E+00	7.58E-02
T Cell Receptor Signaling	4.13E+00	1.19E-01
Aryl Hydrocarbon Receptor Signaling	4.08E+00	9.36E-02
Prolactin Signaling	4.05E+00	1.31E-01
ILK Signaling	4.03E+00	9.27E-02
PI3K Signaling in B Lymphocytes	3.99E+00	1.05E-01
Telomerase Signaling	3.95E+00	1.23E-01
Non-Small Cell Lung Cancer Signaling	3.81E+00	1.20E-01
Calcium Signaling	3.76E+00	8.29E-02
Cyclins and Cell Cycle Regulation	3.68E+00	1.15E-01
Prostate Cancer Signaling	3.54E+00	1.07E-01
Cell Cycle Regulation by BTG Family Proteins	3.54E+00	1.79E-01
Neuropathic Pain Signaling In Dorsal Horn Neurons	3.40E+00	1.10E-01

Table 9. Glioblastoma multiforme signaling was a top canonical pathway enriched in 080-E47 cells treated with 4-hydroxytamoxifen by Ingenuity pathway analysis.

Symbol	Ensembl	Log Ratio	p-value	False Discovery Rate (q-value)	Networks
PDGFRB	ENSMUSG00000024620	-1.350	1.73E-06	7.06E-05	10
PLCL1	ENSMUSG00000038349	-1.333	6.88E-04	1.27E-02	7
PLCL2	ENSMUSG00000038910	-1.298	6.73E-04	1.25E-02	7
CCND1	ENSMUSG00000070348	-0.984	2.11E-04	4.75E-03	6
PIK3CG	ENSMUSG00000020573	-0.882	2.47E-03	3.74E-02	20
CDK6	ENSMUSG00000040274	-0.855	3.12E-06	1.17E-04	5
PIK3CD	ENSMUSG00000039936	-0.642	2.34E-04	5.12E-03	4
MYC	ENSMUSG00000022346	-0.526	2.51E-04	5.43E-03	1
FNBP1	ENSMUSG00000075415	-0.373	3.43E-03	4.89E-02	8
CTNNB1	ENSMUSG00000006932	0.495	6.12E-10	4.53E-08	11
PLCB2	ENSMUSG00000040061	0.602	2.08E-05	6.26E-04	18
CDKN1B	ENSMUSG00000003031	0.798	2.04E-05	6.17E-04	6
RND2	ENSMUSG00000001313	0.883	3.36E-06	1.25E-04	14
ITPR1	ENSMUSG00000030102	1.018	4.38E-04	8.77E-03	
PIK3R5	ENSMUSG00000020901	1.373	3.30E-10	2.57E-08	20
CCNE1	ENSMUSG00000002068	1.472	7.96E-07	3.45E-05	8
E2F2	ENSMUSG00000018983	1.567	1.58E-11	1.55E-09	12
EGFR	ENSMUSG00000020122	1.738	7.39E-04	1.35E-02	4
CDKN1A	ENSMUSG00000023067	1.937	4.53E-14	6.62E-12	9

Table 10. Genes within PTEN signaling pathway that were differentially expressed in 080- E47 after 4-HT treatment are shown.

Symbol	Ensembl	Log Ratio	p-value	False Discovery Rate (q-value)	Networks
PDGFRB	ENSMUSG00000024620	-1.350	1.73E-06	7.06E-05	10
CCND1	ENSMUSG00000070348	-0.984	2.11E-04	4.75E-03	6
PIK3CG	ENSMUSG00000020573	-0.882	2.47E-03	3.74E-02	20
FOXO3	ENSMUSG00000048756	-0.787	9.37E-04	1.66E-02	9
PIK3CD	ENSMUSG00000039936	-0.642	2.34E-04	5.12E-03	4
PDPK1	ENSMUSG00000024122	0.613	1.83E-03	2.88E-02	9
RPS6KB2	ENSMUSG00000024830	0.636	2.50E-03	3.77E-02	9
CDKN1B	ENSMUSG00000003031	0.798	2.04E-05	6.17E-04	6
BCL2L11	ENSMUSG00000027381	0.835	6.84E-08	3.62E-06	16
GSK3A	ENSMUSG00000057177	0.897	1.51E-03	2.46E-02	
DDR1	ENSMUSG00000003534	1.143	0.00E00	0.00E00	23
PIK3R5	ENSMUSG00000020901	1.373	3.30E-10	2.57E-08	20
NTRK3	ENSMUSG00000059146	1.431	3.35E-04	6.99E-03	4
EGFR	ENSMUSG00000020122	1.738	7.39E-04	1.35E-02	4
CDKN1A	ENSMUSG00000023067	1.937	4.53E-14	6.62E-12	9
BCL2L1	ENSMUSG00000007659	2.042	0.00E00	0.00E00	11

cells (1.53- and 1.56 fold respectively). Remarkably, the Pik3cg and Pik3cd enzymes have been targets of kinase inhibitors in various cancer types including T-ALL and chronic lymphocytic leukemia (CLL)[135-137]. We believe the Granzyme A pathway was significantly enriched in 080 cells due to the downregulation of the Histone 1 cluster in this cell line (Table 11).

One top canonical pathway of both 027 and 080 cell lines was the cell cycle G1/S checkpoint (Table 7 and Table 8). *Ccne1* is responsible for the G1/S transition. Due to the arrest seen in the G1 →S transition, we hypothesized that there would be a decrease of *Ccne1* mRNA in the lines that underwent growth arrest upon E47 homodimerization. Cdkn1b is important for inhibiting the function of cyclins important for the G1/S transition, therefore we hypothesized that there will be an increase in Cdkn1b transcripts in the lines that underwent growth arrest upon E47 homodimerization. As expected the 027-E47-4HT cells showed a 2.4 fold increase in *Ccne1* mRNA while the 080-E47_4HT cell line showed a 1.3 fold decrease in *Ccne1* mRNA. Likewise, Cdkn1b mRNA was decreased 1.3 fold in 027-E47_4HT cells but showed a 1.6 fold mRNA increase in 080-E47_4HT cells.

Table 11. The Granzyme A signaling pathway was enriched in 080-E47.

Symbol	Ensembl	Log Ratio	p-value	False Discovery Rate (q-value)	Networks
HIST1H1B	ENSMUSG00000058773	-2.959	8.56E-06	2.88E-04	22
HIST1H1E	ENSMUSG00000051627	-2.638	1.06E-08	6.47E-07	22
GZMA	ENSMUSG00000023132	-2.159	4.77E-13	5.94E-11	17
HIST1H1A	ENSMUSG00000049539	-2.087	8.92E-07	3.79E-05	12
HIST1H1D	ENSMUSG00000052565	-2.002	2.04E-06	8.13E-05	22
APEX1	ENSMUSG00000035960	-0.455	2.18E-04	4.85E-03	12
H1F0	ENSMUSG00000096210	0.847	2.73E-03	4.06E-02	22

Discussion

Both human T-ALL studies and mouse models of T-ALL suggest that LMO2 and its paralogs are responsible for inducing T-ALL via a functional defect of E2A proteins, E12 and E47. *E47*$^{-/-}$ mice spontaneously develop T-ALL and upon rescue of E47, cells undergo apoptosis. We predicted that if Lmo2 induced a functional deficiency of E47, then enforced expression should cause similar effects observed in rescued *E47*$^{-/-}$ T-ALL cells. E47 expression was enforced using an E47-ER fusion protein allowing homodimerization to be induced using 4HT. Stable Lmo2 induced T-ALL cell lines expressing E47-ER were established and grew similar to their parental counterparts. Upon E47-ER homodimerization using 4HT, two cell lines underwent growth arrest while two cell lines continued to grow similar to their parental lines, unresponsive to E47 homodimerization. We were able to determine that the growth arrest was in the G1→S transition of the cell cycle using BrdU labelling. Surprisingly, apoptosis was only induced in one of four cell lines (080) upon E47-ER homodimerization. We also found that the *CD4* gene was activated in all the cell lines independent of the growth arrest seen with E47-ER homodimerization. These data suggest that apoptosis is not a prominent cellular pathway employed by E47 in Lmo2-induced T-ALLs.

In our studies we assessed the cellular distribution of E47-ER in all four cell lines and found that there was no difference in E47-ER distribution between the cell lines sensitive to inhibitory growth effects versus the cell lines that were resistant. Using RNA-seq we analyzed global gene expression in one cell line that was resistant (027) to E47-induced growth inhibitory effects and a cell line

that was sensitive (080) to E47-induced growth inhibitory effects. Gene expression analysis revealed striking similarities and differences between the two cell lines. Upon E47 homodimerization in 027 cells there were more genes downregulated compared to 080-E47 cells. One explanation for this trend is that 080 cells are lacking co-repressors that are necessary for gene expression regulation. For instance, the 080 cell line lacked the myeloid translocation gene 16(Mtg16), a component of the Lmo2 complex, while it was present in the 027 cell line. Mtg16 binds both E2A proteins and in instances of Mtg16 loss there may be a disruption in protein balance that may result in the regulation of transcription targets. Although Mtg16 is required for normal T-cell development, it does not seem to be required for the development of Lmo2-induced T-ALL because of its absence in 080 cells. To determine whether the lack of Mtg16 in 080 cell lines played a role in E47-homodimerization growth arrest, we tried to express Mtg16 in 080-E47 cells. Unfortunately, coexpression of E47-ER and Mtg16, using retroviral transductions, was not achieved which may suggest that they may work together to induce growth arrest in T-ALL cells. On the other hand, validated targets that are repressed by E47 were effectively downregulated in 080 cell lines upon E47 homodimerization. This would suggest that Mtg16 is not a vital co-repressor for these targets. Instead, Mtg16 function may be compensated for by another protein such as myeloid translocation gene, related-1 (Mtgr1) which was present in both cell lines.

Gene expression analysis also revealed similar patterns in the induction and repression of genes involved in the G1→ S phase transition. We found that

in both cell lines the G1/S checkpoint pathway was a significant pathway regulated by E47 in both cell lines. An explanation for this similarity in gene expression and difference in growth inhibitory effect of E47 in 080 cells may be post-transcriptional. One main example is that CD4 mRNA was upregulated in both cell lines but the level of protein expression was different.

One intriguing observation we made was that the two cell lines (020 and 080) that were sensitive to E47 homodimerization inhibitor effects are more mature than the cell lines that were resistant. One explanation for this finding is that the E47 targets may have different chromatin states based on the differentiation state of the cell line. Although the molecular basis for E47-induced growth arrest is still unclear, our results show that E47 deficiency is not a universal feature of Lmo2-induced T-ALL. This finding supports an important role for Lmo2 in transcriptional regulation and argues for further analysis of its chromatin occupancy and its binding partners in T-ALL.

CHAPTER IV

Hhex plays a role in T-ALL development

Background and Significance

The deregulation of homeodomain transcription factor expression has been a common characteristic of many neoplasms[138-140]. Homeodomain genes are often targets of retrovirus-induced hematological malignancies[141,142]. The oncogenic potential of many of these genes has been assessed through insertional mutagenesis studies; which have been crucial for identifying genes involved in the induction of hematological malignancies. One such gene identified is the homeodomain transcription factor hematopoietically expressed homeodomain (Hhex) which when misexpressed, can induce the onset of hematological malignancies[71].

Lmo2-associated complexes occupy the promoter and enhancer of Hhex. Gene expression analysis of both human T-ALL and CD2-*Lmo2* transgenic mouse models revealed that Lmo2 is expressed in two mutually exclusive profiles, one of which includes Hhex[104]. Hhex is a direct target of Lmo2 in which Lmo2 occupies the Hhex promoter and enhancer[104]. Lmo2, Lyl1 and Hhex are all upregulated in a very difficult to treat subset of T-ALL known as ETP-ALL. T-ALL patients with Hhex overexpression have a significantly worse prognosis.

Results

Enforced Hhex expression in T-cells results in differentiation block

To assess the ability of Hhex to induce T-ALL independent of Lmo2, we retrovirally transduced double negative thymocytes from WT mice with either

mouse stem cell virus ires GFP-Hhex (MIG-Hhex) or empty MIG virus. Thymocytes were co-cultured on OP9-DL1 stromal cells with cytokines Fl3L and IL-7[121]. Retrovirus expression was assessed weekly by flow cytometry for GFP. We found that GFP was higher in the group that received Hhex versus the group that received empty MIG vector (Figure 18). This would suggest that MIG-Hhex provides thymocytes with a growth advantage. We also consistently observed an accumulation of double negative (DN) cells in the cultures that received MIG-Hhex, while the MIG only (data not shown) and untransduced WT cultures were able to differentiate to double positive (DP) cells (Figure 19). DN thymocytes can be further divided into four subpopulations (DN1-4) based on CD44 and CD25 expression[143]. Further analysis into the differentiation of these cells revealed that the MIG-Hhex cells were blocked at the DN2 stage of T-cell development (Figure 20). Surprisingly, while these cells were T-cells the MIG-Hhex population had high B220 antigen, a marker of B cells (Figure 21).

Loss of Hhex attenuates Lmo2-induced T-ALL

In order to analyze the role of *Hhex* in the development of Lmo2-induced T-ALL, we bred *Hhex* $^{lox/lox}$ and *Hhex cKO* mice to CD2-*Lmo2* transgenic mice; which are known to spontaneously develop T-ALL. We found that there was a significant difference between T-ALL onset in *CD2-Lmo2* transgenic and CD2-*Lmo2;Hhex cKO*. While all *CD2 Lmo2* transgenic mice developed T-ALL, only 3 out of 16 CD2-Lmo2; Hhex cKO mice developed T-ALL (Figure 22). At steady state Hhex cKO mice had normal thymic cellularity and phenotype.

We performed PCR analysis to determine knockout efficiency of Hhex in the three tumors that developed in the *CD2-Lmo2; Hhex cKO* mice. We found that one tumor sample showed incomplete knockout of Hhex while the other two showed complete knockout of Hhex (Figure 24). This data suggests that Hhex plays a crucial role in the development of Lmo2-induced T-ALL.

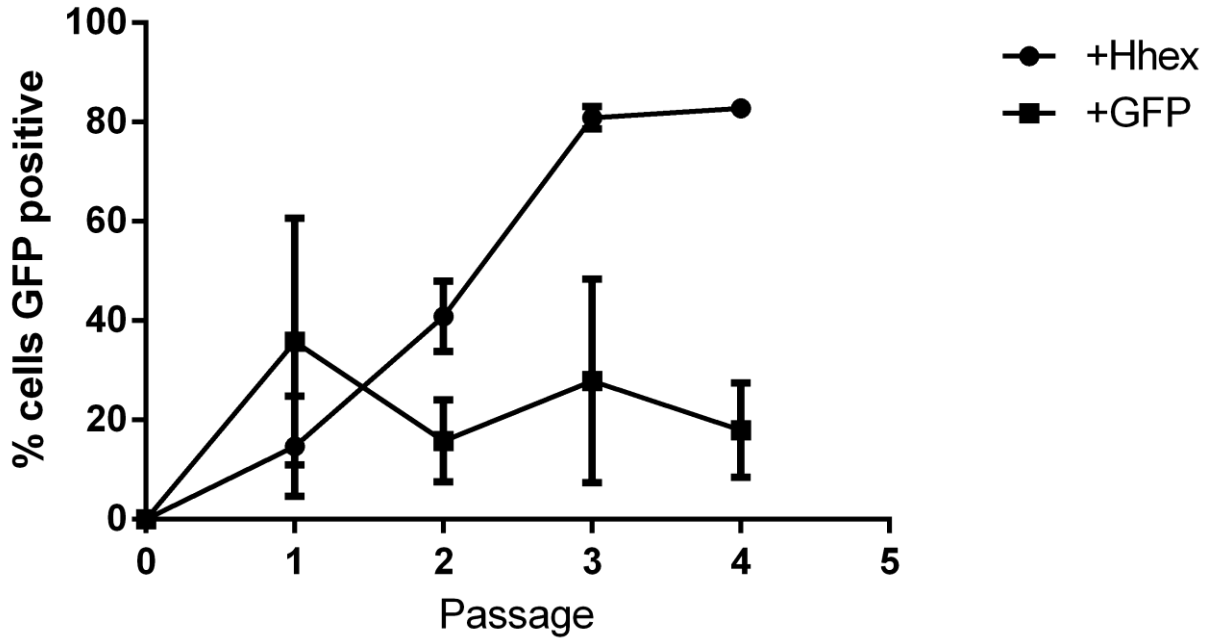

Figure 18. GFP expression in thymocytes transduced with MIG-Hhex or empty vector.

Double negative thymocytes were transduced with either MIG-Hhex or empty vector and plated on OP9-DL1 cells in the presence of cytokines. Every 7 days cells were tested for GFP using flow cytometry. The x-axis shows the number of times each group was passaged and the y-axis shows the proportion of cells that were GFP positive.

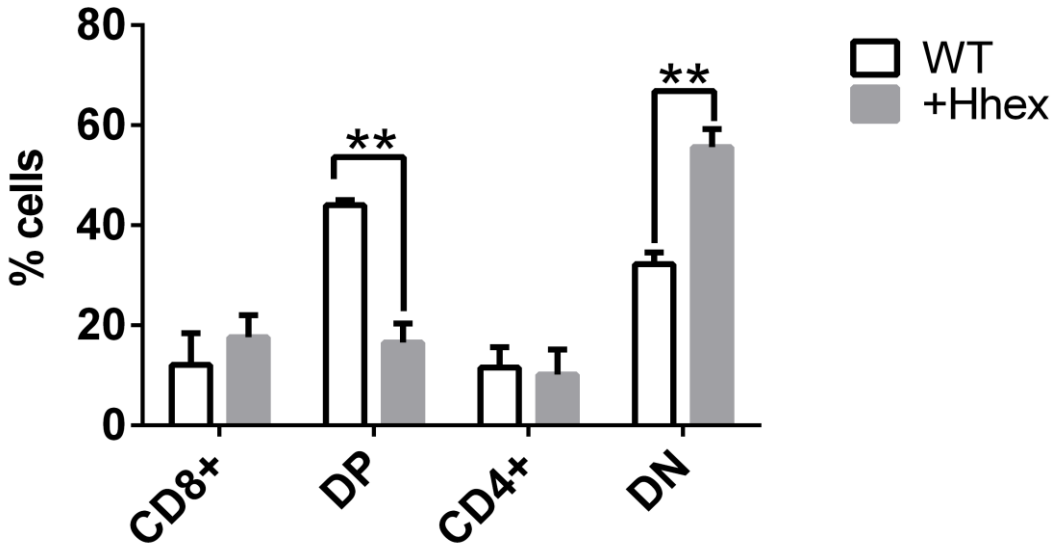

Figure 19. MIG-Hhex cells accumulate at the DN stage of differentiation.

Double negative thymocytes were transduced with either MIG-Hhex or empty vector and plated on OP9-DL1 cells in the presence of cytokines. Every 7 days cells were analyzed for CD4 and CD8 using flow cytometry. Cells transduced with retrovirus was gated on GFP and then analyzed for CD4 and CD8 expression. *, $P \leq 0.05$; **, $P \leq 0.01$; ***, $P \leq 0.001$; ****, $P \leq 0.0001$

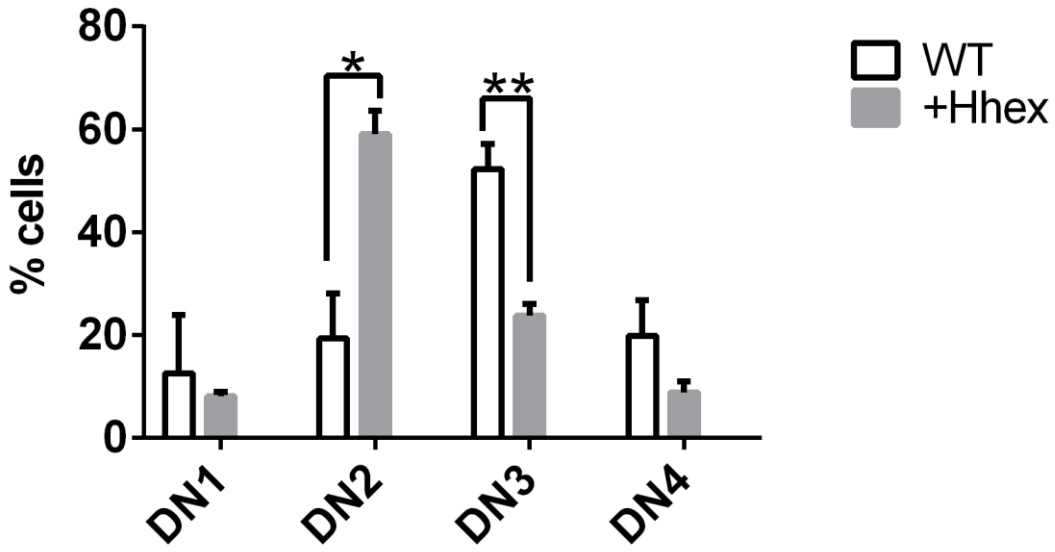

Figure 20. Enforced Hhex expression results in an accumulation of DN2 block cells.

Double negative thymocytes were subtyped, by flow cytometry, for DN1-4 using CD44 and CD25 staining. Bar graphs show percent of cells per subtype. *, P ≤ 0.05; **, P ≤ 0.01; ***, P ≤ 0.001; ****, P ≤ 0.0001

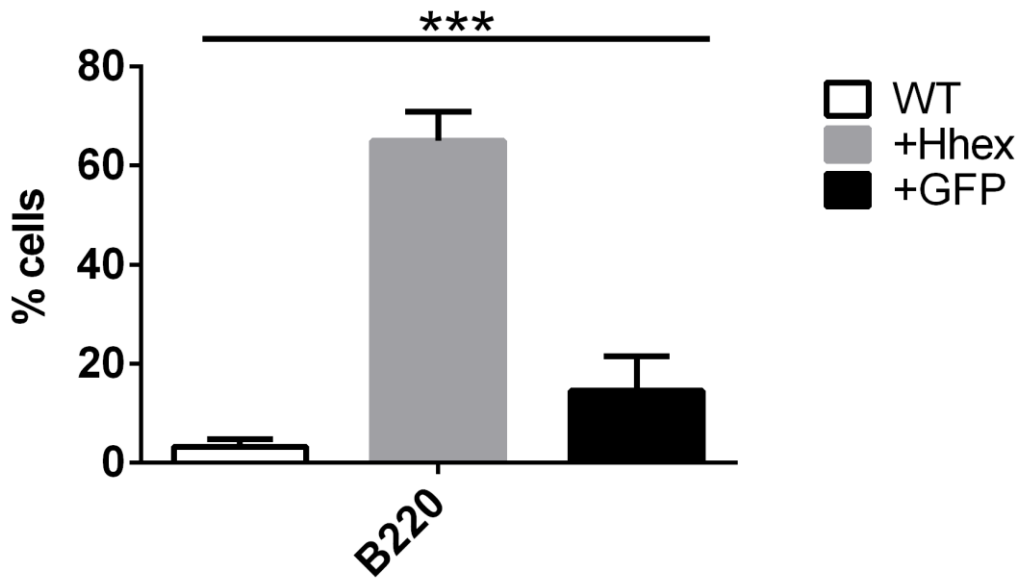

Figure 21. Hhex expression results in increased B220 expression.

Double negative thymocytes were assessed for B220 expression using flow cytometry. Bar graphs show percent of cells that were B220 positive. ***, $P \leq 0.001$;

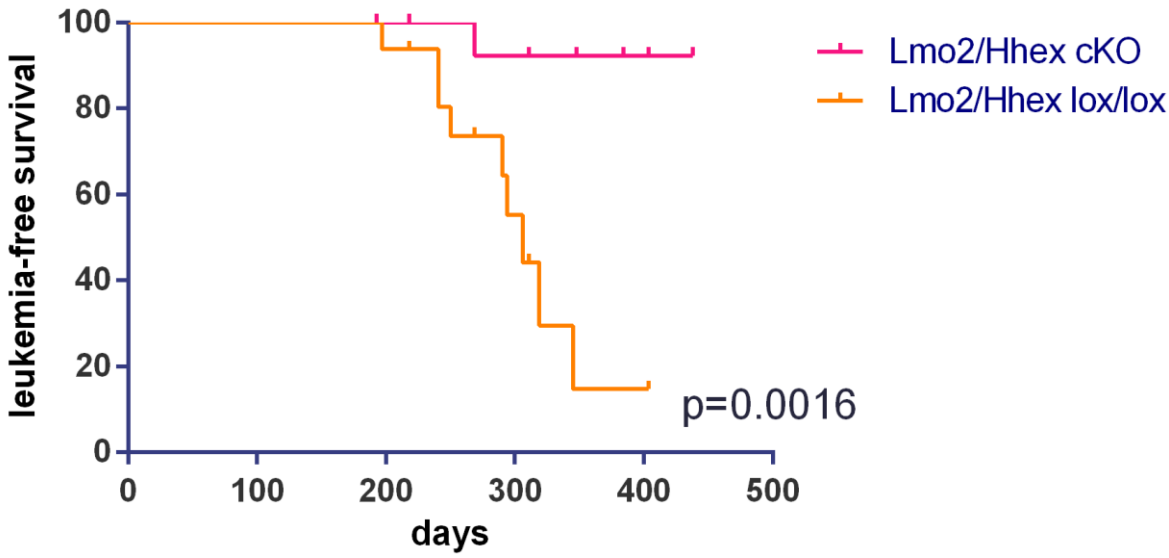

Figure 22. Loss of Hhex attenuates Lmo2 induced T-ALL.

Graph shows survival analysis of Lmo2/Hhex cKO and Lmo2/Lmo2lox/lox mice (n=16 per genotype). The median survival of Hhex lox/lox mice was 306 days. P-value represents the comparison of survival by Log-rank test.

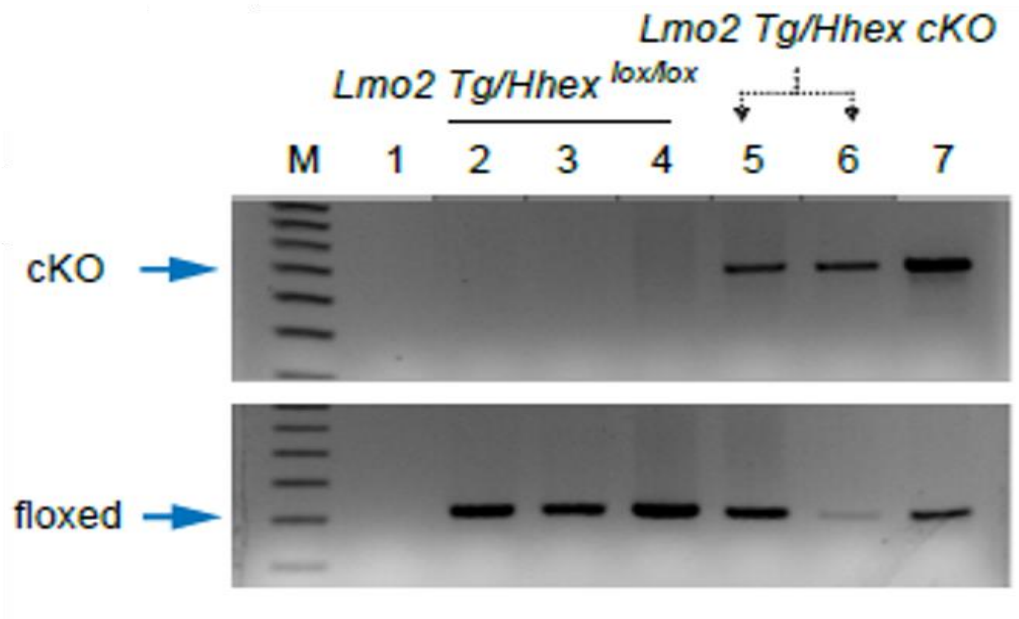

Figure 23. Genotyping of T-ALL tumors.

Genomic DNA was prepared from T-ALL thymic tumors from Lmo2/Hhexlox/lox (n=3) and Lmo2/Hhex cKO (n=2) mice.

Discussion

We demonstrated that Hhex enforced expression in thymic progenitors resulted in a differentiation block similar to Lmo2. This would suggest that Hhex may be functioning downstream of Lmo2. We showed that Hhex expressing thymocytes show impaired development at the DN2 stage of differentiation in vitro. These cells were also able to survive longer in culture than WT cells. Little is known about the mechanism by which Hhex induces T-ALL. To further understand the role Hhex is playing in vitro T-cell differentiation we will assess proliferation and quiescence of Hhex overexpressing thymocytes versus WT thymocytes using BrdU labelling and Hoechst 33342 and pyronin Y staining.

In vitro, Hhex is able to induce T-ALL after bone marrow transduction and transplant. Using various Hhex point mutations we can elucidate the structure/function mechanism behind Hhex induction of T-ALL. We predict that the DNA binding activity of Hhex will be important for T-ALL induction.

Although the mechanism for how Lmo2 leads to Hhex activation is still unknown, we found that Hhex is important for the oncogenic activity of Lmo2; as demonstrated by the difference in T-ALL latency in CD2-Lmo2 transgenic mice when Hhex was deleted versus when Hhex was expressed. This was also demonstrated by the incomplete loss of Hhex in one T-ALL developed in CD2-Lmo2; Hhex cKO mouse. Further analysis of CD2;Hhex lox/lox T-ALL cells can yield valuable information needed to understand whether Hhex is also required for the maintenance of T-ALL by using Cre to knockdown Hhex in these tumor cells. We predict that Hhex is also required to maintain Lmo2-induced T-ALL

therefore knockdown of Hhex in these tumor cell lines will result in the inability of these cells to proliferate similarly to their parental counterparts.

CHAPTER V

Hhex is required for B cell development

Background and Significance

Hematopoietically expressed homeobox protein (Hex or Hhex), also known as proline- rich homeodomain (PRH) protein is a transcription factor that contains a well characterized DNA binding homeodomain. Hhex has both repressive and activating effects on transcription via direct and indirect mechanisms[53,54,58-66]. Hhex is a transcription factor that has an important role in embryonic development and hematopoiesis[54,64,26]. Hhex regulates embryonic development transcriptionally and post transcriptionally [64] and is important for cell proliferation. Hhex can directly bind to the promoter sites and intronic regions of genes and cause transcriptional repression by recruitment of Groucho/TLE family co-repressor proteins[54]. Hhex may also repress transcription by competing with TATA Binding Protein (TBP) at TATA boxes[64]. Hhex can activate transcription by directly binding to promoters and forming complexes with other DNA binding proteins to activate transcription such as at the NTCP promoter[56,57].

The role of Hhex in specific hematological malignancies has been previously studied. *Hhex* is a common integration site in retroviral insertional mutagenesis studies and it induces T-ALL in bone marrow transduction and transplantation mouse models[71]. HHEX is hypothesized to be a tumor suppressor gene in acute myeloid leukemia (AML) based on an unusual post-transcriptional regulation by repressing mRNA transport and translation of CCND1 by disrupting the activity of the eukaryotic initiation factor 4E (eIF-4E)[73].

Data from the Immunological Genome Project revealed that Hhex expression is

observed in many hematopoietic lineages. Hhex expression is highest in hematopoietic stem and progenitor, myeloid and developing B cells. Hhex expression is also high in ETP cells and double negative T-cell progenitors but is not expressed in subsequent T-cell differentiation stages. Knockout of Hhex results in embryonic lethality at embryonic stage E10.5[67,68]. Due to embryonic lethality, little is known about the role of Hhex in normal adult hematopoiesis. To study the role of Hhex in adult hematopoiesis, we created *Hhex cKO* mice and characterized the role of Hhex in normal adult hematopoiesis. Using flow cytometry we quantified lymphoid and myeloid mature lineages.

Results

Hhex conditional knockout mice show reduced bone marrow and splenic cellularity

In order to study the role of Hhex in adult hematopoiesis we created *Hhex cKO* mice by crossing mice with lox P sites flanking *Hhex* exons 2-4 (Hhex $^{lox/lox}$) to Vav-iCre transgenic mice. When *Vav-iCre* mice are bred to mice containing lox P sites flanking a gene of interest, Cre-mediated recombination results in the deletion of the gene in the entire hematopoietic compartment of the offspring[144,145]. Deletion via Cre-mediated recombination occurs around E12.5; which is consistent with *vav* itself being undetectable prior to E11.5[146,147]. These *Hhex cKO* mice were viable and born in normal litter sizes. PCR analysis of genomic DNA taken from bone marrow, spleen and thymus revealed highly

efficient knockout of the Hhex gene, with no presence of the floxed alleles (Figure 24). Peripheral blood counts were performed on WT and *Hhex cKO* mice.

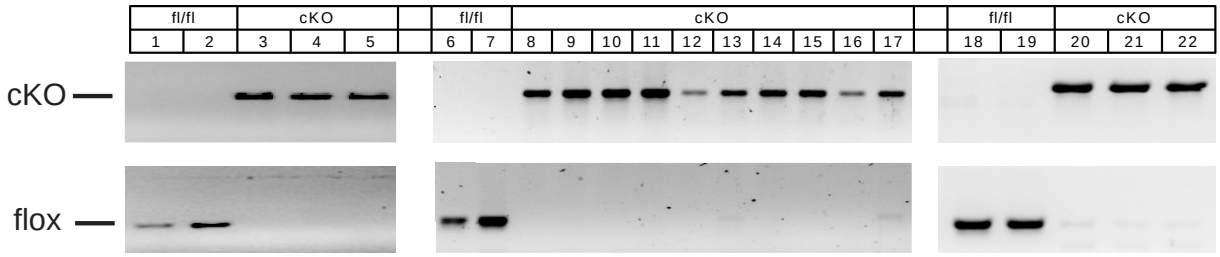

Figure 24. Knockout efficiency in Hhex cKO mice.

PCR genotyping of bone marrow, spleen and thymus cells taken from *WT* and *Hhex cKO* mice. Genotyping for splenocytes was carried out in both B220+(lanes 6,8,10,12,14,and 16) and B220-(lanes 7,9,11,13,15,and 17) splenocytes.

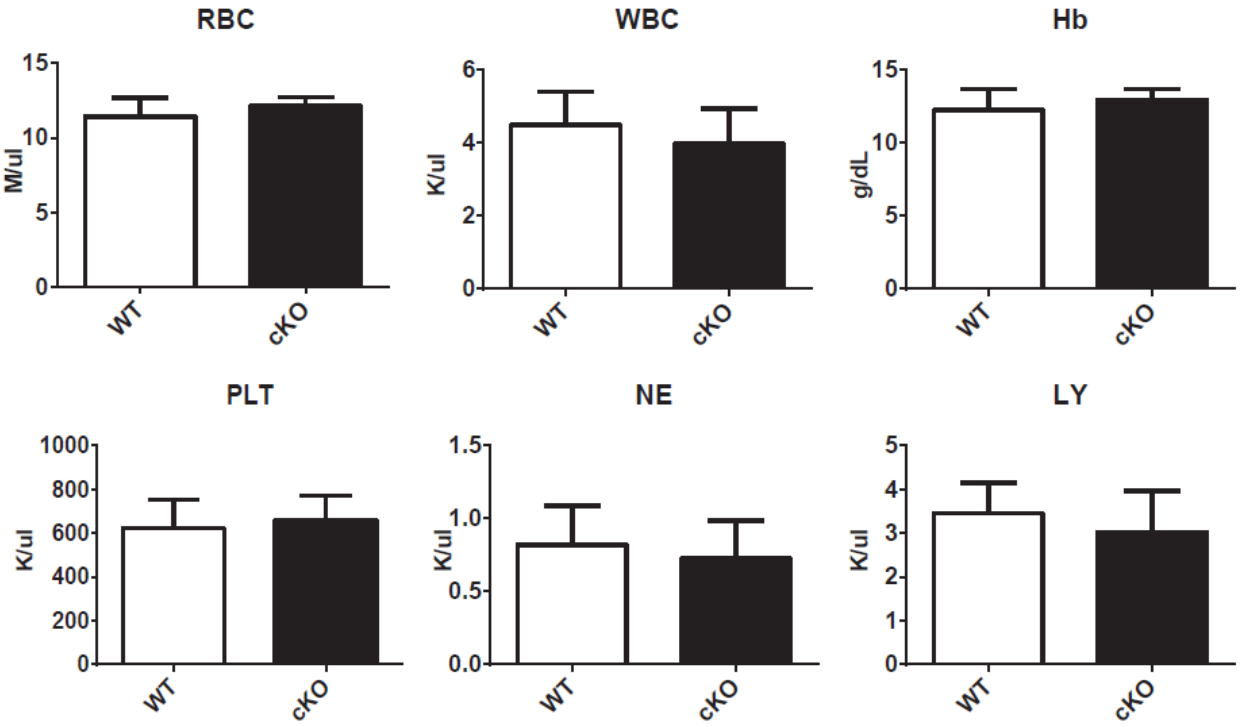

Figure 25. Hhex cKO mice show normal blood counts at steady state.

Peripheral blood cells and hemoglobin were analyzed by an automated Hemavet (cell counter) machine for WT (n=5) and Hhex cKO (n=6) mice at steady state. Bar graphs show the means ± SEM for RBC, red blood cells; WBC, white blood cells; Hb, Hemoglobin; PLT, platelets; NE, neutrophils; and, LY, lymphocytes. White bars are WT and black bars are Hhex cKO samples.

We determined that *Hhex cKO* mice had normal peripheral blood counts (Figure 25). Next we investigated total cellularity of the bone marrow, spleen and thymus of Hhex cKO mice. We found that while Hhex cKO mice showed normal cellularity in their thymi, there was a significant reduction in bone marrow and spleen cellularity; this defect in cellularity was seen in both young and adult Hhex cKO mice (Figure 26).

Hhex cKO mice have markedly reduced numbers of B cells

Flow cytometry analysis using lineage specific antibodies confirmed all hematopoietic lineages were present in *Hhex cKO* mice (Figure 27, Figure 28, and Figure 29), but there was a significant reduction in B cells in both the bone marrow and the spleen (Figure 30). Gross dissection of the spleen revealed that *Hhex cKO* mice had smaller spleens with distorted architecture (Figure 31). Immunohistochemical staining revealed that the spleens of *Hhex cKO* mice had T cells (CD3+) but significantly reduced B cells (B220+) (Figure 31).

Next, we wanted to determine at what stage of B-cell development Hhex was necessary. We used flow cytometry to analyze immature and mature B-cell subsets of the bone marrow and the spleen using previously described B cell markers (Figure 32 and Figure 33). Hhex cKO mice had reduced numbers at all stages of B-cell differentiation from as early as the pro-B stage to as late as the recirculating B cell (Figure 34). We quantified the IL7R on pro-B cells and showed significantly reduced levels in *Hhex cKO* mice compared to WT mice. This was expected because the number of pro-B cells were markedly reduced; however, the mean fluorescent intensity was significantly higher in Hhex cKO

pro-B cells compared to WT (Figure 35). This would suggest that these pro-B cells may have more IL7R molecules on their surface when compared to WT. We then looked at V-D-J recombination in splenic B220+ and B220- cells (Figure 36).

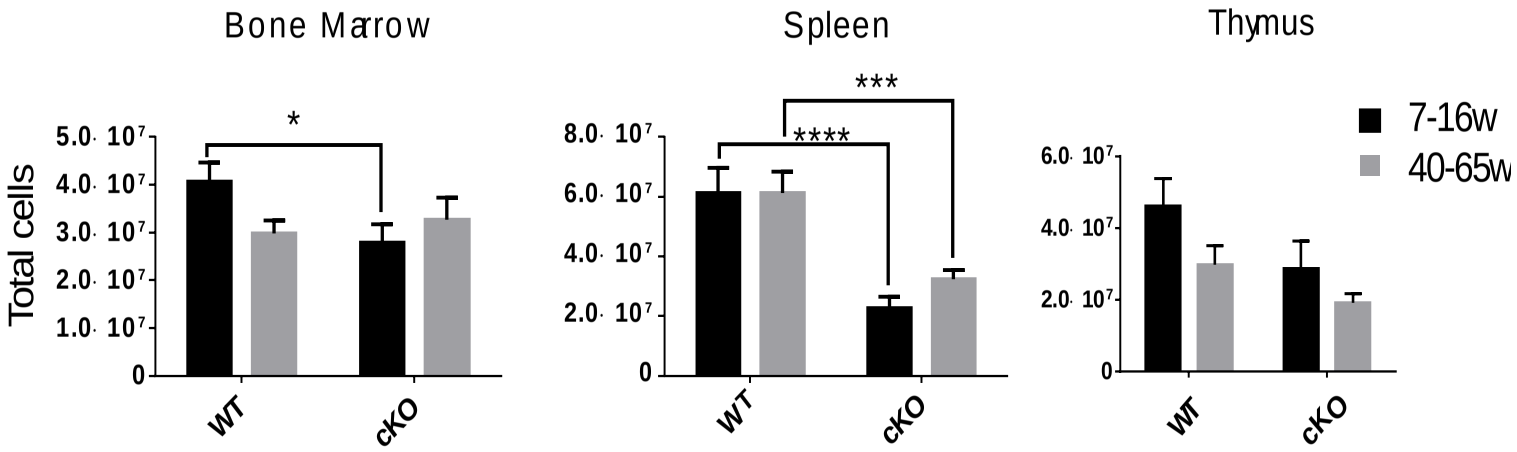

Figure 26. Hhex cKO mice show reduced cellularity in their bone marrow and spleens.

Total cellularity was determined by counting the live cells. Bone marrow (femurs and tibiae), splenic and thymic cellularity of WT and Hhex cKO mice between 7-16 weeks and 40-65 weeks. Bone marrow (WT 7-16wks, n=22; WT 40-65wks, n=12; cKO 7-16 wks, n=21; cKO 40-65 wks, n=12). Spleen (WT 7-16wks, n=20; WT 40-65wks, n=11; cKO 7-16 wks, n=22; cKO 40-65 wks, n=11). Thymus (WT 7-16wks, n=11; WT 40-65wks, n=11; cKO 7-16 wks, n=11; cKO 40-65 wks, n=11). Bar graphs are means ± SEM, n=11. *, $P \leq 0.05$; **, $P \leq 0.01$; ***, $P \leq 0.001$; ****, $P \leq 0.0001$.

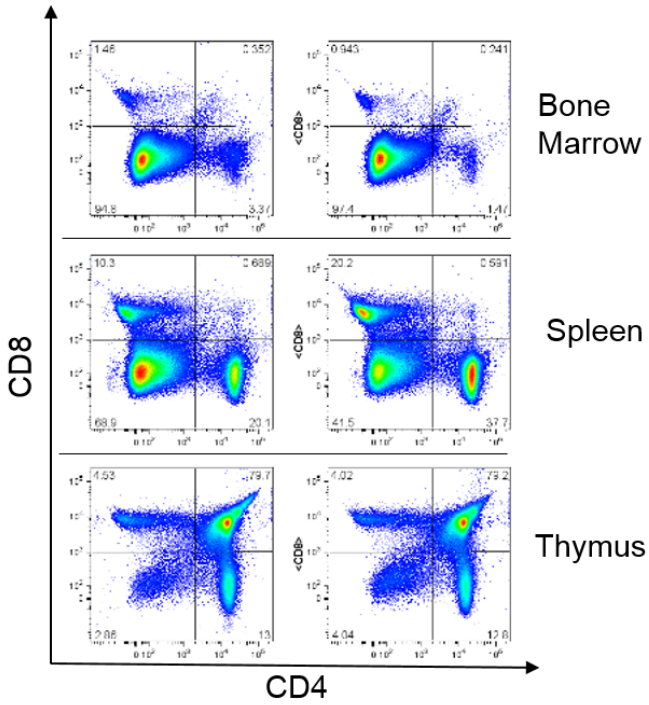
CD8
CD4
Bone Marrow
Spleen
Thymus

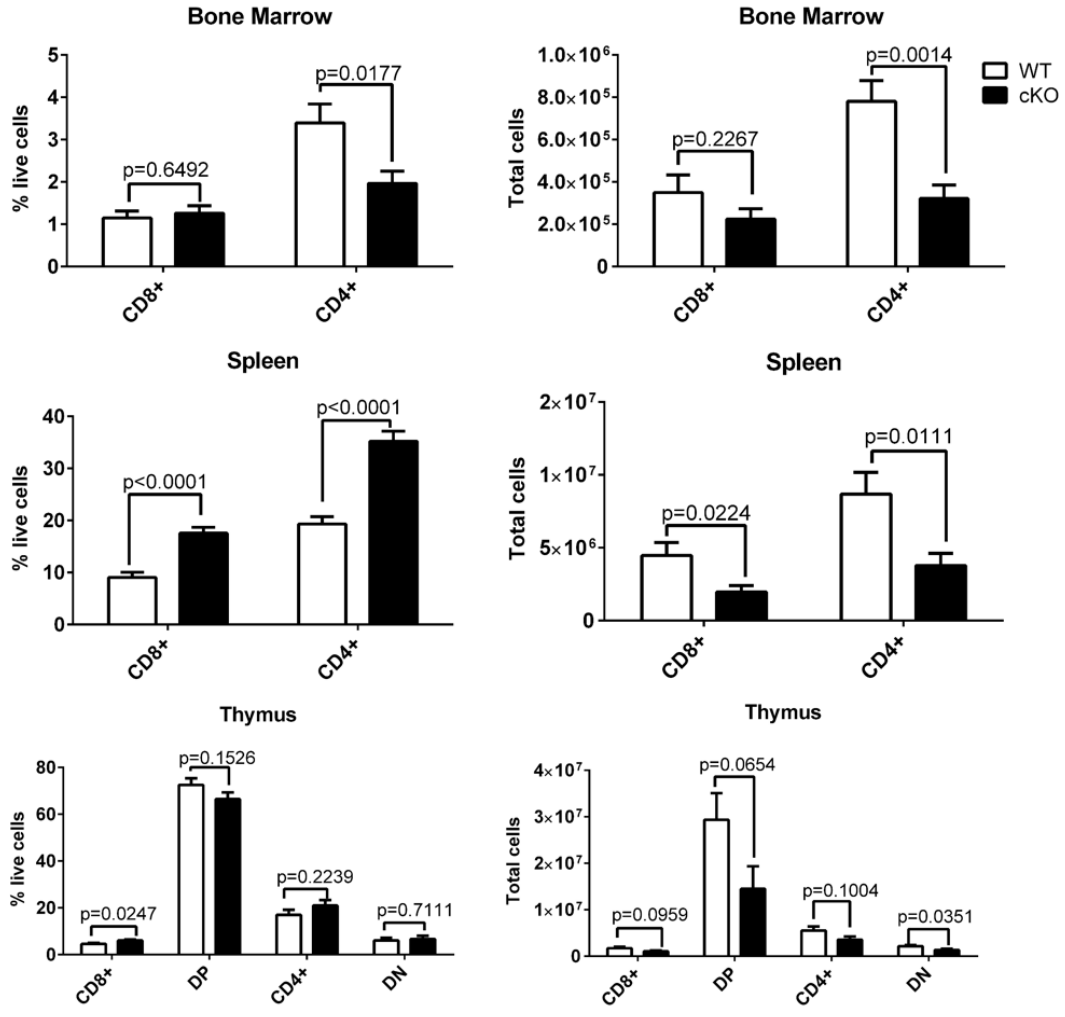
Bone Marrow
% live cells
p=0.6492
p=0.0177
CD8+
CD4+
Bone Marrow
Total cells
p=0.2267
p=0.0014
WT
cKO
Spleen
% live cells
p<0.0001
p<0.0001
Spleen
Total cells
p=0.0224
p=0.0111
Thymus
% live cells
p=0.0247
p=0.1526
p=0.2239
p=0.7111
CD8+
DP
CD4+
DN
Thymus
Total cells
p=0.0959
p=0.0654
p=0.1004
p=0.0351

Figure 27. Comparison of T cells in WT and Hhex cKO mice.

Representative flow cytometry plots are shown for CD4 and CD8 stained cells in the bone marrow, spleens and thymi isolated from WT and *Hhex cKO* mice. The bottom panels shows bar graphs representing the proportions and absolute numbers of each T-cell population. Total cells were calculated based on the total number of cells multiplied by the percentage of each population and represented as mean ± SEM, n=9-10 for WT and cKO. P-values were generated by student's t-test.

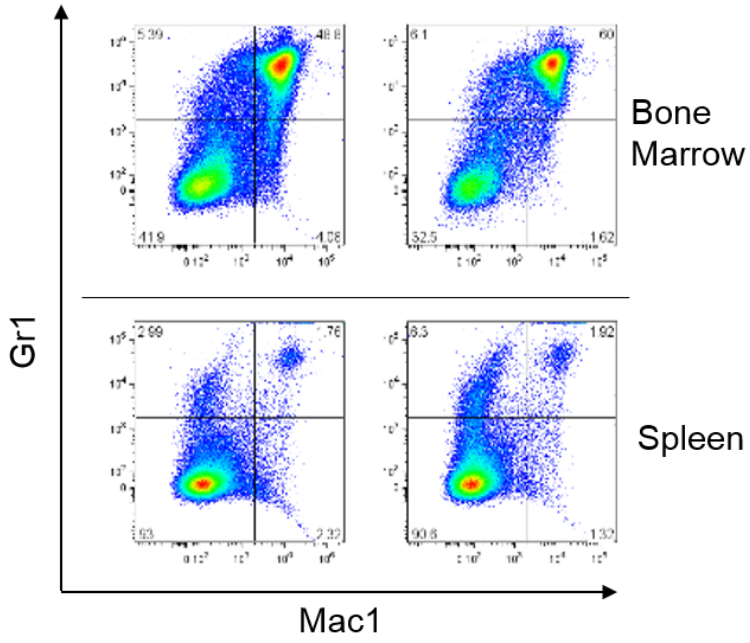
Gr1
Mac1
Bone Marrow
Spleen

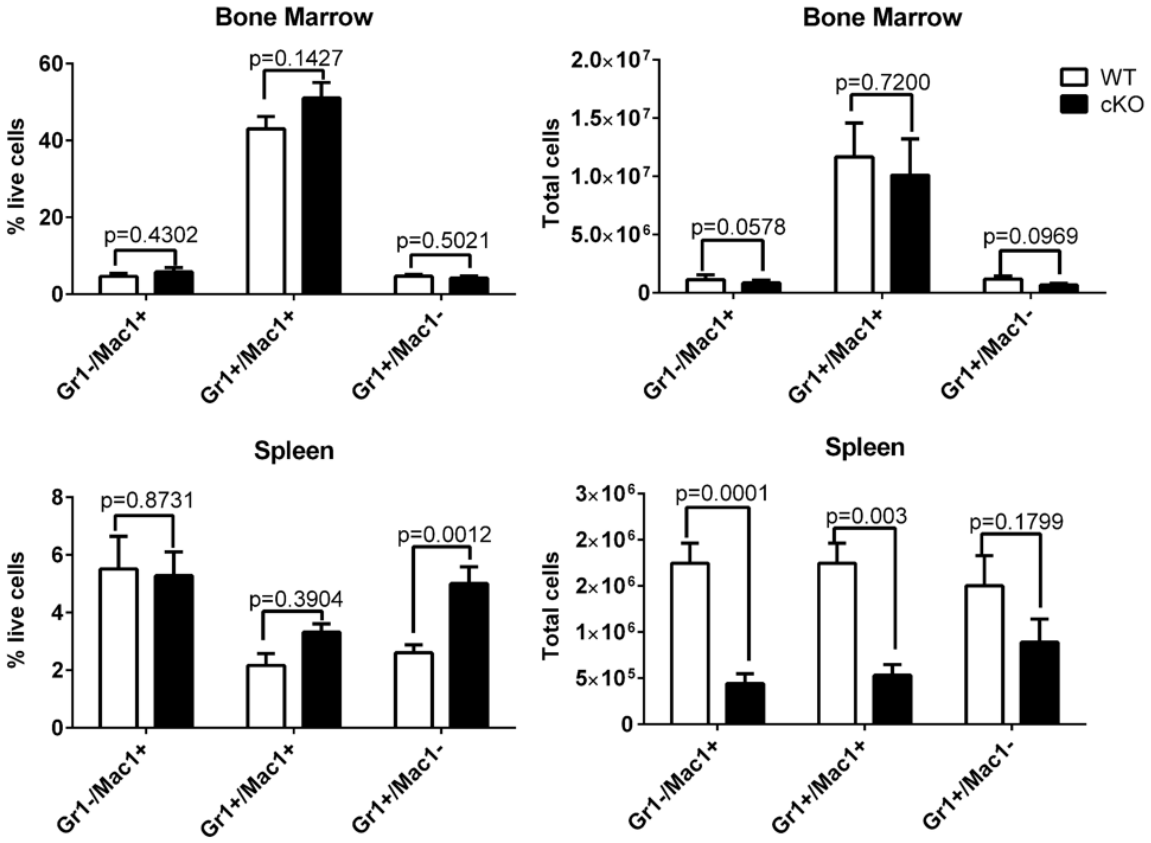
Bone Marrow
% live cells
p=0.4302
p=0.1427
p=0.5021
Gr1-/Mac1+
Gr1+/Mac1+
Gr1+/Mac1-
Bone Marrow
Total cells
WT
cKO
p=0.0578
p=0.7200
p=0.0969
Spleen
% live cells
p=0.8731
p=0.3904
p=0.0012
Spleen
Total cells
p=0.0001
p=0.003
p=0.1799

Figure 28. Comparison of macrophages and granulocytes in WT and Hhex cKO mice.

Representative flow cytometry plots for Mac-1 (or CD11b) and Gr-1 are shown for stained cells from the bone marrow and spleen of WT and Hhex cKO mice. Bar graphs show the proportions and absolute number of each myeloid population in the bone marrow, and spleen. Total cells were calculated based on the total number of cells multiplied by the percentage of each population and represented as means ± SEM, n=9-10. P-values were generated by student t-test.

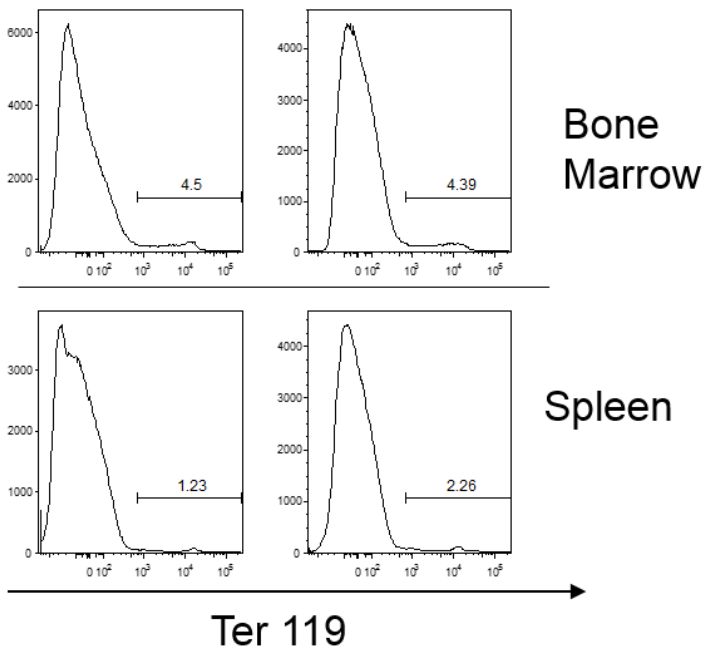
4.5
4.39
Bone Marrow
1.23
2.26
Spleen
Ter 119

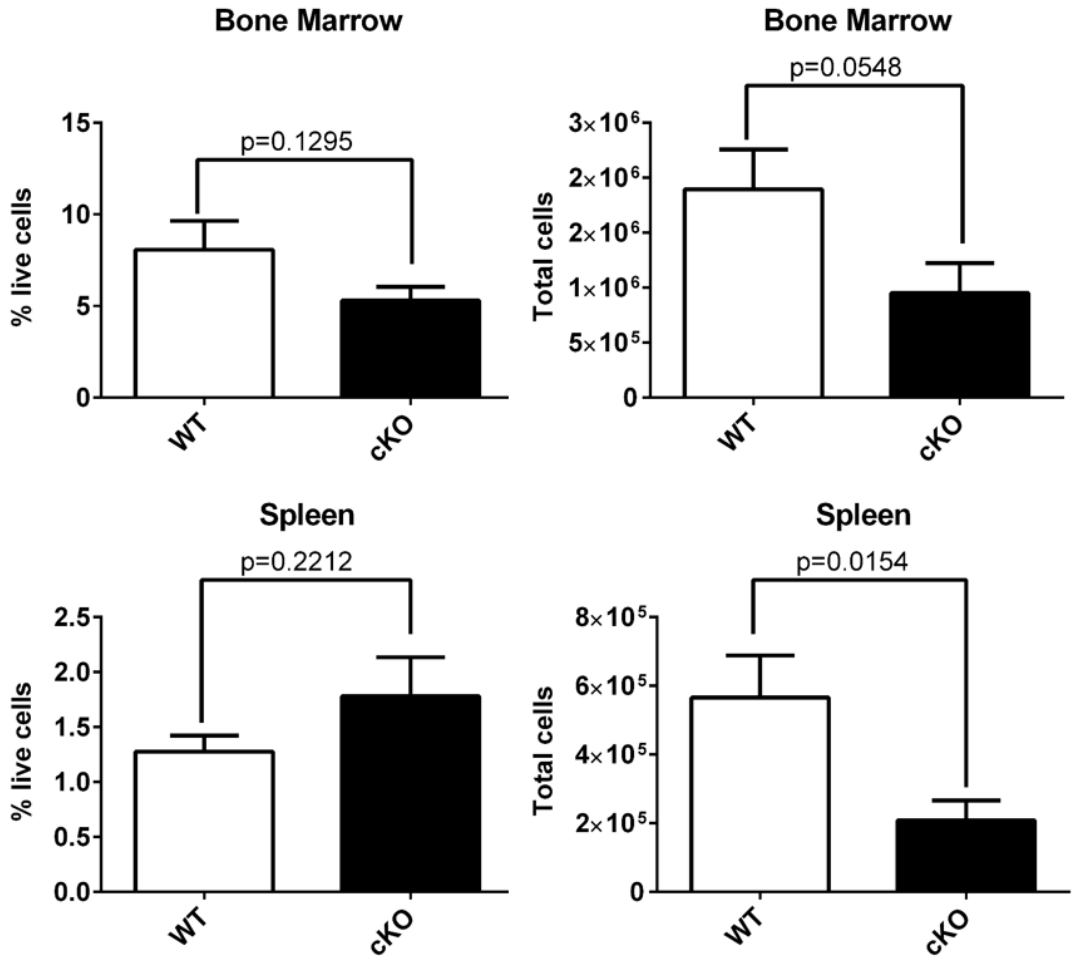
Bone Marrow
p=0.1295
% live cells
WT
cKO
Bone Marrow
p=0.0548
Total cells
Spleen
p=0.2212
% live cells
Spleen
p=0.0154
Total cells

Figure 29. Comparison of erythroid progenitors in WT and Hhex cKO mice. Histograms show flow cytometry analysis for Ter119 staining done on bone marrow and spleen cells isolated from WT and *Hhex cKO* mice. Bar graphs show the proportion and absolute number of erythroid cells in the bone marrow and spleen. Total cells were calculated based on the total number of cells multiplied by the percentage of each population and represented as means ±

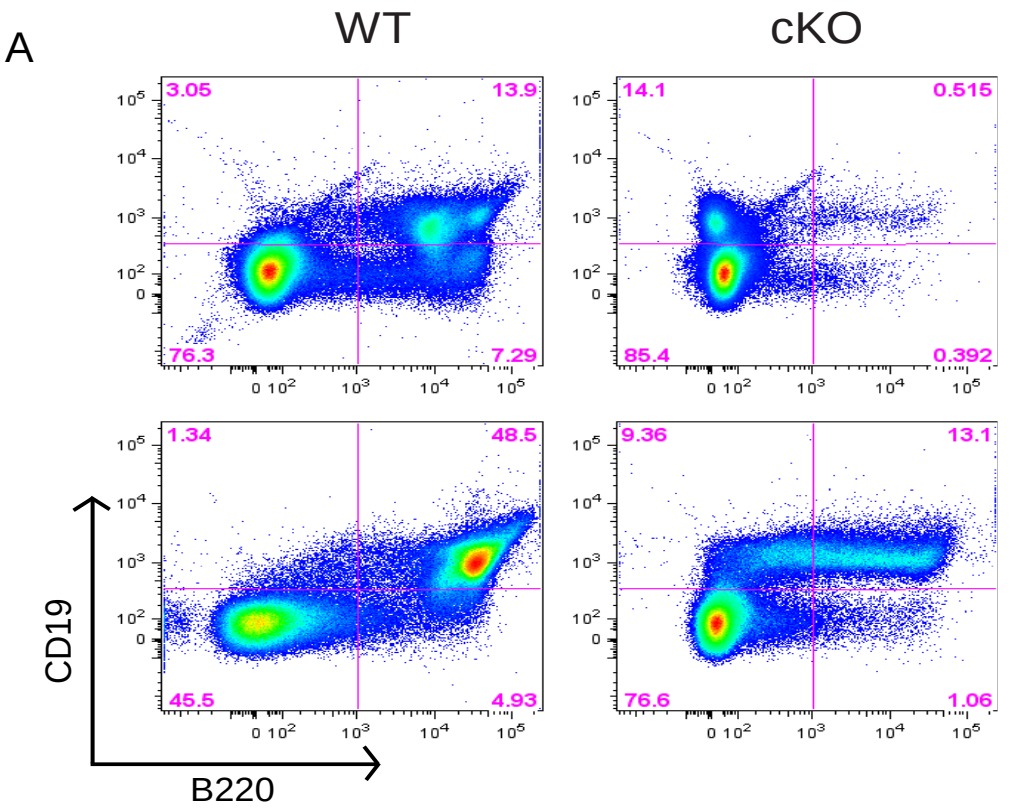
A
WT
cKO
3.05
13.9
76.3
7.29
14.1
0.515
85.4
0.392
1.34
48.5
45.5
4.93
9.36
13.1
76.6
1.06
CD19
B220

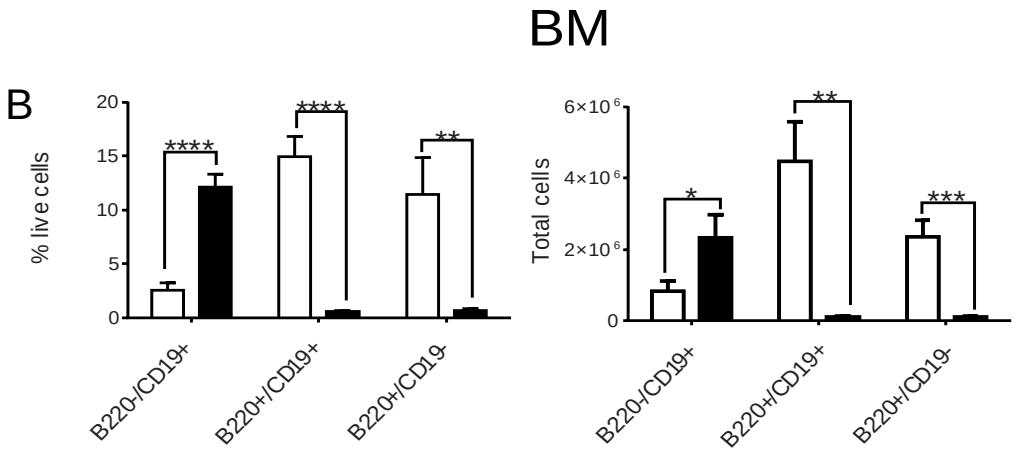
BM
B
% live cells
Total cells
B220-/CD19+
B220+/CD19+
B220+/CD19-

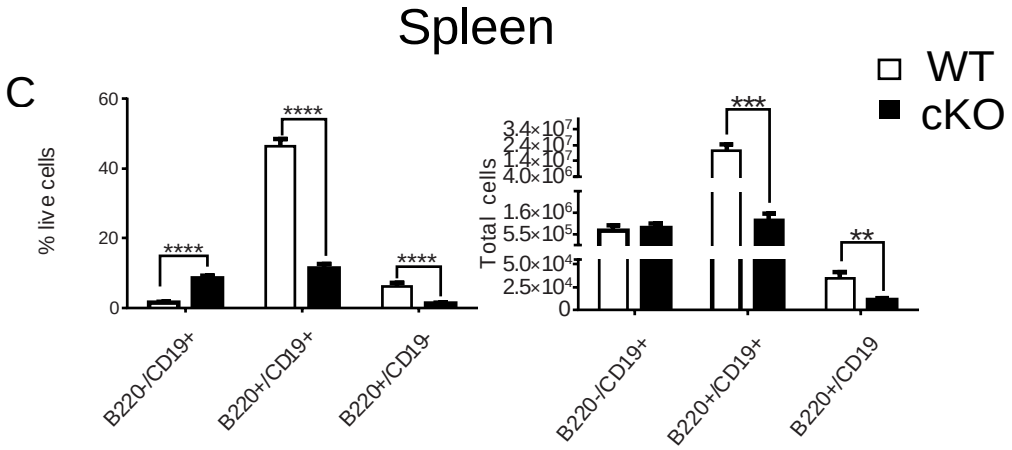
Spleen
C
WT
cKO
% live cells
Total cells
B220-/CD19+
B220+/CD19+
B220+/CD19-

Figure 30. Loss of Hhex results in B-cell defects.

(A) Representative FACS plots for B220 and CD19 for bone marrow and spleen cells isolated from WT and *Hhex cKO* mice. (B) Bar graphs show mean (± SEM, n=9) proportions (% live cells) and absolute numbers of B cells in the bone marrow. Absolute numbers were calculated based on the total number of cells multiplied by the percentage of each population. (C) Bar graphs show mean (± SEM, n=8) proportions (% live cells) and absolute numbers of B cells in the bone marrow. Calculation was same as for BM.

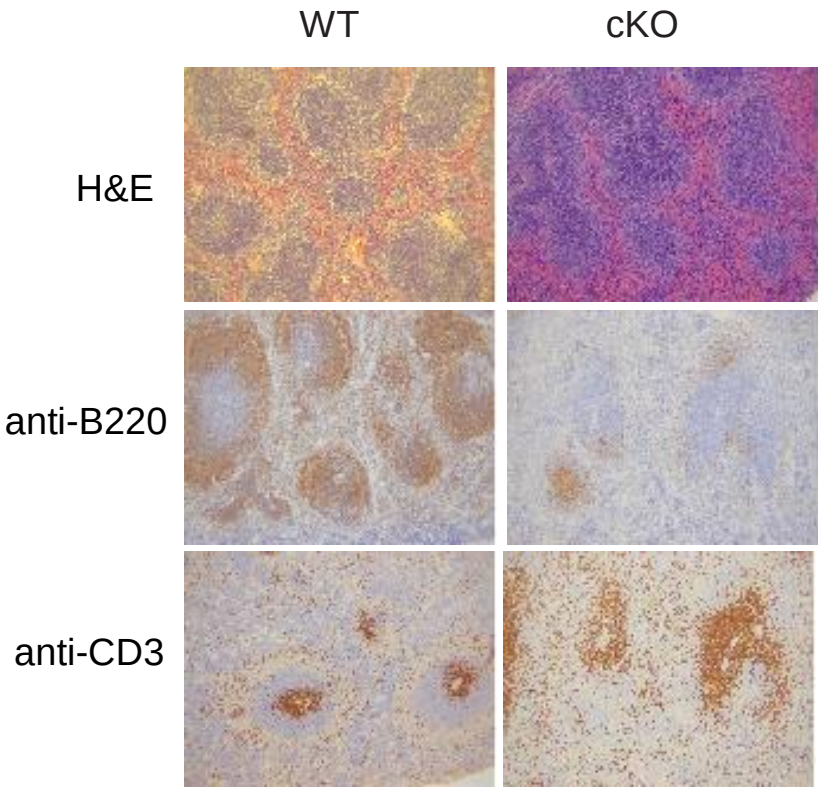

Figure 31. Immunohistochemical analysis of spleens.

Sections were stained with H&E (hematoxylin and eosin), anti-B220 or anti-CD3 antibodies.

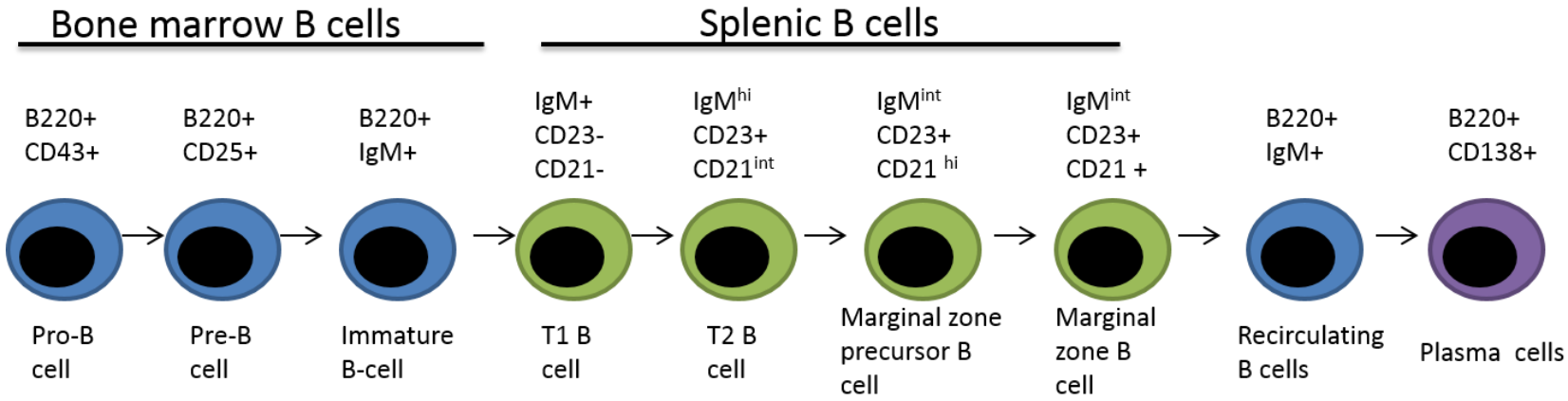

Figure 32. B cell development schematic.

B cells at various stages of differentiation can be identified and purified using various cell surface markers.

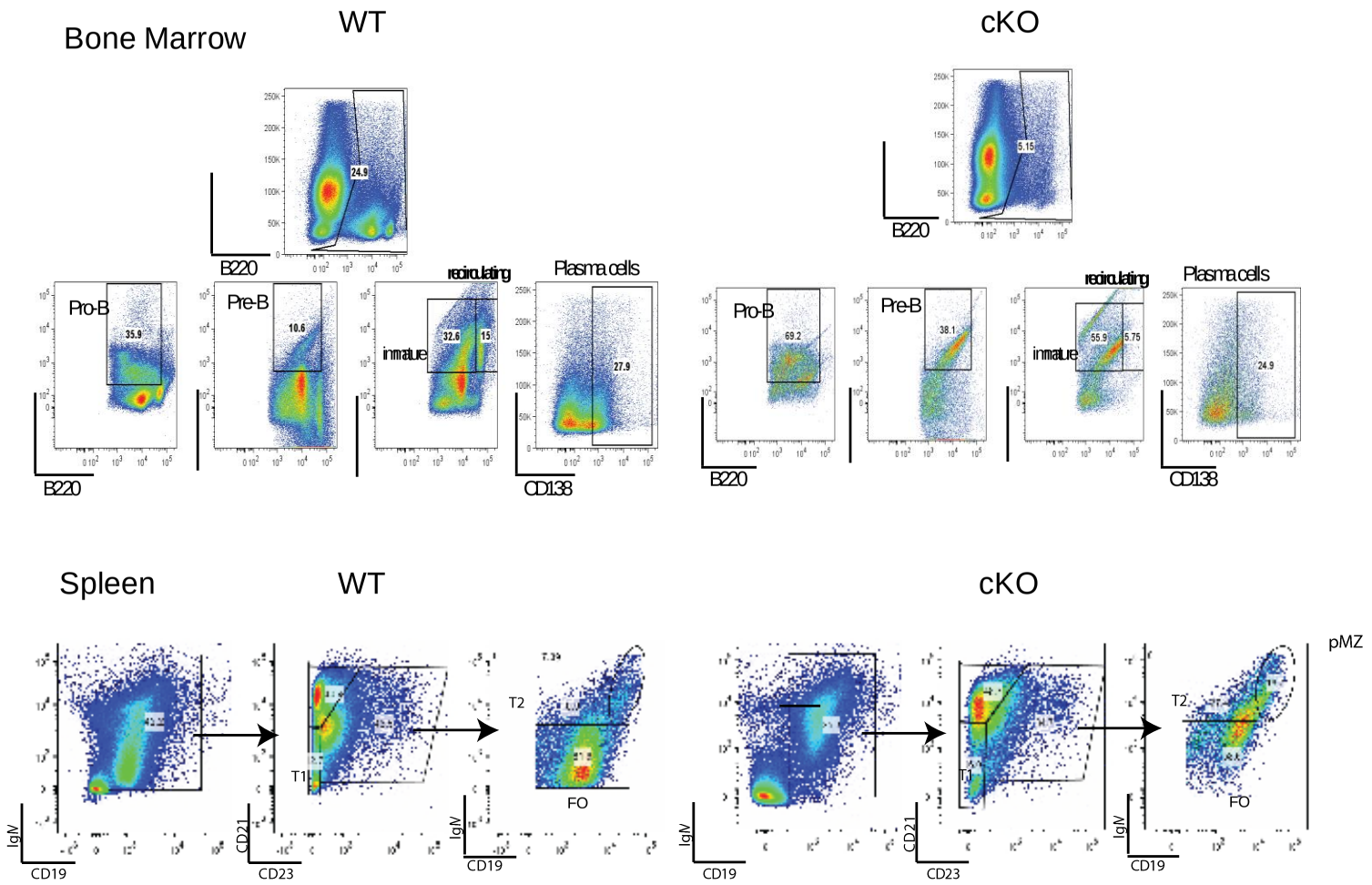

Figure 33. Gating schemes for B-cell subsets.

Representative flow plots of B-cell subsets of the bone marrow and the spleen of WT and *Hhex* cKO mice.

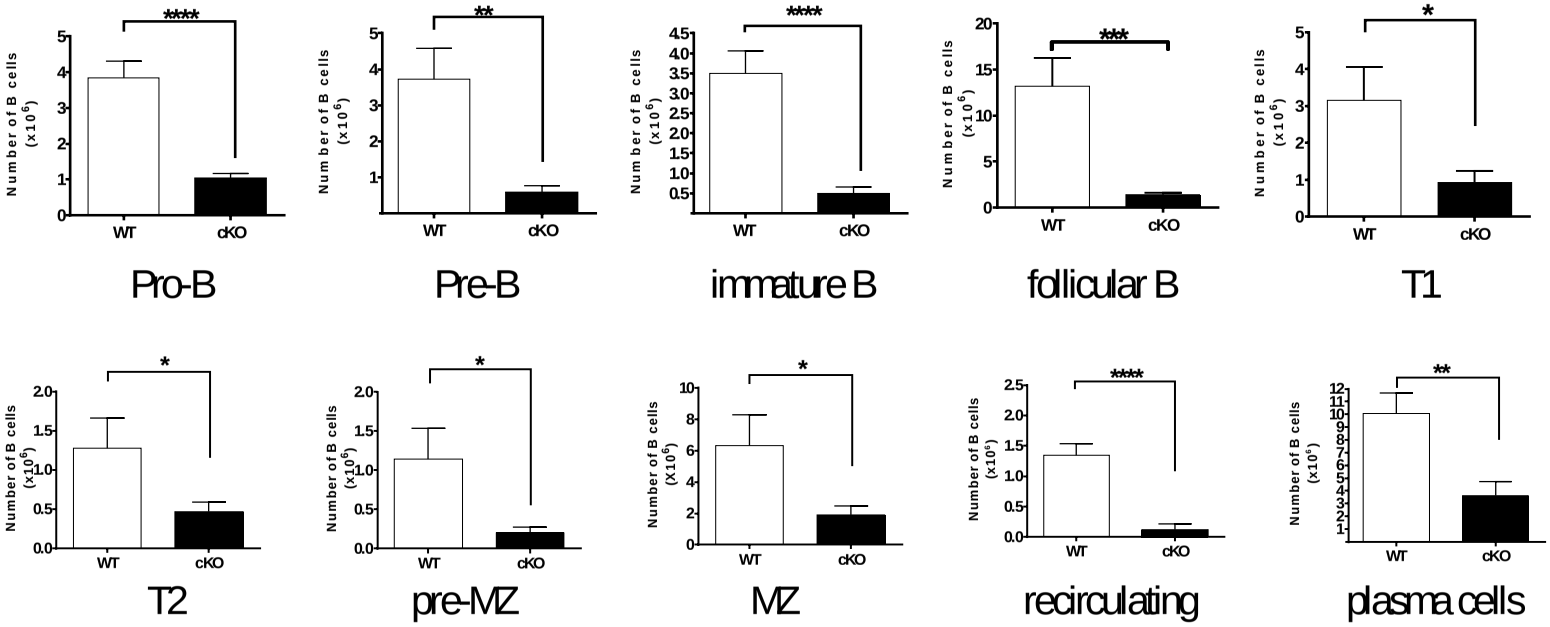

Figure 34. Hhex cKO mice show defect in all B cell subsets.

Bar graphs representing the mean size of B cell subset in the bone marrow and spleen of WT and Hhex cKO mice. Values are means ± SEM, WT; n=10 and Hhex cKO; n=9. Two-tailed Student's t tests were applied to determine the statistical significance. *, P ≤ 0.05; **, P ≤ 0.01; ***, P ≤ 0.001; ****, P ≤ 0.0001. Mice in these experiments were between 7-16 weeks old.

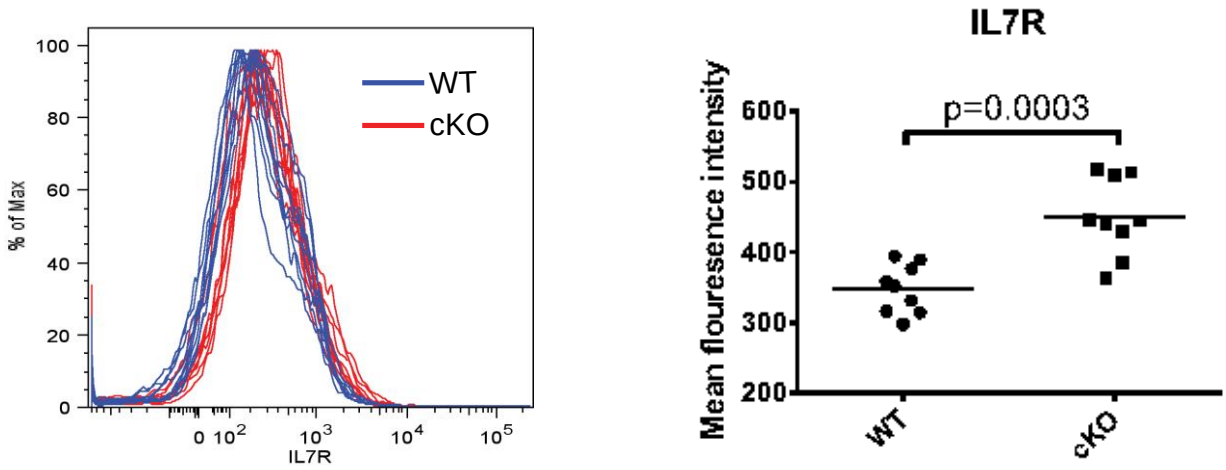

Figure 35. Mean fluorescent intensity of IL7R on pro B cells.

Histogram depicting the mean fluorescence intensity (MFI) of IL7R staining in the bone marrow of WT and *Hhex* cKO mice. Graph representing MFI of IL7R in bone marrow of WT and *Hhex* cKO mice. Bars represent mean of n=9. P value was generated by Student t test.

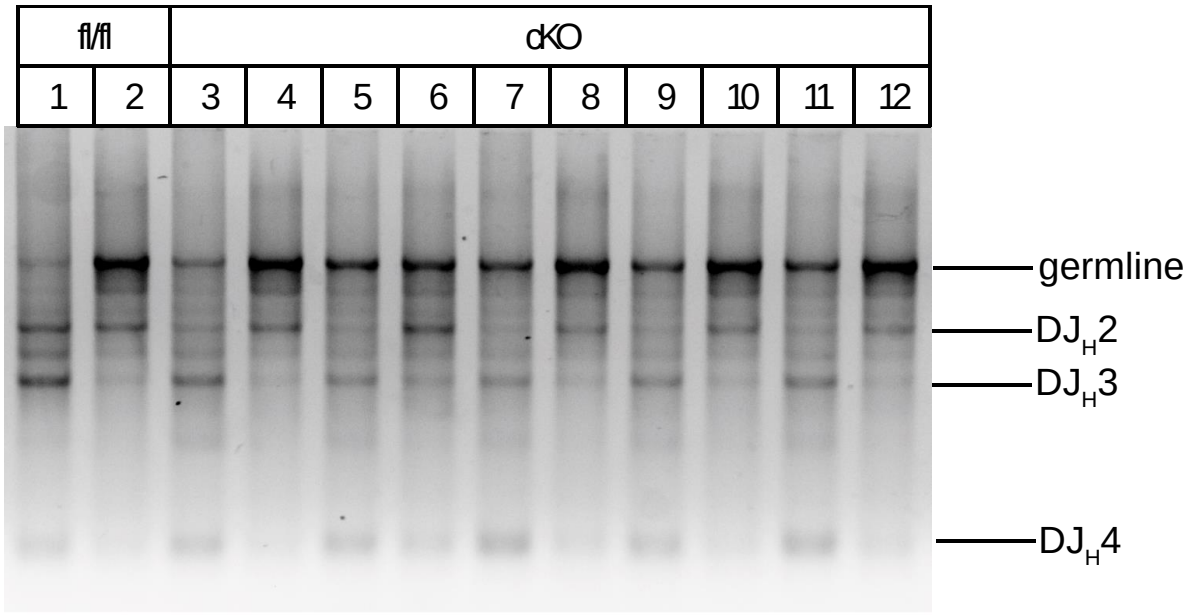

Figure 36. IgH recombination in splenic cells.

Nested PCR analysis of DJ recombination was used to amplify four possible junctions between D-Q25 and JH regions from genomic DNA. IgH rearrangement was analyzed in $B220^{+}$ (odd lanes) and $B220^{-}$ (even lanes) sorted splenocytes from WT and *Hhex* cKO mice. Both *Hhex cKO* and WT gDNA showed the same pattern of DJ recombination.

While V-D-J recombination occurs in Hhex cKO cells, the bands were fainter than WT which may be due to fewer cKO cells. These data suggest that Hhex cKO mice are able to produce major B cells but at numbers well below WT mice.

To further determine at what stage is Hhex important for B cell development we performed an OP9-GFP assay to differentiate lineage$^-$ sca1$^+$ c-kit$^+$ (LSKs) cells to B cells in vitro. We found that LSKs plated on OP9-GFPs had a proliferation defect when compared to WT cells (Figure 37A). Flow cytometry analysis, looking at the B cell markers CD19 and B220, one week post plating revealed that Hhex cKO LSKs were also unable to differentiate into B cells in vitro (Figure 37B). Next, we used flow cytometry to determine whether Hhex cKO LSKs were differentiating to myeloid cells instead by assessing the antigens Gr1 and Mac1. We were able to determine that there were no more myeloid cells present in Hhex cKO cultures when compared to WT cultures (Figure 37C). While there was less proliferation in Hhex cKO cultures, surprisingly, Hhex cKO cultures did not show an increase in cell death (Figure 37D). RNA-seq analysis was carried out on samples prior to plating and one week post plating and we found that WT cells turned on a B-cell specific transcriptional program, consisting of genes such *as Blk, Cd19, Ebf1, Vpreb1-3 and Clec7a*, while Hhex cKO cells were unable to upregulate these same genes (Figure 38). Taken together, these data suggest that Hhex is important for the earliest stages of B cell development.

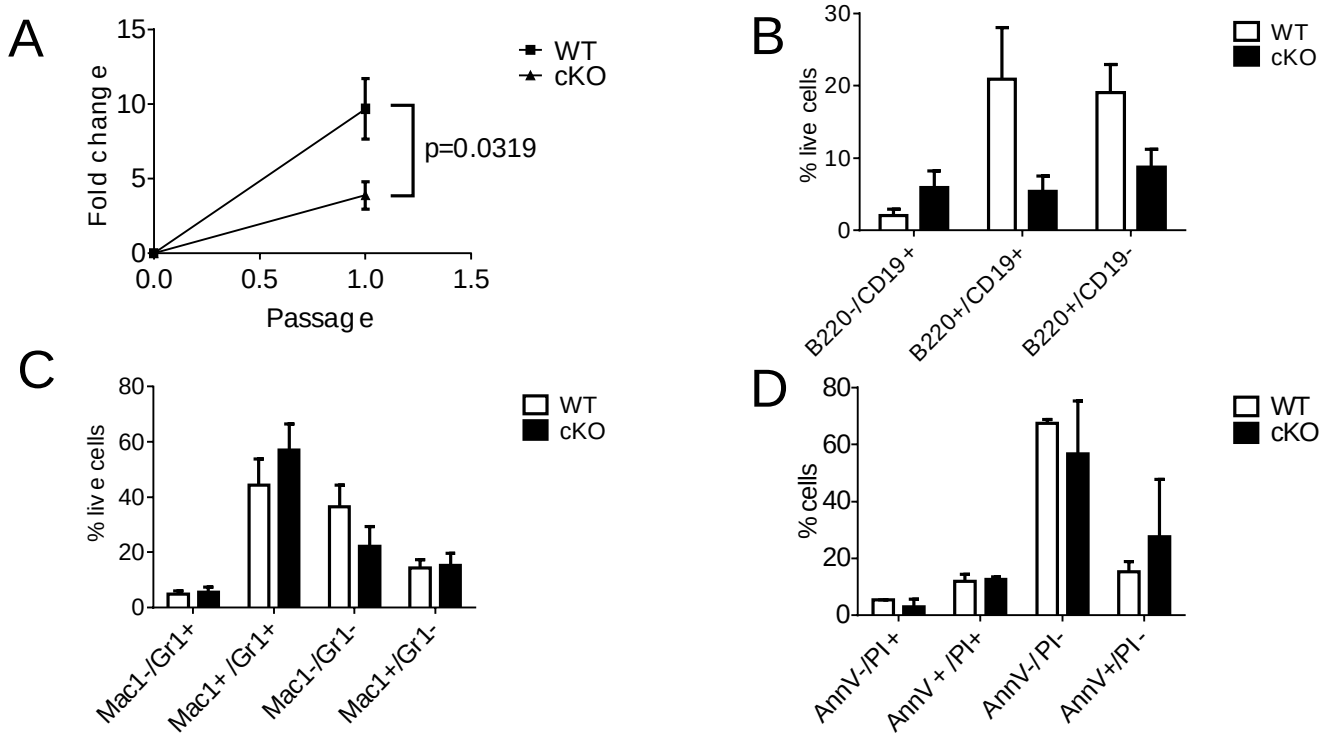

Figure 37. Hhex LSKs are unable to proliferate and differentiate.

(A) Graph shows fold change versus passage number for WT and *Hhex* cKO cells plated on irradiated OP9-GFP stromal cells. (B) 7 days after the initiation of culture, the remaining cells were stained for B220 and CD19. Bar graphs represent percentage of B cell populations. Values are means ± SEM. (C) 7 days after the initiation of culture, the remaining cells were stained for CD11b and Gr1. Bar graphs represent myeloid populations. Values are means ± SEM. (D) Apoptosis was measured by flow cytometry 7 days after the initiation of culture, using Annexin V and PI. Bar graphs represent percentage of populations. Values are means ± SEM.

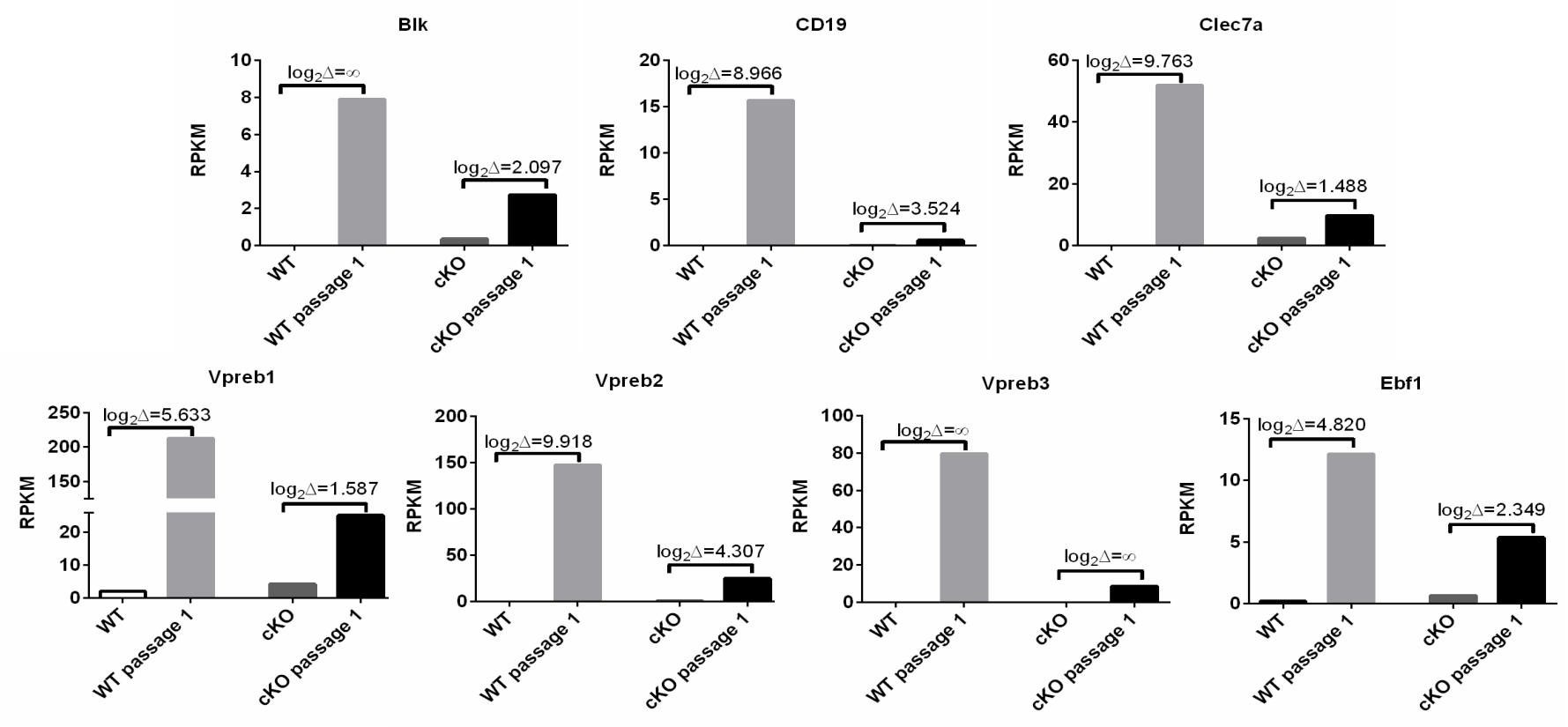

Figure 38. Gene expression analysis reveals defect in B-cell program activation in Hhex cKO cells.

RNA-seq analysis of LSK cells after enrichment from bone marrow and at passage 1 (7 days of co-culture with OP9 cells).

Discussion

Our data show a defect in bone marrow and splenic development in *Hhex cKO* mice. Further dissection of these organs revealed a profound defect in B cell development. Our data show that loss of *Hhex* results in impaired B-cell development in the bone marrow and spleen of *Hhex cKO* mice. Hhex cKO mice have markedly reduced absolute numbers of the earliest B-cell progenitors, pro-B cells. This would suggest a defect in B-cell commitment. The data obtained from the in vitro OP9 assay were consistent with our in vivo assay, by demonstrating an impaired proliferation and commitment of LSK cells to B cells. The intense loss of B cell progenitors and mature B cells at steady state implicated Hhex in the development of the B cell lineage at an early point of commitment (i.e. MPP, LMPP or CLP) to pro-B cells.

Hhex has been implicated in embryonic development[60,67,148-153]; however, little is known about Hhex regulated target genes. Mechanistically, the defect in B-cell development can be traced to changes in gene expression patterns that are associated with B-cell development. These genes include *Blk, Cd19, Ebf1, Vpreb1-3 and Clec7a.* Gene expression profiling identified a decrease in mRNA transcripts; providing a potential mechanism for how loss of Hhex affects B-cell development. Further studies will be required to determine the exact nature of regulation of these genes by Hhex.

Further studies to determine the transcript levels of lymphoid priming genes in Hhex overexpressing T-ALL samples may yield new targets for T-ALL treatment. We predict that there will be an increase in lymphoid priming genes in

ETP-ALL T-cells. These studies may also yield potential mechanisms for how Hhex affects T-ALL development.

CHAPTER VI

Hhex is critical for normal stem cell function

Background and Significance

In order to maintain homeostasis, the balance between hematopoietic stem cell (HSC) differentiation and self-renewal must be maintained[154]. HSCs are able to differentiate to form mature blood cells and at the same time they can replicate themselves, a process known as self-renewal. Loss of this balance can negatively affect the viability of long-term stem cells and lead to bone marrow failure or the development of cancer. By identifying genes that control this balance we can study their role in tumorigenesis and use the information in clinical applications.

Homeobox proteins play a role in stem cell functions[155]. Overexpression of the homeobox proteins Hoxb4[34] and Hoxa9[156] results in an expansion of stem cell pools. Additionally, gene expression data show that Hhex is expressed in hematopoietic stem and progenitor populations; suggesting Hhex may be important for stem cell function.

Results

Hhex cKO bone marrow is compromised in competitive repopulation of lethally irradiated host mice

Competitive repopulation bone marrow transplant experiments were performed to prove a cell-autonomous role for Hhex in B-cell development. First, Hhex cKO or WT B6.CD45.2 (donor) bone marrow was mixed with B6.CD45.1 (host) congenic bone marrow at a ratio of 4:1, then injected into lethally irradiated

CD45.1 host mice (Figure 39). We analyzed peripheral blood of host mice 3-9 weeks after transplant, for CD45.1 and CD45.2 via flow cytometry. We found there were very few Hhex cKO donor cells in peripheral blood (Figure 40). To assess donor contributions to hematopoiesis we assessed host and donor contributions to blood cells 12 weeks post-transplant (Figure 41). We found that while WT donor cells were able to contribute to the mononuclear cells of the bone marrow, spleen and thymus of host mice, Hhex cKO bone marrow contributed to the repopulation of the host mice at a reduced ratio than the input of 4:1 and the contribution to the spleen and thymi was minor (Figure 41). Upon rescue with WT Hhex, the donor contribution of Hhex cKO increased in the thymus of host mice.

Next, Hhex cKO or WT B6.CD45.2 (donor) bone marrow was mixed with B6.CD45.1 (host) congenic bone marrow at a ratio of 6:1, then injected into lethally irradiated CD45.1 host mice (Figure 42). We analyzed peripheral blood of host mice 3-12 weeks after transplant, for CD45.1 and CD45.2 via flow cytometry. We found there were very little Hhex cKO donor cells in peripheral blood (Figure 43). To assess donor contributions to long-term hematopoiesis we assessed host and donor contributions to blood cells 16 weeks post-transplant. While WT donor cells contributed to mononuclear cells of the bone marrow, spleen and thymus of host mice, Hhex cKO bone marrow contributed to the repopulation of host bone marrow at a reduced ratio than the input of 6:1 and the contribution to the spleen and thymi was minor (Figure 44).

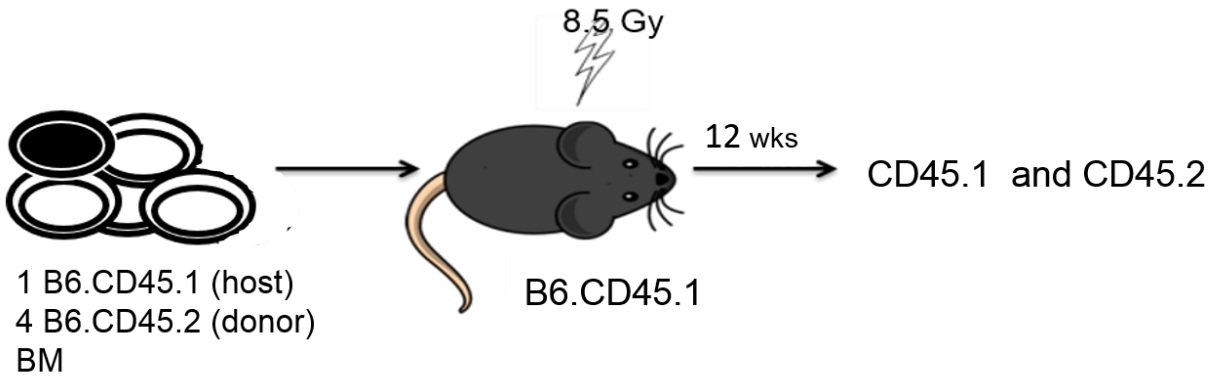

Figure 39. BMT schematic.

Lethally irradiated CD45.1 mice were injected with mixed bone marrow from CD45.1 and CD45.2 mice at an input ratio of 1:4. Twelve weeks post-transplant mice were sacrificed and flow cytometry was used to quantify CD45.1 and CD45.2 in the bone marrow, spleens and thymi of mice.

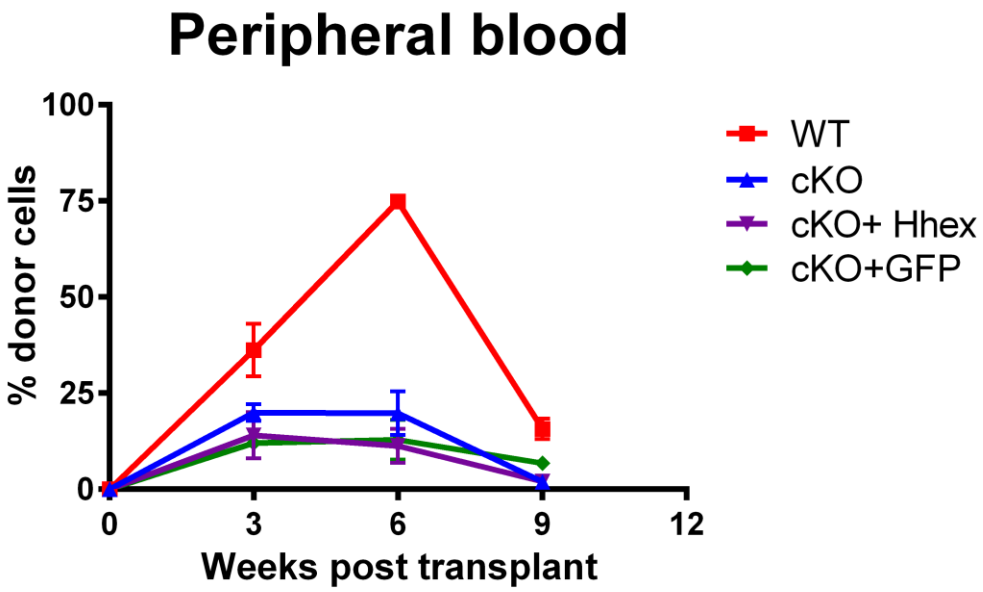

Figure 40. Peripheral blood analysis of recipient mice.

Donor chimerism shown as the percentage of peripheral blood of recipient mice that were $CD45.2^{+}$ 3, 6, and 9 weeks post-transplant.

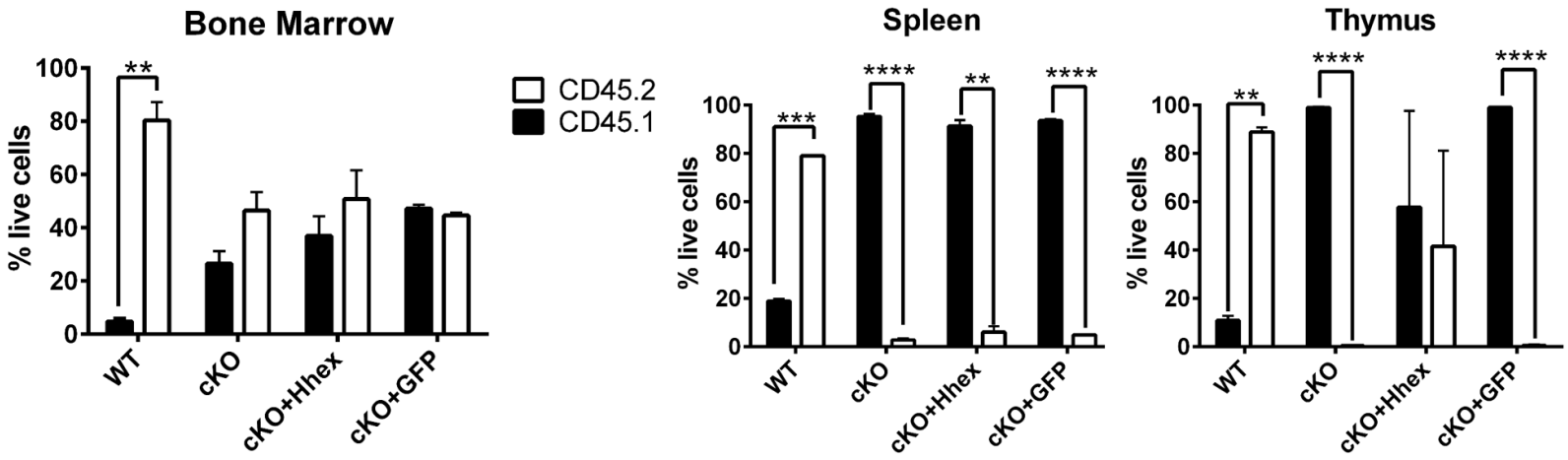

Figure 41. Hhex cKO mice show defect in spleen and thymus repopulation of lethally irradiated host mice.

Twelve (12) weeks post-transplant recipient mice were sacrificed and their bone marrow, spleens, and thymi were harvested for analysis. Flow cytometry analysis was performed to assess CD45.1 and CD45.2 contribution in each organ.

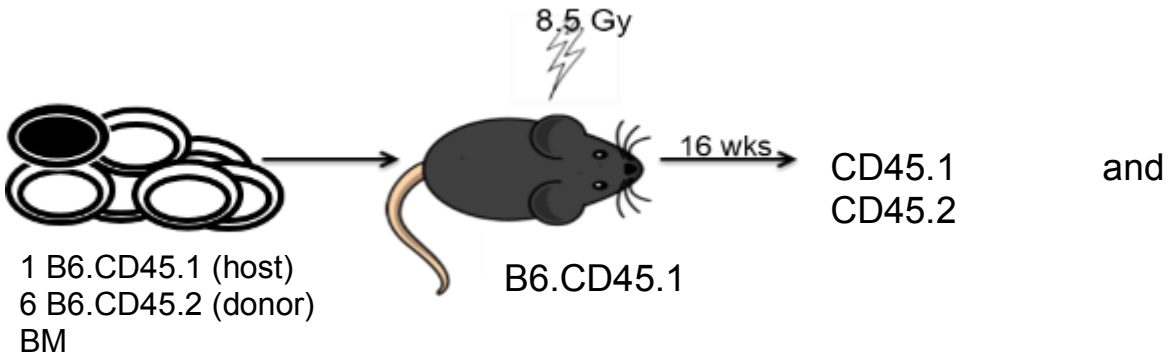

Figure 42. Schematic of competitive BMT.

Schematic of BMT experiments; lethally irradiated recipient mice (CD45.1) were transplanted with whole bone marrow (CD45.2) from WT or Hhex cKO mice; 6-fold more Hhex cKO was injected. Recipient mice were analyzed 16 weeks after injection.

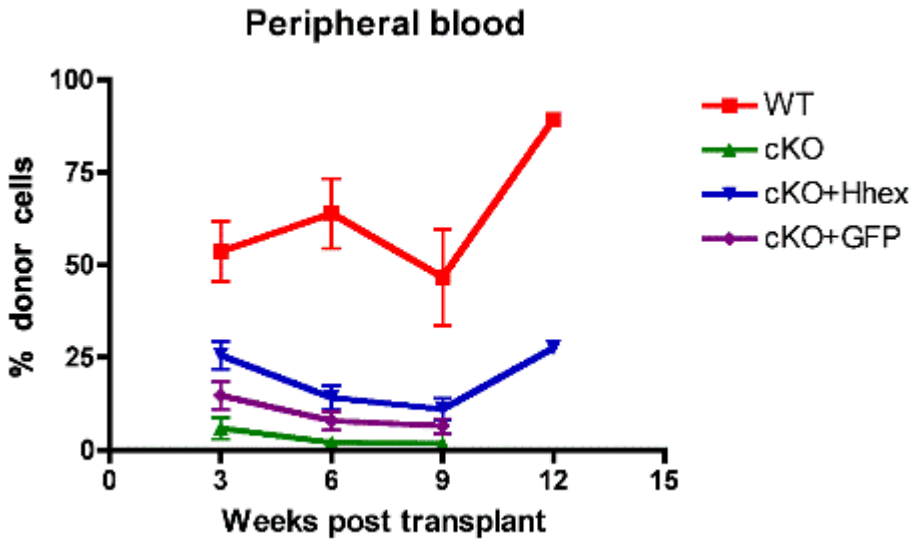

Figure 43. Peripheral Blood analysis of recipient mice.

Donor chimerism is shown as the percentage of peripheral blood of recipient mice that were CD45.2^{+} at the time points indicated.

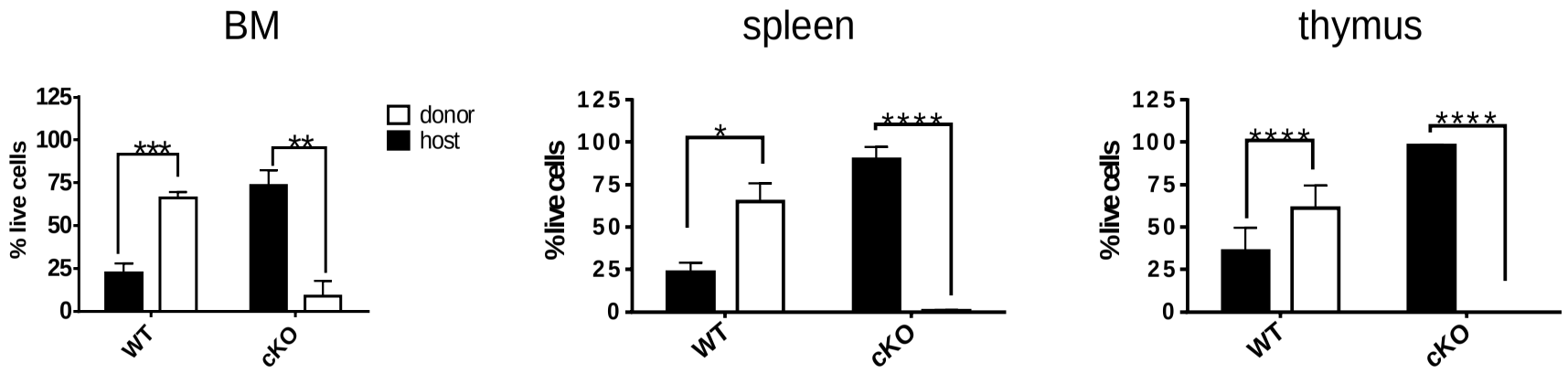

Figure 44. Hhex cKO bone marrow is unable to compete with WT.

Sixteen (16) weeks post-transplant, bone marrows, spleens, and thymi were harvested from BMT mice and analyzed for CD45.1 and CD45.2 for host (i.e. competitor marrow) and donor contributions.

Not only did the bone marrow transplant reveal a cell-autonomous role for Hhex in hematopoiesis but it also revealed a T-cell defect that was not apparent at steady state in Hhex cKO mice.

Hhex cKO bone marrow cells are able to home to and engraft in the bone marrow

The reduced levels of Hhex cKO donor cells in host bone marrow could be due to a homing or engraftment defect in Hhex cKO cells. To assess the homing ability of Hhex cKO cells, bone marrow from B6.CD45.2 donor mice were injected into lethally irradiated mice. Twenty four hours later, the bone marrow of host mice was analyzed by flow cytometry for CD45.2 contribution. We further examined stem and progenitor cells by performing methylcellulose colony formation after bone marrow transplantation and calculated the percentage of stem and progenitor cells that homed to the bone marrow (Figure 45). We found that there was no significant difference in the homing of WT vs *Hhex cKO* cells.

Next we assessed the ability of Hhex cKO cells to engraft in the bone marrow. Bone marrow cells from B6.CD45.2 donor mice were injected into lethally irradiated CD45.1 host mice. Seven (7) days later mice were assessed for CD45.2 cells in the bone marrow, spleen, thymus and peripheral blood (Figure 46). We found that Hhex cKO cells were able to engraft in lethally irradiated host mice (Figure 47).

We then repeated the Hhex cKO bone marrow transplantation after transduction with empty retrovirus (MIG) or MIG-Hhex to test whether we could rescue the defect in reconstitution. MIG-Hhex-transduced bone marrow showed

the highest levels of donor chimerism but not to the same extent as untransduced WT bone marrow. Nevertheless, since both transduced and untransduced bone marrow cells were transplanted into lethally irradiated mice, the MIG-Hhex-transduced GFP^+ and untransduced GFP^- were compared for their contribution to mature cell lineages. The GFP^+ graft (i.e. expressing Hhex) contributed significantly to the B and T cells of the bone marrow and spleen compared to the GFP^- graft (Figure 48 and Figure 49). The proportion of $Gr\text{-}1^+Cd11b^+$ progenitors was the same between GFP^+ and GFP^- grafts although there were decreased $Mac1^+$ and increased $Gr\text{-}1^+$ cells in GFP^+ grafts compared to WT; these mature populations were at comparable proportions at steady state (Figure 50). Thus, MIG-Hhex was able to rescue the T and B cells reconstitution defects observed after Hhex cKO bone marrow transplantation albeit at lower efficiency probably due to poor retroviral transduction and a possible functional defect of LT-HSCs.

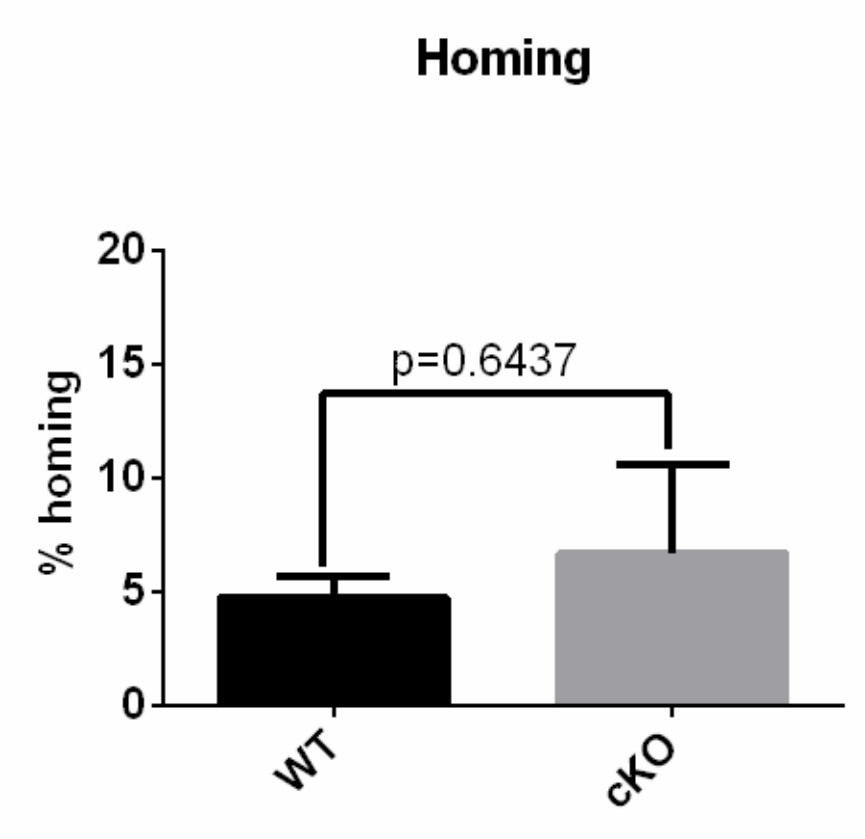

Figure 45. Homing of HSCPs to bone marrow.

In vivo homing assay: colony forming units were quantified from bone marrow of lethally irradiated mice 16 hours after injection with WT or *Hhex* cKO bone marrow.

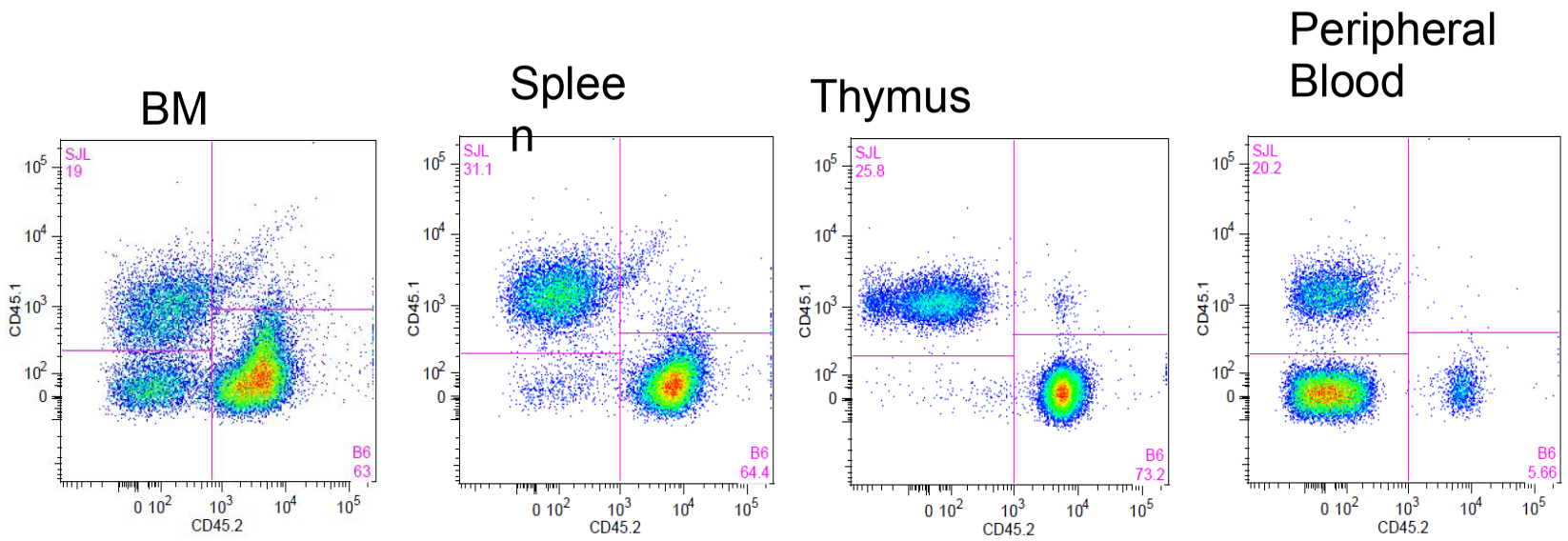

Figure 46. Flow cytometry analysis of donor engraftment.

Representative flow plots of Hhex cKO (CD45.2) engraftment into irradiated CD45.1 mice 7 days post injection.

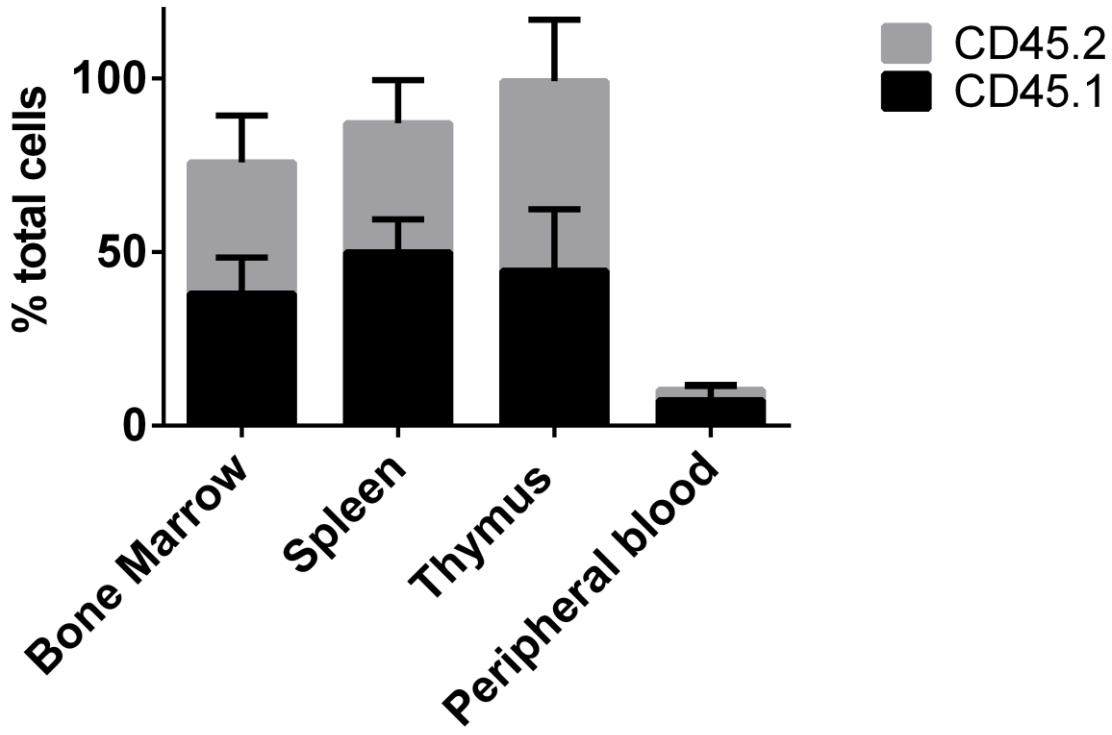

Figure 47. Hhex cKO mice are able to engraft in lethally irradiated host.

In vivo engraftment assay: bar graphs represent percent donor and host cells in bone marrow, spleen, thymus and peripheral blood of host mice 7 days post-transplant. Values are means ± SEM.

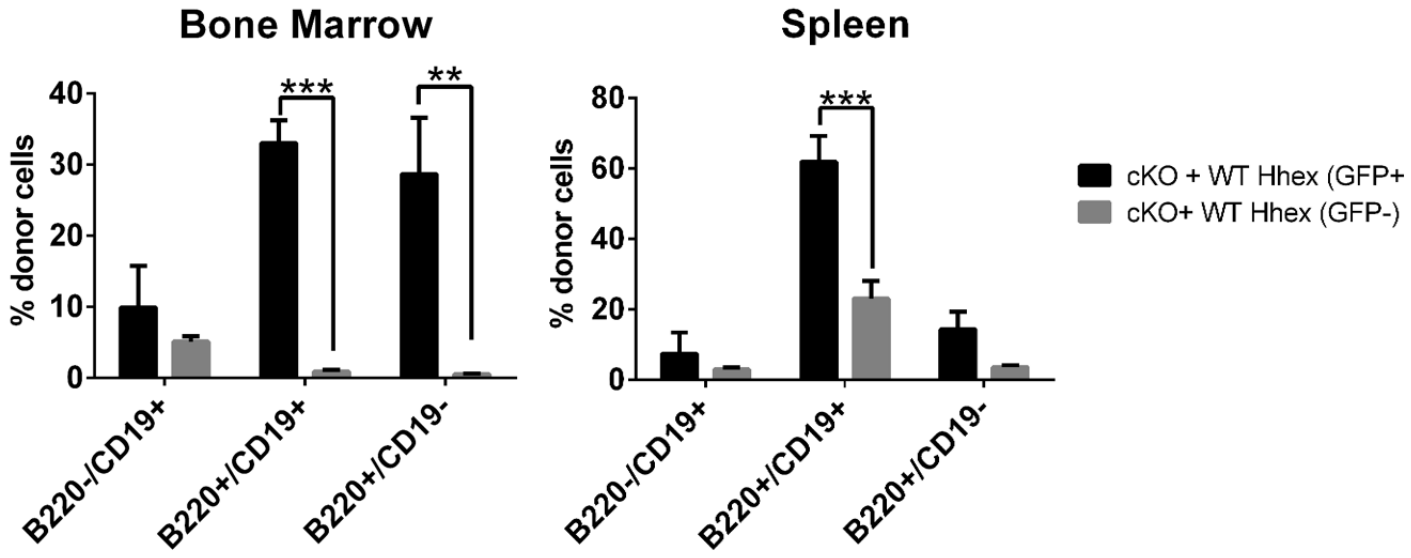

Figure 48. WT Hhex is able to rescue B cell defect.

Proportion of donor B cells in the bone marrow and spleen of host mice 16 weeks after *MIG-Hhex* transduction and BMT are shown gating on GFP^+ and GFP^- cells. Values are means ± SEM, n=7. Two-tailed Student t tests generated P values as shown: *, $P \leq 0.05$; **, $P \leq 0.01$; ***, $P \leq 0.001$; ****, $P \leq 0.0001$.

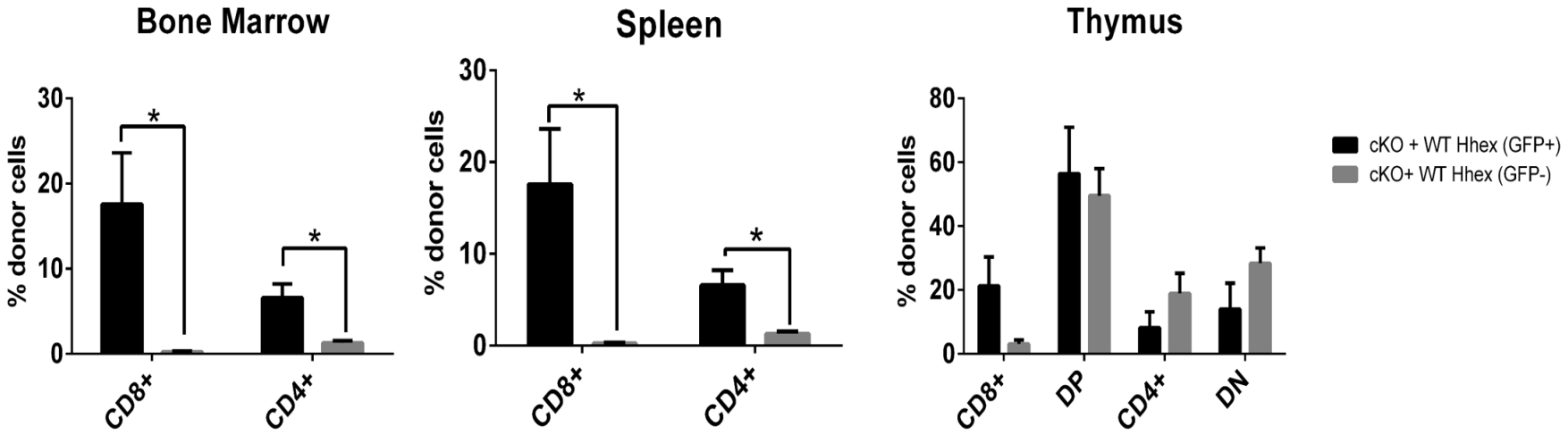

Figure 49. Hhex is able to rescue T cell defect.

Proportion of donor T cells in the bone marrow, spleen and thymus of host mice 16 weeks after *MIG-Hhex* transduction and BMT. Values are means ± SEM, n=7. Two-tailed Student t tests generated P values as shown: *, P ≤ 0.05; **, P ≤ 0.01; ***, P ≤ 0.001; ****, P ≤ 0.0001.

Sublethal irradiation reveals lymphoid defect in Hhex cKO mice

The stress hematopoiesis of bone marrow transplantation revealed a T-cell defect that was not present at steady state in *Hhex cKO* mice. To further assess lymphoid development under stress conditions we induced stress hematopoiesis by sublethally irradiating WT and *Hhex cKO* mice at 6.5 Gy and then allowing their hematopoietic organs to be repopulated by endogenous stem and progenitor cells (Figure 51). We then assessed cellularity of the bone marrow, spleen and thymus after 3, 6, or 9 weeks. We found that the bone marrow of *Hhex cKO* mice was able to repopulate at levels similar to WT mice; however, the spleens and thymi of *Hhex cKO* mice showed reduced cellularity as late as 9 weeks post irradiation (Figure 52). We found that myeloid populations were similar in Hhex cKO and WT mice at 6 weeks (Figure 53). The previously described B-cell defect observed at steady state was still evident under stress conditions (Figure 54). Hhex cKO mice showed a decrease in T-cell populations in both the spleen (Figure 55) and thymus (Figure 56) at 3, 6 and 9 weeks post irradiation. Analysis of thymic progenitors revealed a reduction in early thymic progenitor (ETP) cells at 6 weeks post irradiation in Hhex cKO mice (Figure 57). We also analyzed stem and progenitor populations at 3, 6 and 9 weeks post irradiation and at 3 weeks we observed a significant increase in stem and progenitor populations in Hhex cKO bone marrow when compared to WT (Figure 58).

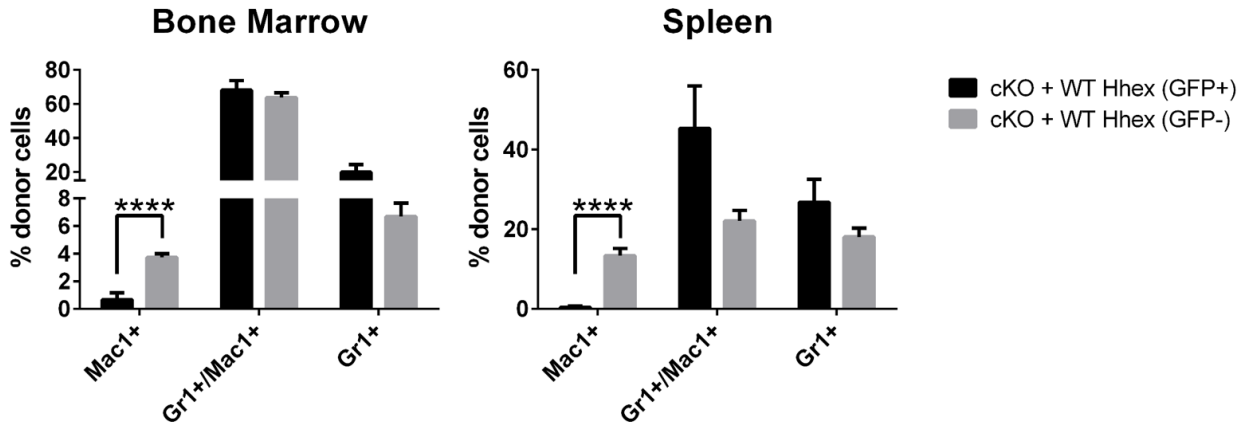

Figure 50. Loss of Hhex results in an increase in Mac1+ cells.

Proportion of donor myeloid cells in the bone marrow and spleen of host mice 16 weeks after *MIG-Hhex* transduction and BMT are shown gating on GFP^+ and GFP^- cells. Values are means ± SEM, n=7. Two-tailed Student t tests generated P values as shown: *, $P \leq 0.05$; **, $P \leq 0.01$; ***, $P \leq 0.001$; ****, $P \leq 0.0001$.

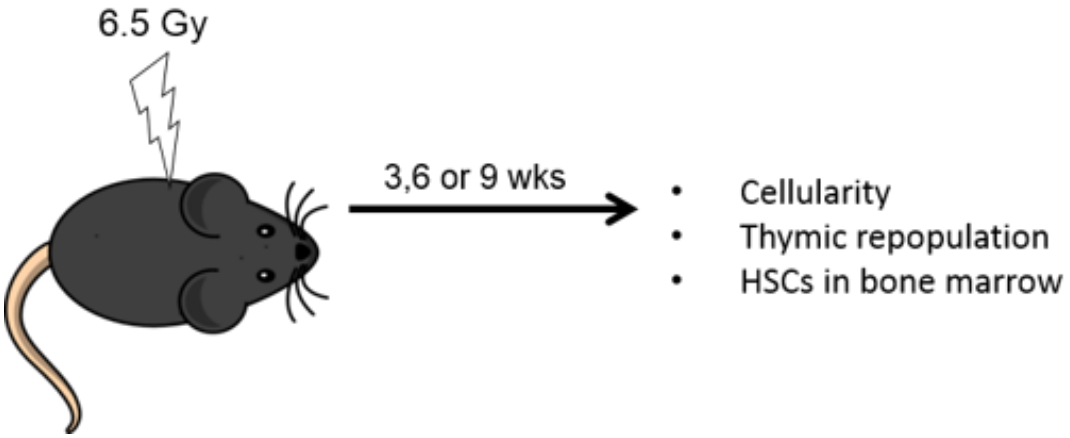

Figure 51. Schematic shows the experiment outline of sublethal irradiation experiment.

WT and Hhex cKO mice were irradiated with 6.5 Gy and bone marrows, spleens, and thymi were analyzed at 3,6, and 9 weeks.

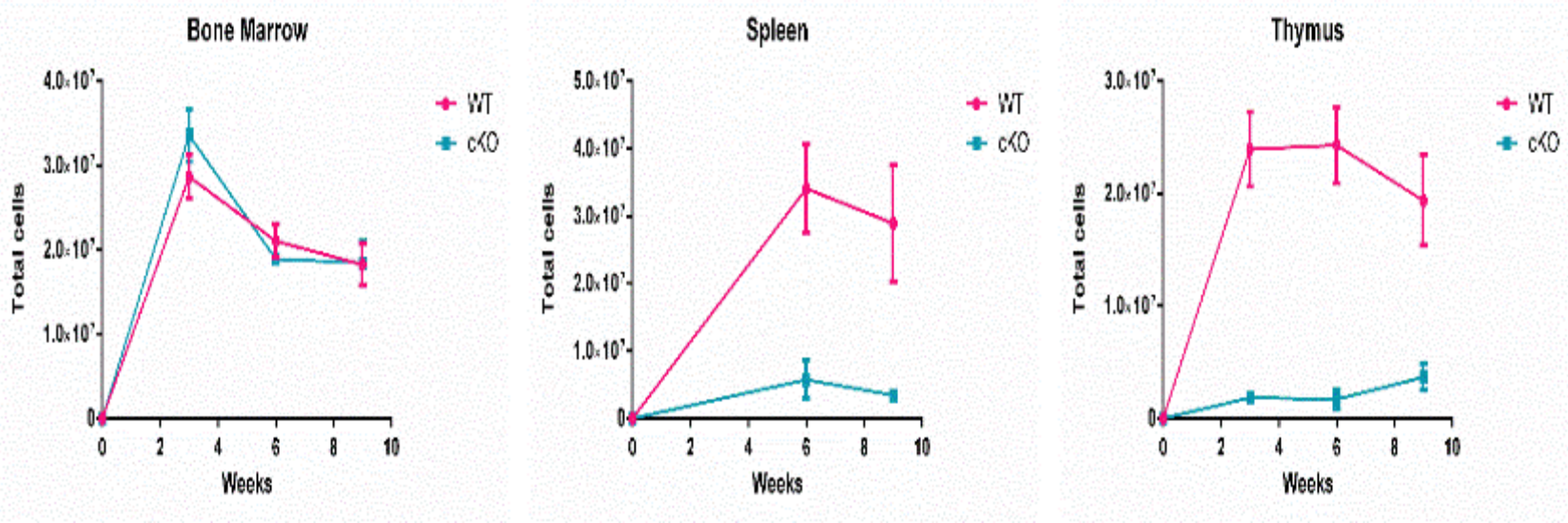

Figure 52. Hhex cKO mice are not able to repopulate their spleen and thymi after sublethal irradiation.

Graph shows total cellularity versus time post-irradiation in weeks for bone marrow, spleen and thymus of WT and Hhex cKO mice. Two tailed Student t test was done to generate P values: *, $P \leq 0.05$; **, $P \leq 0.01$; ***, $P \leq 0.001$; ****, $P \leq 0.0001$.

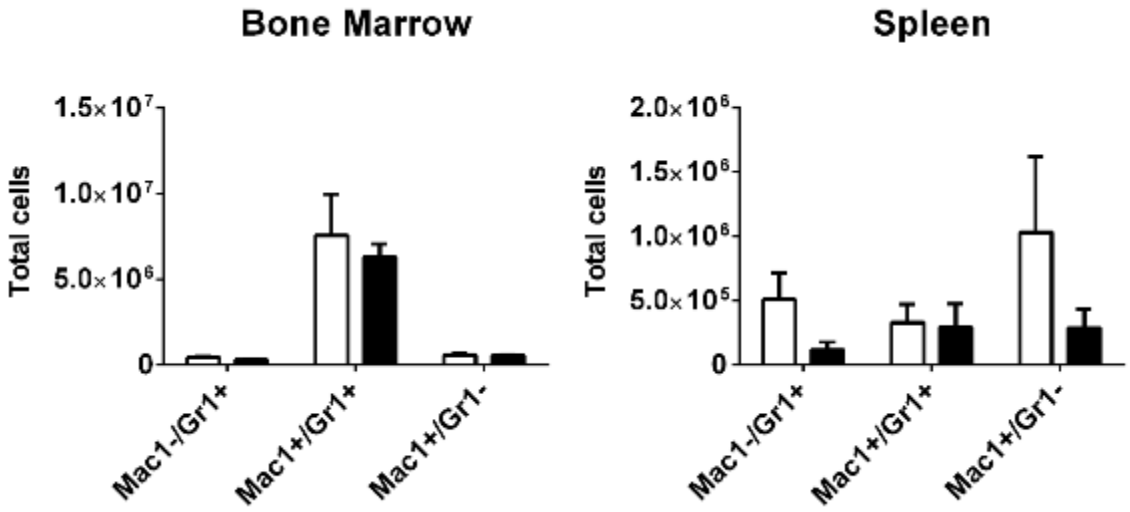

Figure 53. Myeloid cells are able to repopulate the BM and spleen of sublethally irradiated mice.

Bar graphs show the mean numbers of myeloid in the bone marrow and spleens of WT and Hhex cKO mice at 6 weeks post irradiation. WT in white bars, Hhex cKO in black bars. Total cells were calculated based on the total number of cells multiplied by the percentage of each population.

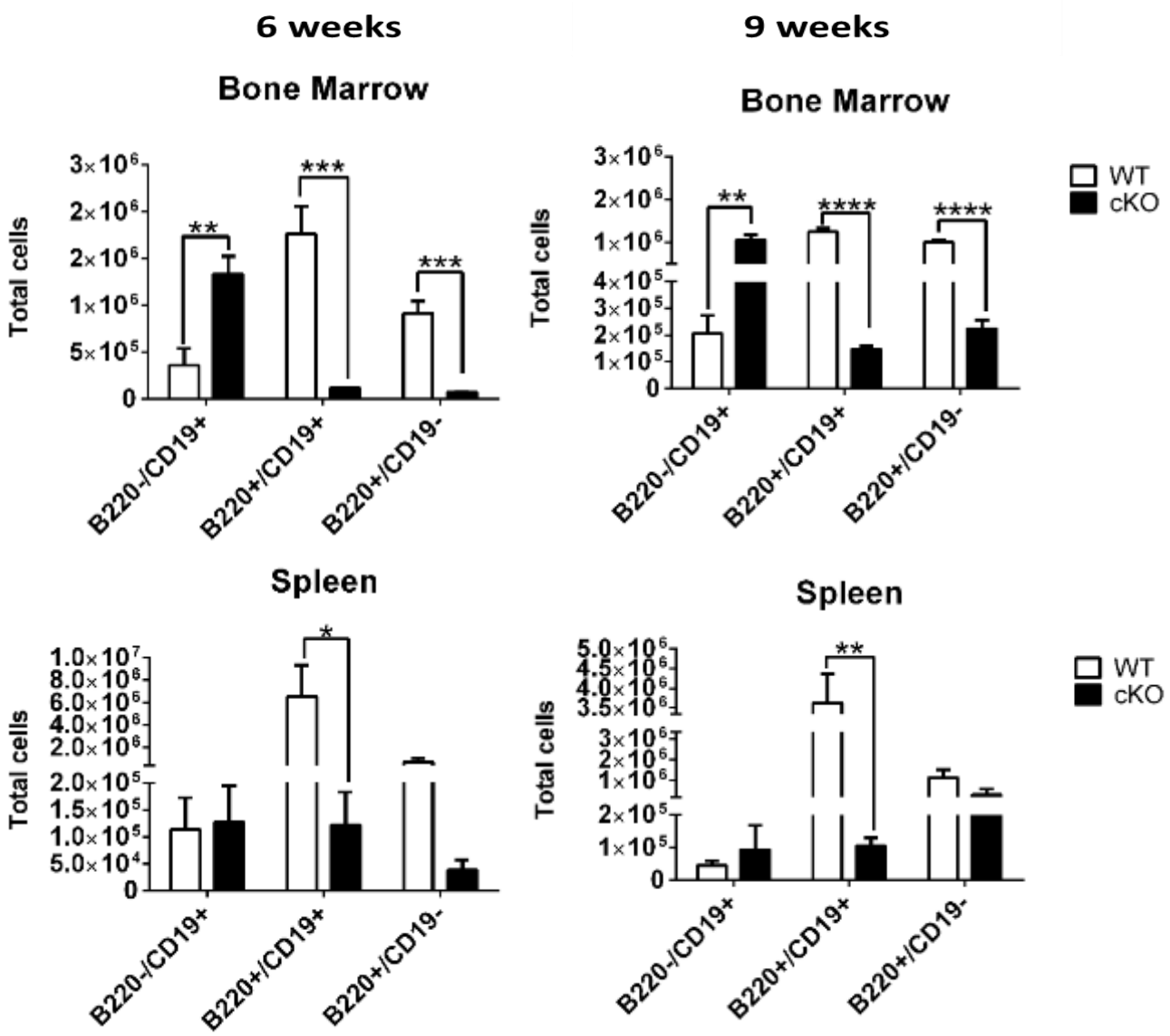

Figure 54. Hhex cKO show a B cell defect post sublethal irradiation.

Bar graphs show the mean numbers of B cells in the bone marrow at 6 weeks (column 1), and 9 weeks (column 2) post sublethal irradiation. WT in white bars, Hhex cKO in black bars. Total cells were calculated based on the total number of cells multiplied by the percentage of each population. Two tailed Student t test was done to generate P values: *, $P \leq 0.05$; **, $P \leq 0.01$; ***, $P \leq 0.001$; ****, $P \leq 0.0001$.

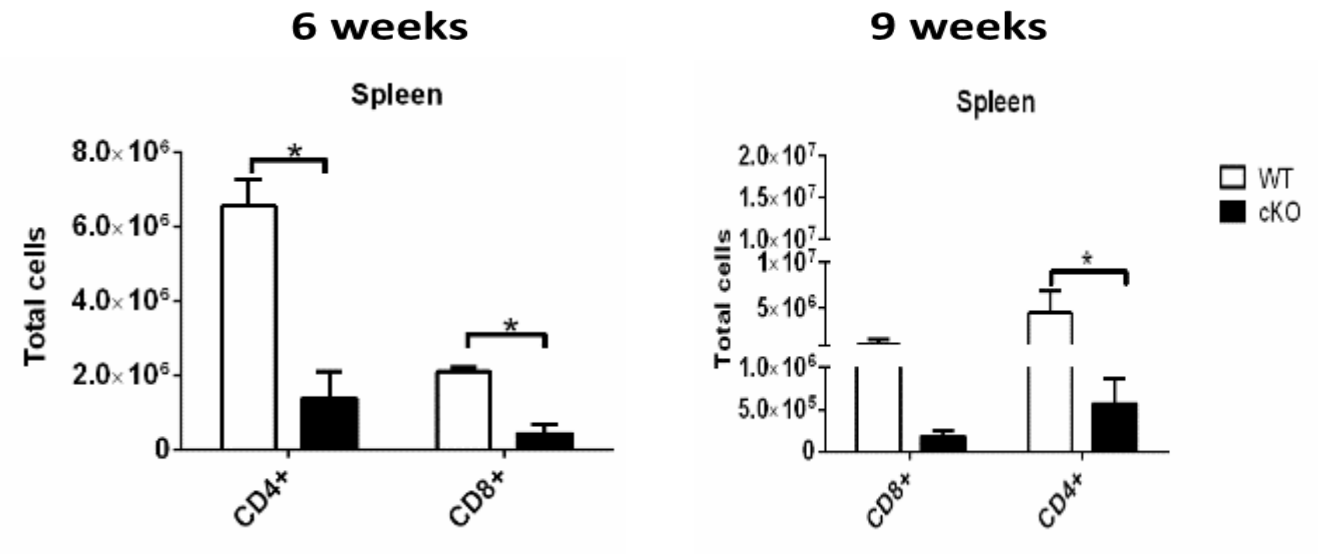

Figure 55. Hhex cKO mice have a defect in splenic T cells post sublethal irradiation.

Bar graphs show the mean ± SEM of mature T cell populations in the spleen; WT; n=3, cKO; n=5. Two tailed Student t test was done to generate P values: *, P ≤ 0.05; **, P ≤ 0.01; ***, P ≤ 0.001; ****, P ≤ 0.0001.

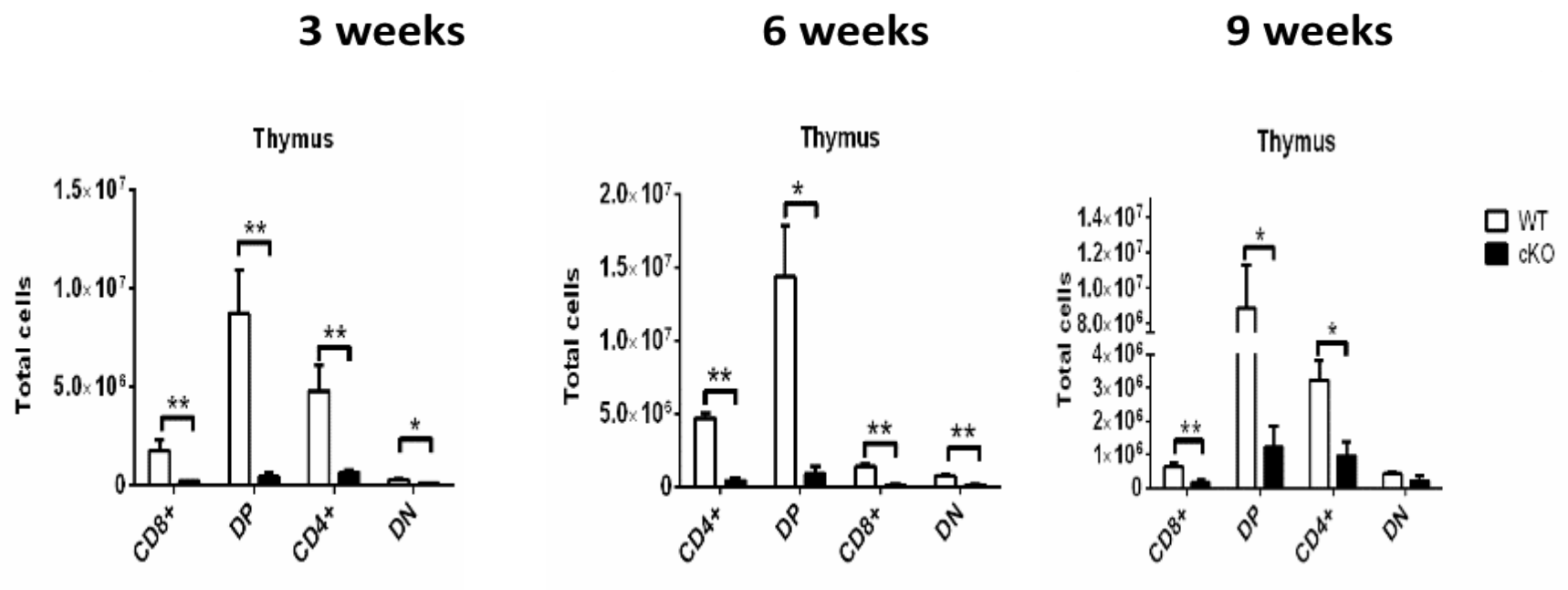

Figure 56. Hhex cKO mice show a defect in thymic T-cell reconstitution post irradiation.

Bar graphs represent the sizes of each T cell population in the thymus at 3 weeks (column 1), 6 weeks (column 2), and 9 weeks (column 3). WT in white bars, Hhex cKO in black bars. Total cells were calculated based on the total number of cells multiplied by the percentage of each population. Two tailed Student t test was done to generate P values: *, $P \leq 0.05$; **, $P \leq 0.01$; ***, $P \leq 0.001$; ****, $P \leq 0.0001$.

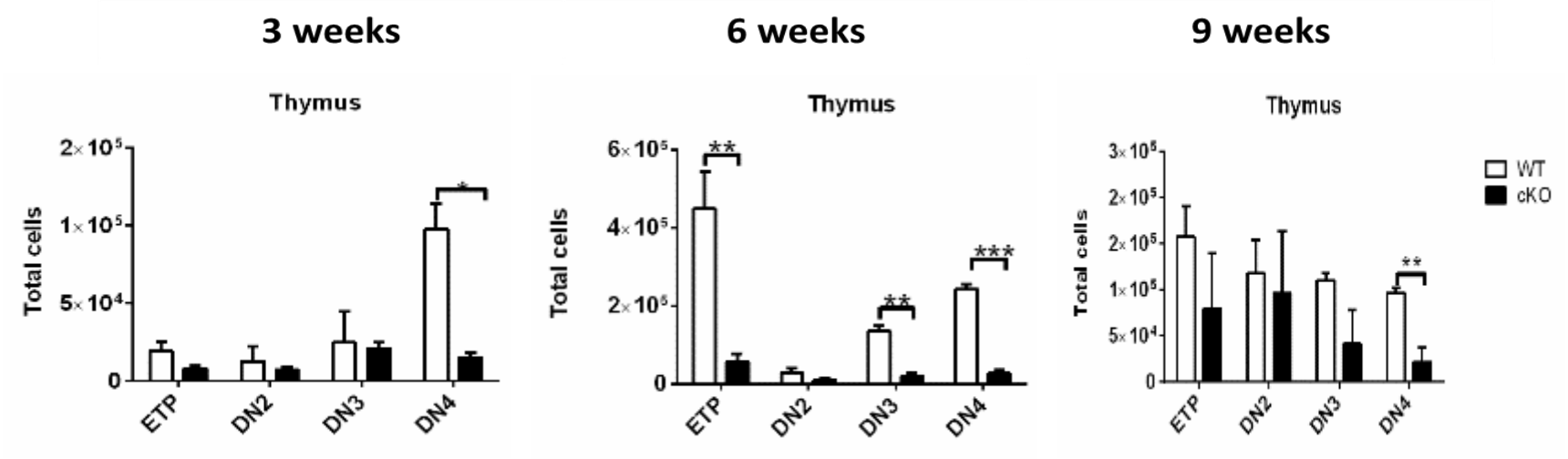

Figure 57. Hhex cKO mice show thymic progenitor defects post sublethal irradiation.

Bar graphs represent the sizes of each T cell progenitor population in the thymus at 3 weeks (column 1), 6 weeks (column 2), and 9 weeks (column 3). WT in white bars, Hhex cKO in black bars. Total cells were calculated based on the total number of cells multiplied by the percentage of each population. Two tailed Student t test was done to generate P values: *, $P \leq 0.05$; **, $P \leq 0.01$; ***, $P \leq 0.001$; ****, $P \leq 0.0001$.

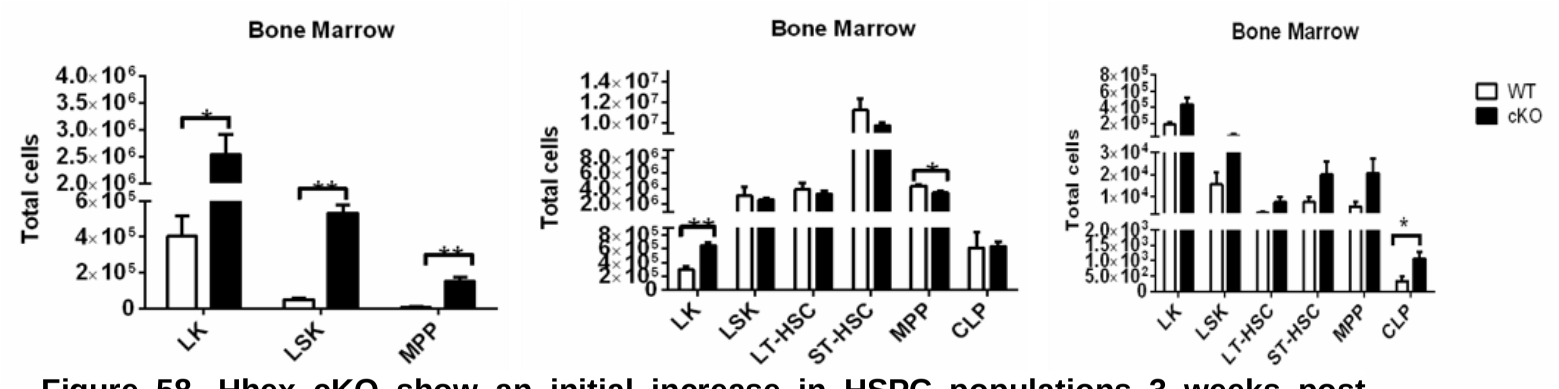

Figure 58. Hhex cKO show an initial increase in HSPC populations 3 weeks post irradiation.

Bar graphs show the mean numbers of stem and progenitor populations in the bone marrow at 3 weeks (column 1), 6 weeks (column 2), and 9 weeks (column 3). WT in white bars, Hhex cKO in black bars. Total cells were calculated based on the total number of cells multiplied by the percentage of each population. Two tailed Student t test was done to generate P values: *, $P \leq 0.05$; **, $P \leq 0.01$; ***, $P \leq 0.001$; ****, $P \leq 0.0001$.

Hhex cKO mice have reduced numbers of LT-HSCs at steady state

The competitive bone marrow transplant suggests that there may be a defect in the stem cell populations, while the sublethal irradiation experiment suggests a defect in progenitor populations of Hhex cKO mice. To further determine where the Hhex cKO hematopoietic defect is occurring we used previously established cell surface markers to quantify the stem and progenitor populations in Hhex cKO mice. We quantified LSK cells which contain stem and progenitor populations. Analysis revealed no difference in the absolute numbers of LSKs in WT and Hhex cKO mice (Figure 59). To differentiate between stem and progenitor populations the LSK population was further divided based on flt3 expression (Figure 60A). The long-term HSCs (LT-HSCs) population, defined as LSKflt3^{-}, was significantly reduced in *Hhex cKO* mice while short-term HSCs (ST-HSCs), and multipotent progenitors (MPPs) showed no significant difference (Figure 60B). To confirm the reduction in the LT-HSC population, the LSKflt3^{-} population was further fractionated using SLAM markers CD48 and CD150. The LSKfl3^{-}CD48^{-}CD150^{+} population was also significantly reduced in absolute number in *Hhex cKO* mice compared to WT mice (Figure 60B).

Hhex cKO mice show an increase in the proportion of CD34- CD150+ CD48- LSK highly enriched HSC population

CD150^{+} CD48^{-} LSK cells are able to generate mature lineages over a long period of time[15]. Previous studies have shown that CD34^{-} LSK cells have more HSC activity while CD34^{+} LSK cells have more MPP activity[16,31]. These findings

led to the identification of a highly enriched functional HSC population (LSK $CD150^{+}CD48^{-}CD34^{-}$ cells)[157].

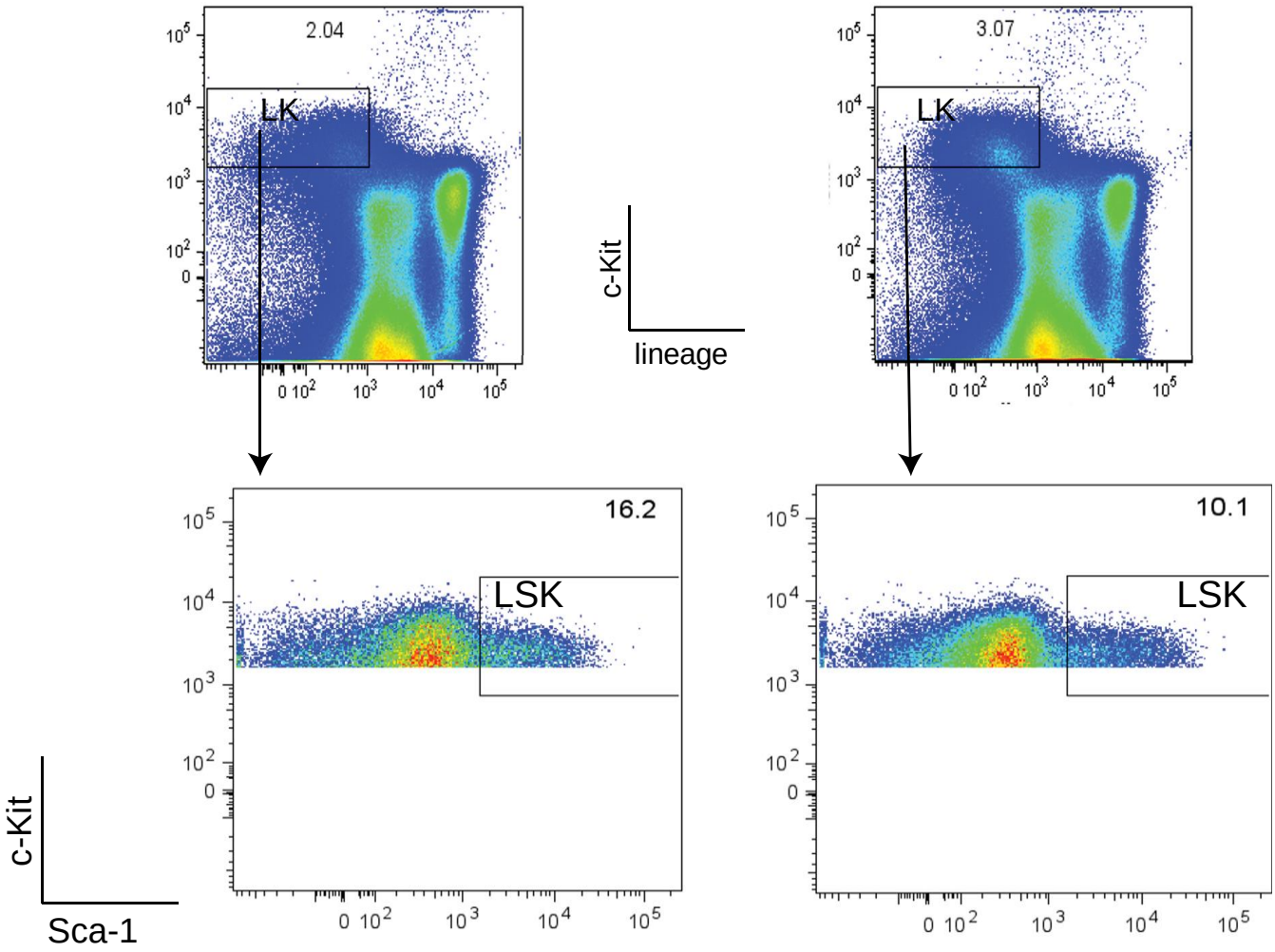
2.04
LK
3.07
LK
c-Kit
lineage
16.2
LSK
10.1
LSK
c-Kit
Sca-1

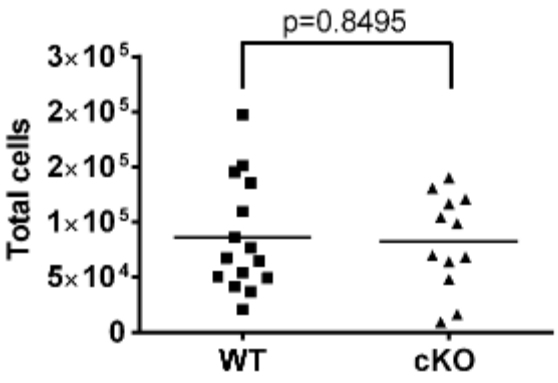
LSK
p=0.8495
Total cells
3×10^5
2×10^5
2×10^5
1×10^5
5×10^4
0
WT
cKO

Figure 59. Hhex cKO mice show no defect in absolute LSK numbers.

A) Representative flow cytometry analysis of the hematopoietic stem populations from the bone marrow of WT and *Hhex* cKO mice at 7-16 weeks of age. The sizes of gated populations as percentages of the parental populations are shown. The plot shows the absolute numbers of LSK: $Lin^{-}Sca\text{-}1^{+}Kit^{+}$ cells in the bone marrow of WT or *Hhex* cKO mice. Total cells were calculated based on the total number of cells multiplied by the percentage of each population, WT, n=15; cKO, n=12. P values were generated by two tailed Student t test: *, $P \leq 0.05$; **, $P \leq 0.01$; ***, $P \leq 0.001$; ****, $P \leq 0.0001$.

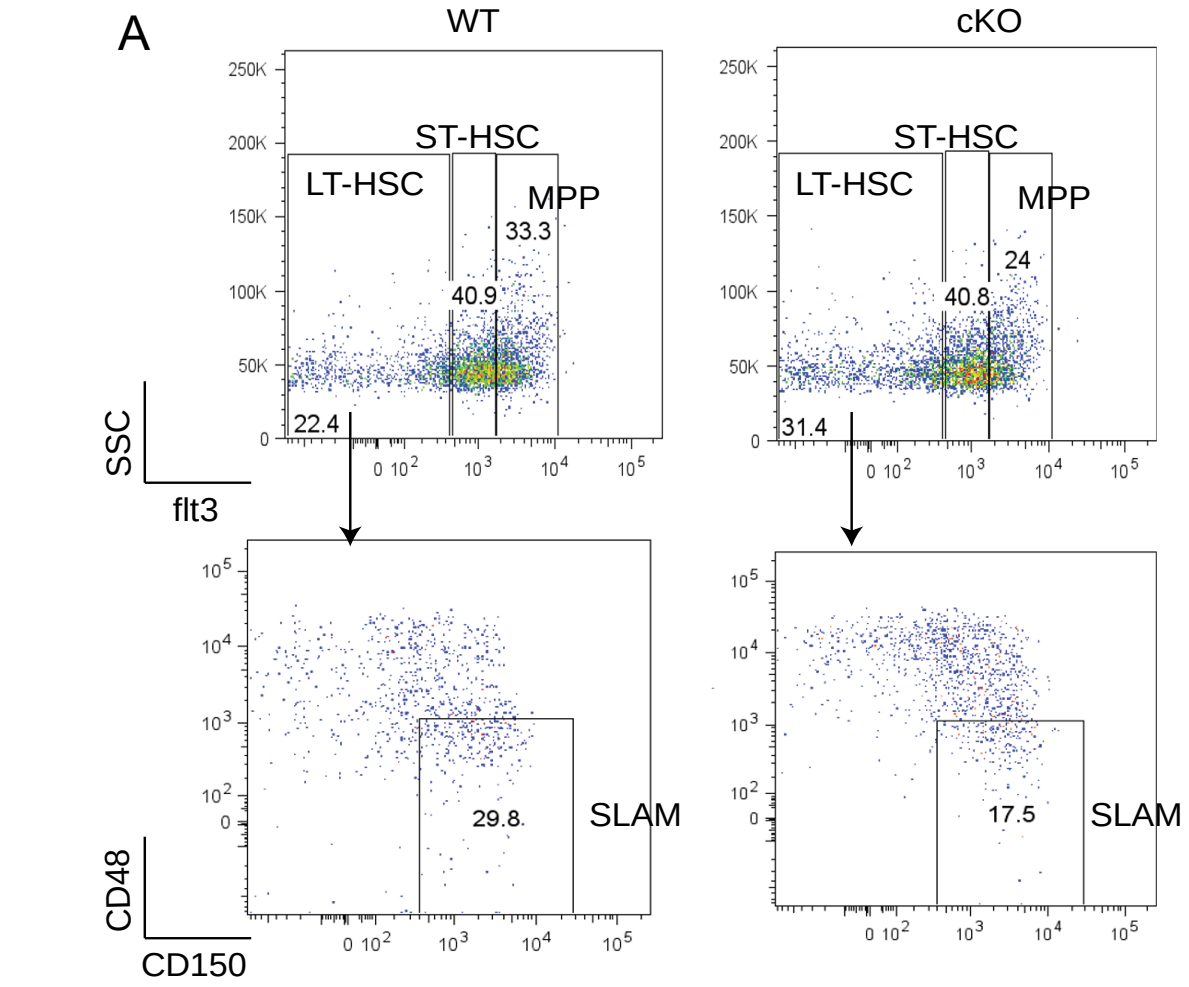
A
WT
cKO
ST-HSC
LT-HSC
MPP
33.3
40.9
22.4
24
40.8
31.4
SSC
flt3
29.8
17.5
SLAM
CD48
CD150

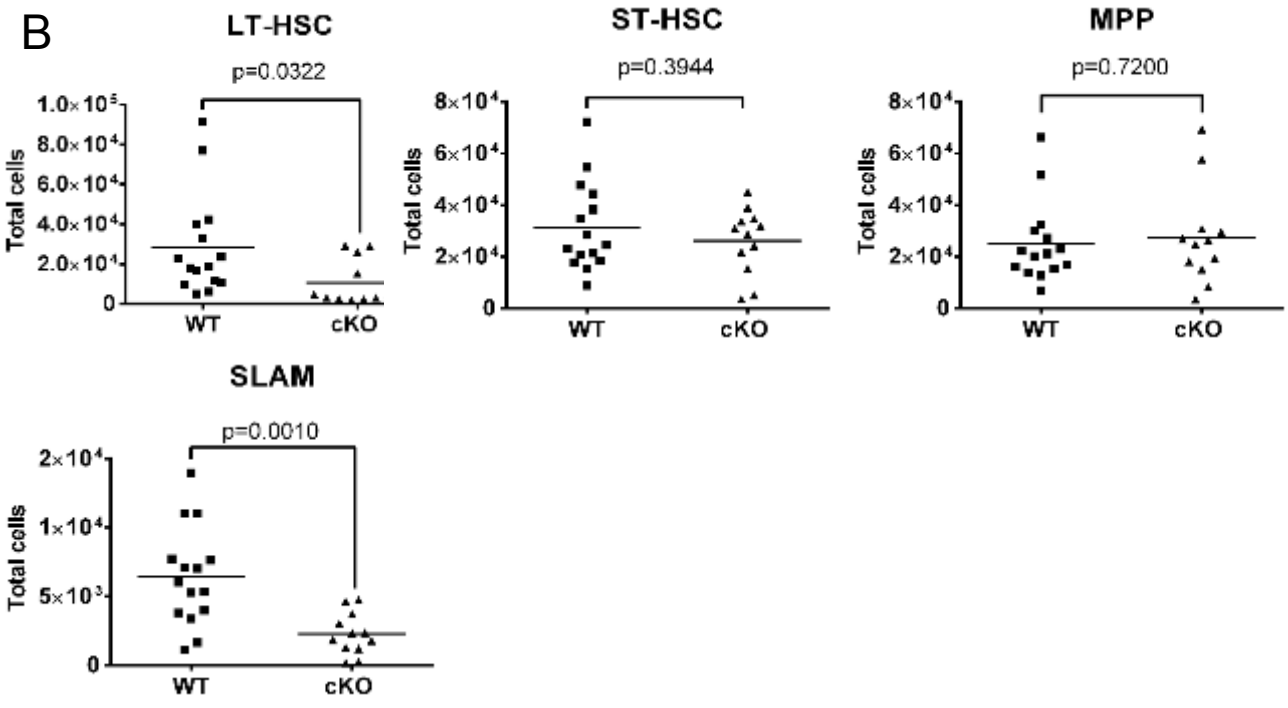
B
LT-HSC
p=0.0322
ST-HSC
p=0.3944
MPP
p=0.7200
SLAM
p=0.0010
Total cells
WT
cKO

Figure 60. Hhex cKO show a decrease in LT-HSCs.

(A) Representative flow cytometry analysis of the hematopoietic stem and progenitor populations from the bone marrow of WT and *Hhex* cKO mice at 7-16 weeks of age. The sizes of gated populations as percentages of the parental populations are shown. (B) Plots show the absolute numbers of each stem and progenitor population in the bone marrow of WT or *Hhex* cKO mice. HSPCs; MPP: multipotent progenitors; ST-HSC: short term HSC; SLAM: CD150; LT-HSC: long term HSC. Total cells were calculated based on the total number of cells multiplied by the percentage of each population, WT, n=15; cKO, n=12. P values were generated by two tailed Student t test: *, $P \leq 0.05$; **, $P \leq 0.01$; ***, $P \leq 0.001$; ****, $P \leq 0.0001$.

To improve our ability to identify HSCs we also assessed CD34 expression in stem cell populations. Using the gating scheme described by Wilson et al., we again assessed the frequency of various stem and progenitor populations[158] (Table 2 and Figure 61). We found that Hhex cKO mice showed an increase in the proportion of HSC cells and a reduction of more differentiated MPP cells (Figure 62). This quantitative defect shown in the proportion of these cells was not evident in total cells. Next we quantified the common lymphoid progenitor (CLP) frequency using flow cytometry and found a significant increase in the CLP population (Figure 63). Together, these data would suggest a functional defect in stem populations of Hhex cKO mice that results in a defect in lymphoid progenitor populations.

Hhex cKO stem and progenitor cells have enhanced proliferation activity

While ST-HSCs, MPPs and CLPs are progeny of LT-HSCs, there was only a defect in CLPs and no defect in parental population. This led us to hypothesize that increased CLPs, in the setting of reduced LT-HSCs (Figure 60), is due to increased proliferation. Stem and progenitor populations underwent in vivo BrdU labeling. We observed significantly higher BrdU labeling in Hhex cKO LSKs when compared to WT (Figure 64A). Hhex cKO had twice the amount of BrdU incorporation into HSCs and MPPs compared to WT. Hhex cKO and WT CLP populations showed comparable levels of BrdU labeling (Figure 64B).

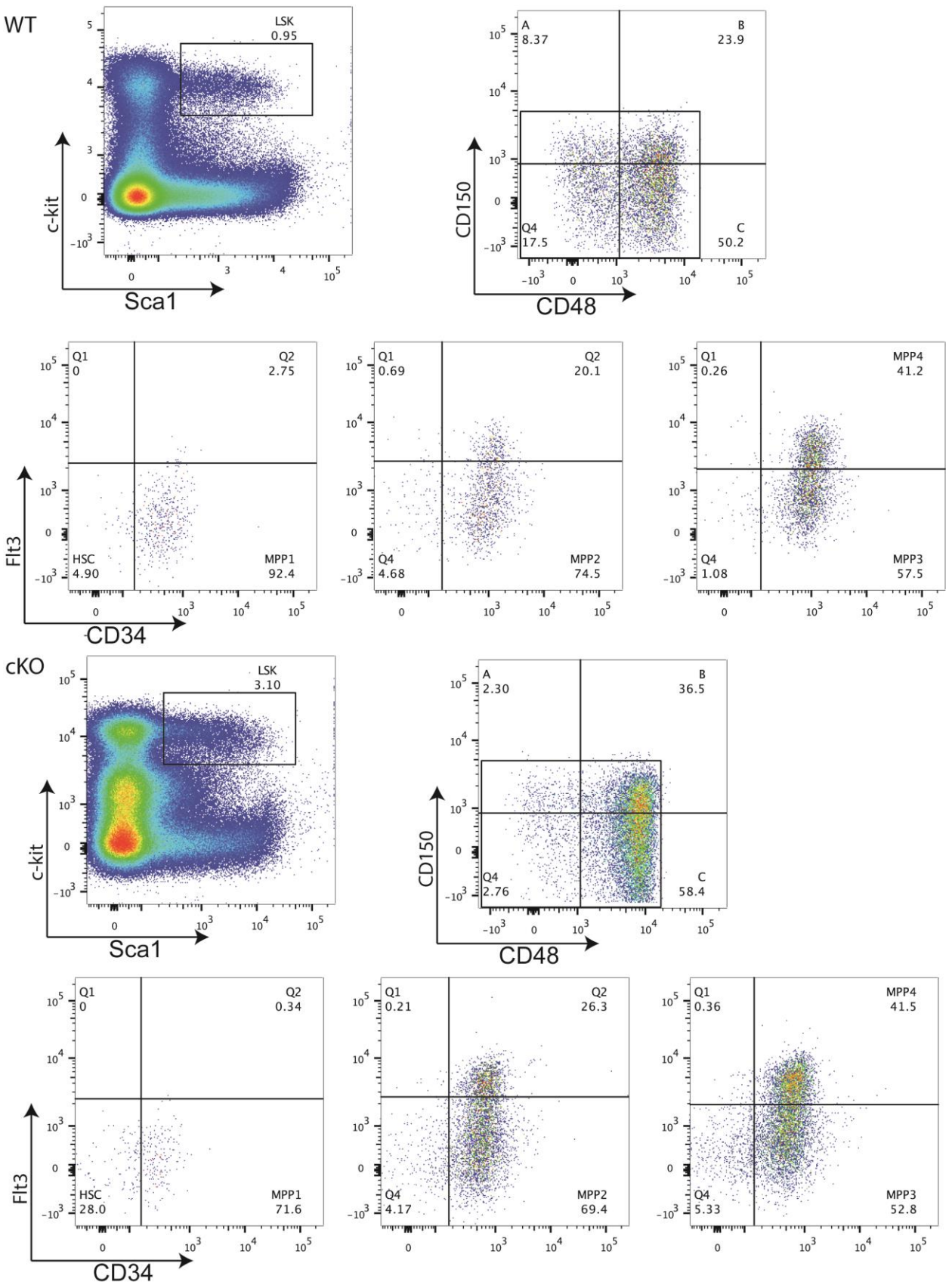
WT
LSK
0.95
c-kit
Sca1
A
8.37
B
23.9
Q4
17.5
C
50.2
CD150
CD48
Q1
0
Q2
2.75
HSC
4.90
MPP1
92.4
Flt3
CD34
Q1
0.69
Q2
20.1
Q4
4.68
MPP2
74.5
Q1
0.26
MPP4
41.2
Q4
1.08
MPP3
57.5
cKO
LSK
3.10
A
2.30
B
36.5
Q4
2.76
C
58.4
Q1
0
Q2
0.34
HSC
28.0
MPP1
71.6
Q1
0.21
Q2
26.3
Q4
4.17
MPP2
69.4
Q1
0.36
MPP4
41.5
Q4
5.33
MPP3
52.8

Figure 61. Representative flow cytometry of HSC populations.

Representative flow cytometry analysis of the hematopoietic stem and progenitor populations from the bone marrow of WT and *Hhex* cKO mice. The sizes of gated populations as percentages of the parental populations are shown.

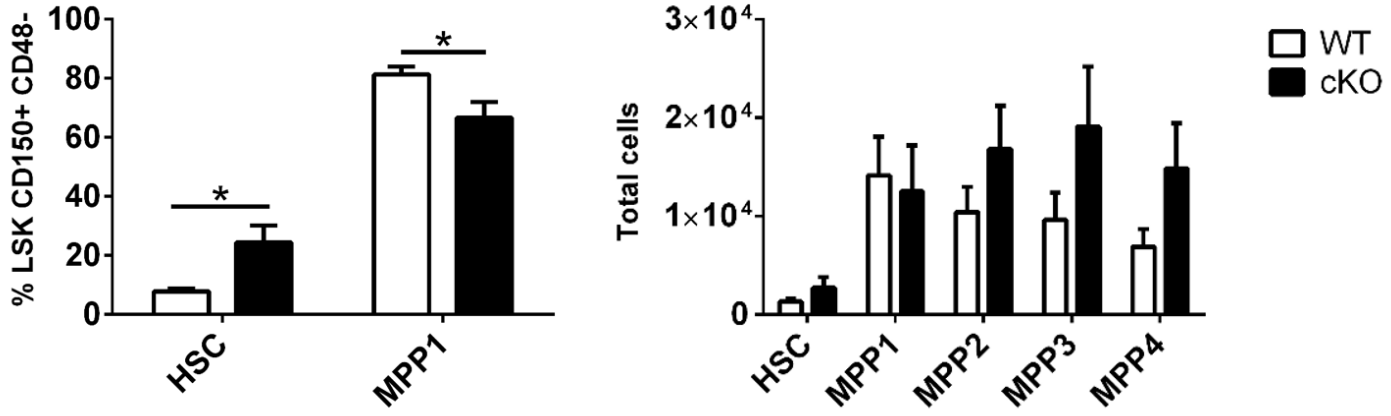

Figure 62. Hhex cKO show an increase in HSC populations.

Bar graphs show the absolute numbers of each stem and progenitor population in the bone marrow of WT or *Hhex* cKO mice. Total cells were calculated based on the total number of cells multiplied by the percentage of each population, WT, n=10; cKO, n=11. P values were generated by two tailed Student t test: *, P ≤ 0.05; **, P ≤ 0.01; ***, P ≤ 0.001; ****, P ≤ 0.0001.

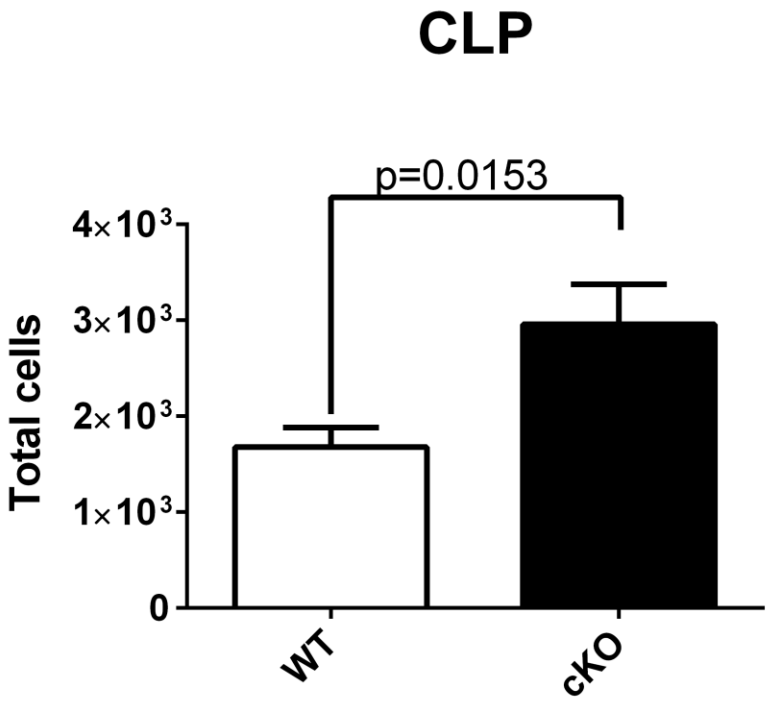

Figure 63. Hhex cKO mice show increase in CLP population.

The plot shows the absolute numbers of common lymphoid progenitors (CLPs) in the bone marrow of WT or *Hhex* cKO mice. Total cells were calculated based on the total number of cells multiplied by the percentage of each population. P value was generated by two tailed Student t test:

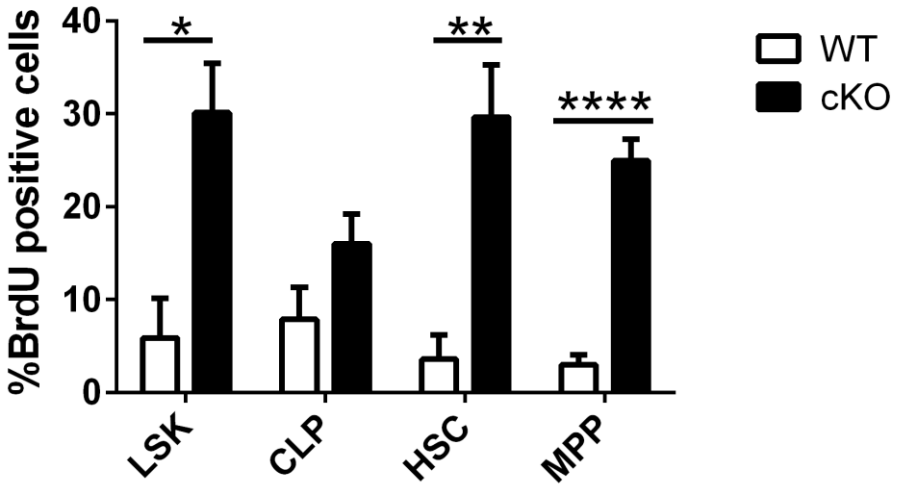

Figure 64. Hhex cKO shows significantly higher BrdU labelling.

Representative flow cytometry analysis of the BrdU in stem and progenitor populations in the bone marrow of WT and Hhex cKO mice. (B) Bar graphs representing the proportion of BrdU in each stem and progenitor population. Values are means ± SEM for WT, n=3; cKO, n=5. Two tailed Student t test was done to generate P values: *, $P \leq 0.05$; **, $P \leq 0.01$; ***, $P \leq 0.001$; ****, $P \leq 0.0001$.

Gene expression analysis reveals lymphoid priming defect in Hhex cKO cells

Our data suggests that Hhex is required for LT-HSC maintenance, lymphoid differentiation and cell cycle regulation. To further analyze the role of Hhex in these processes we sorted HSCs and MPPs based on Flt3 expression in the LSK compartment (Figure 65) and performed RNA-seq. We identified genes that varied by at least 2-fold in pairwise comparisons. MPPs sorted from both WT and Hhex cKO mice had marked downregulation of mRNAs that are associated with megakaryocyte and erythrocyte progenitor (MEP) lineages (Figure 66). This is consistent with the idea that Flt3+ MPPs have little to no MEP potential[4]. Prior to lineage commitment, Flt3+ MPPs upregulate a lymphoid transcriptional program, a process known as lymphoid priming[159]. We observed an increase in lymphoid priming genes (i.e. Blk, Blnk, Rag1, Rag2, Cd79a, Dntt, Vpreb2, and Il7r) in the differentiation of WT HSCs to MPPs (Figure 67). However, the upregulation of these genes was attenuated in Hhex cKO HSC to MPP differentiation.

HHEX regulated the EIF4E-directed transport and stability of CCND1 mRNA in U937 acute myeloid leukemia cells[73]. We also analyzed RNA-seq data to determine if there was a difference in the mRNA of cell cycle regulators between WT and Hhex cKO stem and progenitor populations. Transcripts for cell cycle regulators associated with stem and progenitor cell proliferation and quiescence were comparably expressed between WT and Hhex cKO mice except for Cdkn1a, which was reduced in Hhex cKO cells (Figure 68). This

reduction in Cdkn1a in Hhex cKO HSCs and MPPs may account for the enhanced proliferation in Hhex cKO stem and progenitor populations.

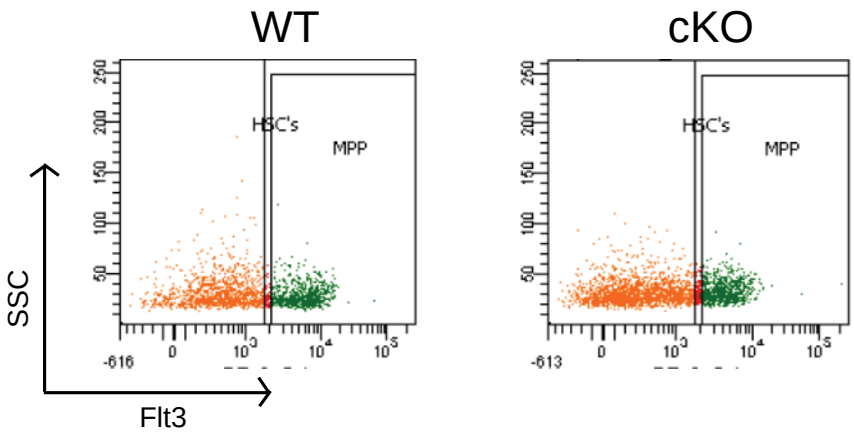

Figure 65. Stem and progenitor cells were sorted for RNA-seq analysis.

Representative flow cytometry analysis of the HSCs and MPPs sorted based on Flt3 expression from the bone marrow of WT and *Hhex* cKO mice.

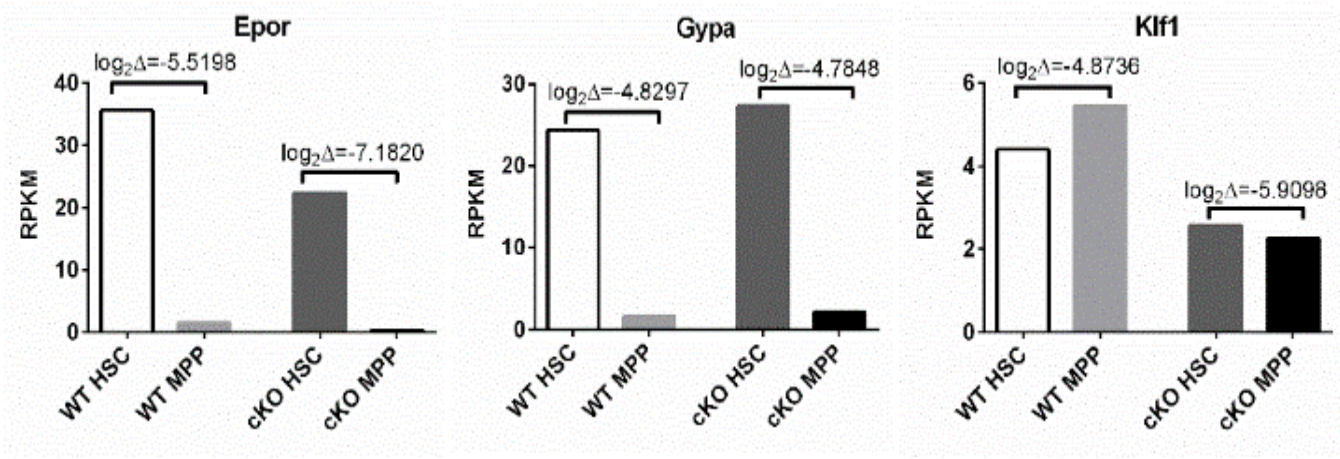

Figure 66. Hhex cKO MPPs are able to downregulate genes involved in MEP.

RNA-seq analysis of sorted HSC and MPP cells from WT and Hhex cKO bone marrows. Genes are specific to the megakaryocytic-erythroid lineage. Y-axes values are in RPKM, reads per kilobase of gene per million reads total. Brackets show $\log_2$ changes between HSC and PP differentiation.

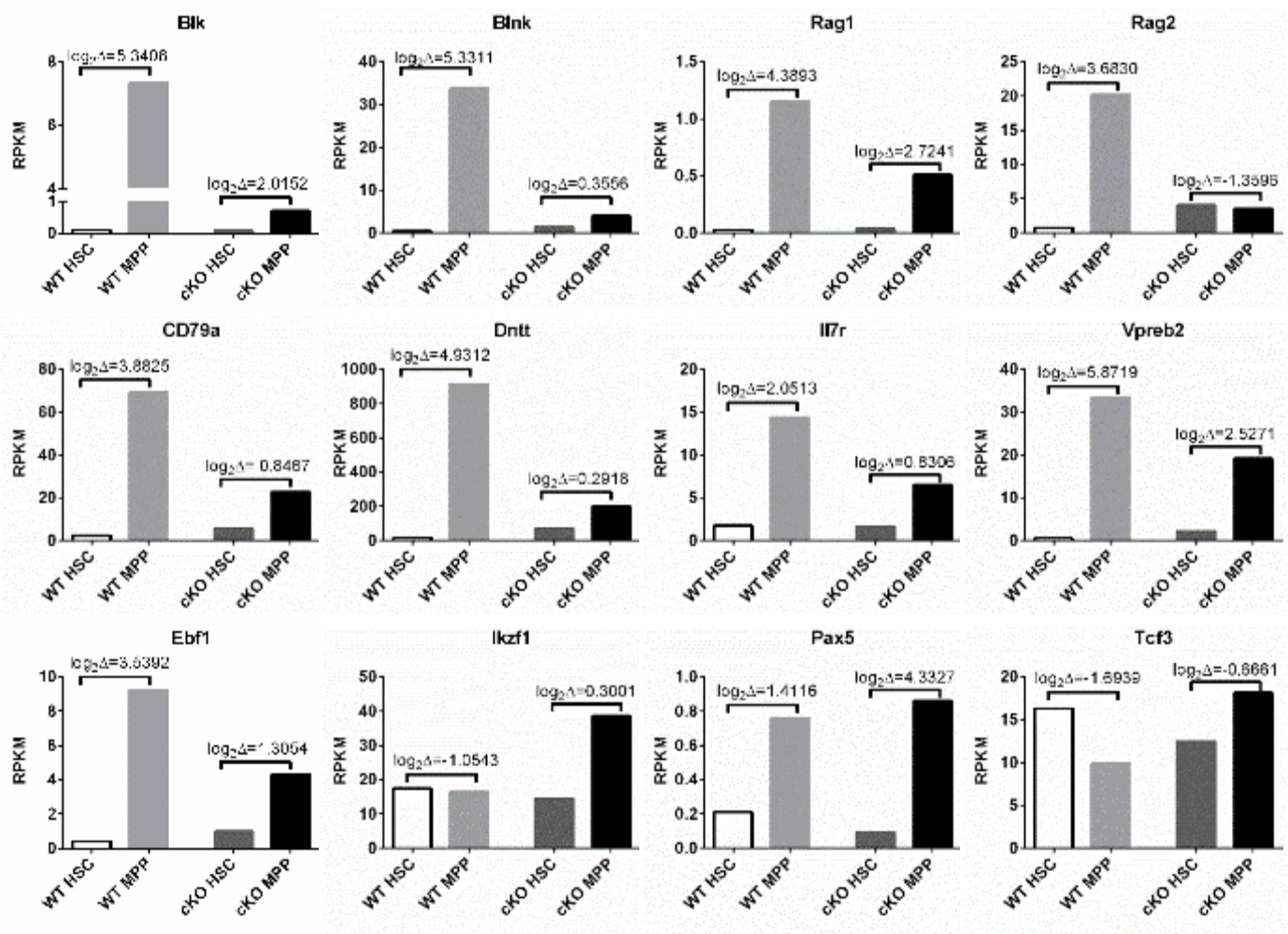

Figure 67. Hhex cKO MPPs are unable to upregulate lymphoid priming genes.

Genes are lymphoid specific transcripts that prime MPPs for lymphoid differentiation. Y-axes values are in RPKM, reads per kilobase of gene per million reads total. Brackets show $\log_2$ changes between HSC and MPP differentiation.

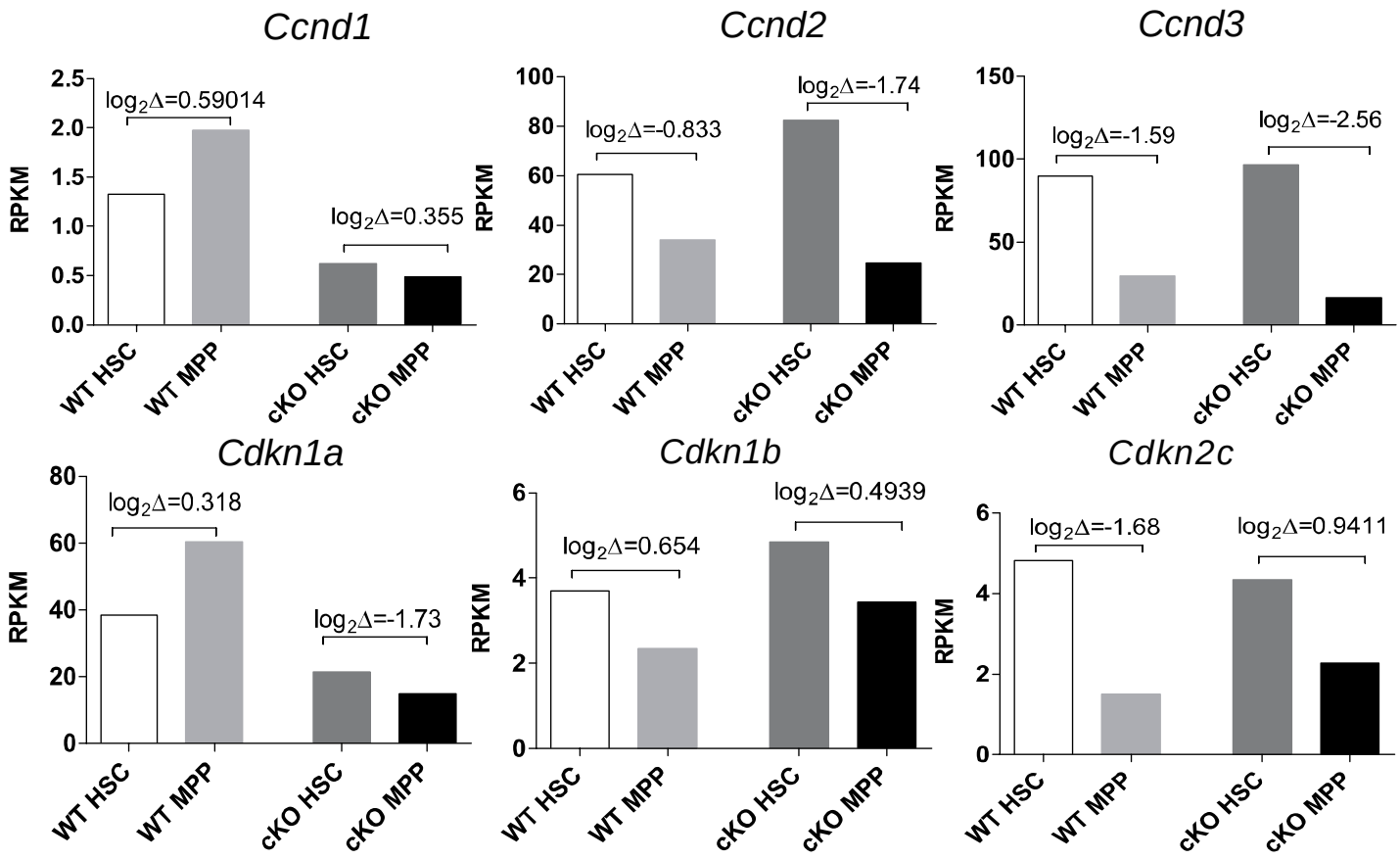

Figure 68. RNA seq analysis reveals a downregulation of Cdkn1a in Hhex cKO cells.

Bar graphs show RPKM values for RNA-seq of HSC and MPP cells sorted from WT or Hhex cKO mice for genes encoding cell cycle regulators. Brackets show log2 fold changes with HSC to MPP differentiation.

Discussion

Our data suggests that Hhex plays a role in the maintenance and proliferation of stem and progenitor cells. While at steady state, *Hhex cKO* mice showed a severe B-cell defect; however, stressed hematopoiesis revealed a more severe phenotype. In a bone marrow transplant setting we observed a lack of hematopoiesis from Hhex cKO donor cells in lethally irradiated host mice. In the setting of sublethal irradiation, *Hhex cKO* mice showed normal myeloid repopulation of the bone marrow but had a severe defect in B- and T-cell reconstitution of the bone marrow.

Quantification of the stem and progenitor populations revealed that the LT-HSCs were severely reduced in number at steady state, but all other progenitor populations were equivalent to WT. Proliferation studies showed that all the stem and progenitor populations had increased proliferation activity in Hhex cKO mice compared to WT mice. These data would suggest that the loss of Hhex may be perturbing the balance between differentiation and proliferation. The increased cycling in the stem and progenitor populations would explain the decreased number of total LT-HSCs and the inability of LT-HSCs to competitively repopulate irradiated host mice. *Cdkn1a* knockout mice showed increased cycling that led to stem cell exhaustion[160]. Gene expression analysis does suggest that this may be a result of reduced Cdkn1a mRNA but we have not investigated whether this may be a direct or indirect effect of Hhex.

Some transcription factors act as master regulators of HSCs, then are downregulated in progenitor cells and are subsequently upregregulated in

specific lineages. We believe that Hhex has a role in HSCs and a separate role in lymphoid development. Transcriptionally, Hhex cKO MPPs are able to downregulate genes with megakaryocyte-erythrocyte progenitor (MEP) potential but were unable to upregulate genes important for lymphoid priming.

CHAPTER VII

Hhex may require DNA binding for normal function

Background and Significance

DNA binding transcription factors are important regulators of gene expression. They often work in combination with non-DNA binding co-repressors and co-activators. Hhex is a DNA-binding transcription factor that is able to regulate genes through various mechanisms[64]. When Hhex is bound to DNA it can act as a transcriptional repressor by recruiting co-repressors such as members of the Groucho/TLE family[54,161-163]. Hhex can also act as an activator of transcription[56]. Hhex regulates transcription in a non-DNA binding manner by regulating the activity of other DNA binding transcription factors[164-166].

While extensive biochemical work on various point mutants of the Hhex protein has been done, little is known about the molecular requirements within the Hhex protein that are necessary for Hhex to function normally. To investigate the molecular determinants for Hhex function we used previously described Hhex mutants[62,161] (Figure 69) to determine if they rescued the lymphoid abnormalties seen in previous in vitro and in vivo studies.

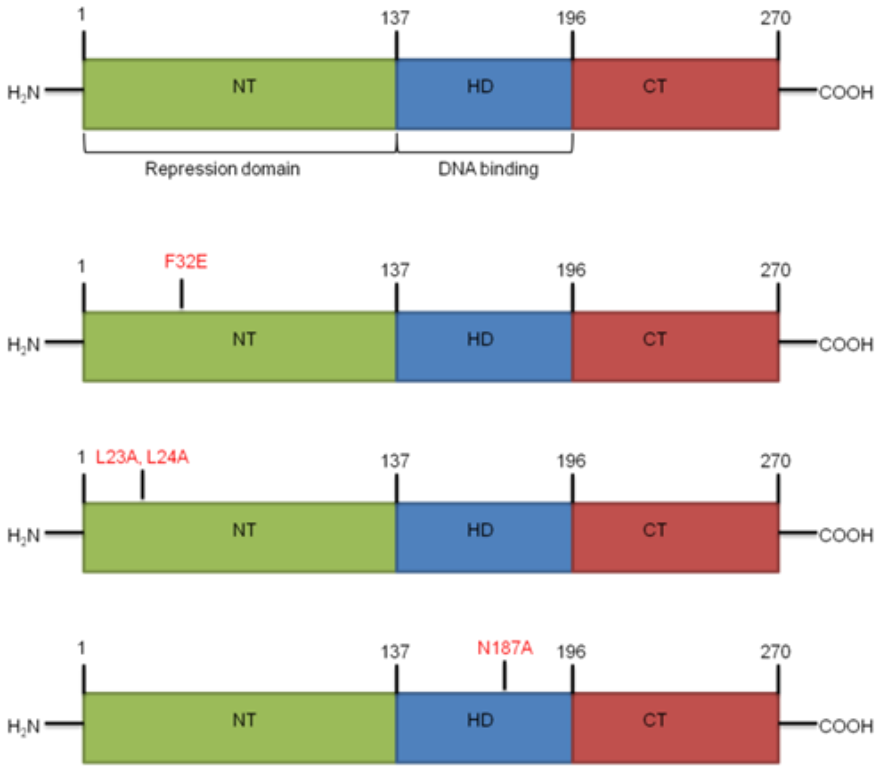

Figure 69. Hhex mutants tested.

The F32E point mutation is unable to bind members of the Groucho/TLE repressor proteins. The L23A, L24A double mutant is unable to bind to eIF-4E and is consequently defective in regulating Cyclin D1 mRNA. The N187A mutant is unable to bind DNA.

Preliminary results

Hhex requires DNA binding to induce T-cell differentiation block

To assess the molecular determinants for Hhex function in vitro, we retrovirally transduced double negative thymocytes from WT mice with mouse stem cell virus ires GFP(MIG) that expressed either WT Hhex, F32E Hhex, L23A, L24A Hhex, N187A Hhex or GFP only. Thymocytes were cocultured on OP9-DL1 stromal cells with cytokines Flt3L and IL7. To assess the expression of each retroviral construct GFP expression was quantified weekly using flow cytometry. GFP expression was lower in N187A Hhex when compared to WT Hhex, F32E Hhex, and L23A, L24A Hhex (Figure 70). This would suggest that unlike WT Hhex, the N187A mutant does not provide a growth advantage in thymocytes. Similar to previous studies, we observed an accumulation of double negative (DN) cells in the cultures that expressed WT Hhex. This accumulation was also observed with the expression of the F32E Hhex and L23A, L24A Hhex mutants, while the N187A mutant culture was able to differentiate to CD4 and CD8 double positive (DP) cells similar to WT and GFP only cultures (Figure 71). This would suggest that Hhex DNA binding ability is important for T cell transformation. Previously we observed an increase in the B cell antigen, B220, on T-cells expressing WT Hhex. We observed this trend in the F32E and L23A, L24A mutants but to a lesser extent compared to WT Hhex (Figure 72). This would suggest that the repressive activity of Hhex is important for B220 expression.

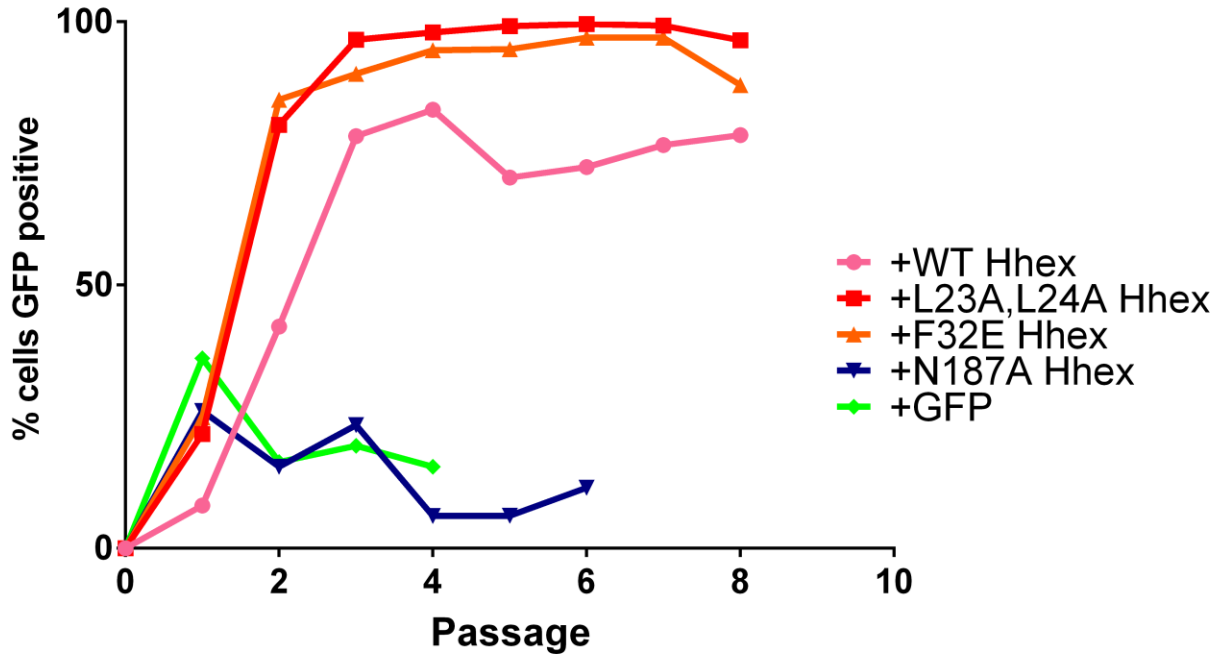

Figure 70. GFP expression in thymocytes transduced with Hhex mutants.

Double negative thymocytes were transduced with either MIG-WT Hhex, MIG-L23A, L24A Hhex, MIG-F32E Hhex, MIG-N187A Hhex or empty vector in the presence of cytokines. Every 7 days cells were analyzed for GFP positivity via flow cytometry. The x-axis shows the number of times each group was passaged and the y-axis shows the proportion of cells that were GFP positive.

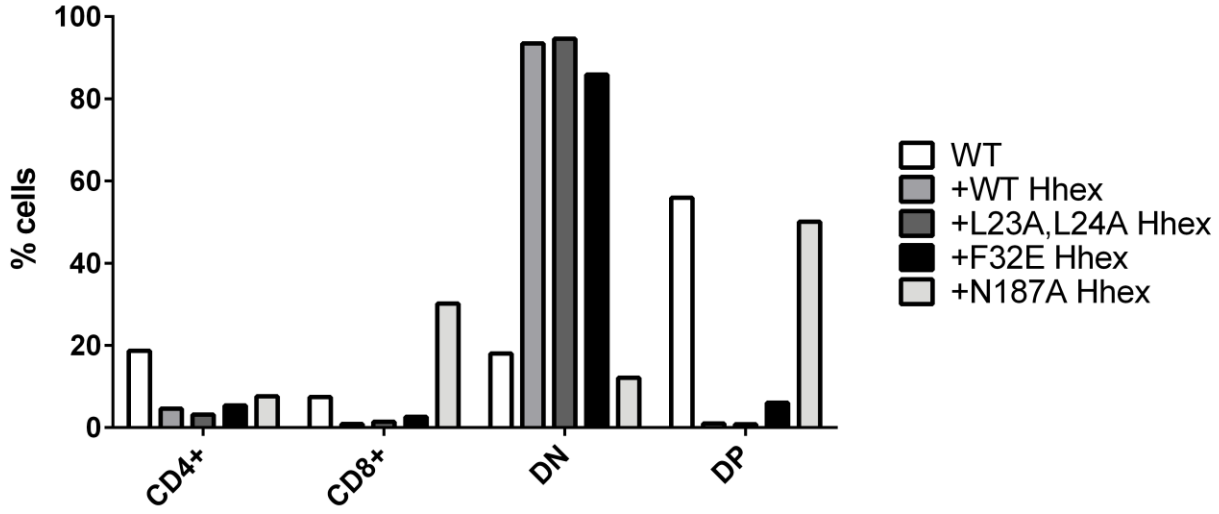

Figure 71. MIG-N187A Hhex cells do not accumulate at the DN stage of T cell differentiation.

Double negative thymocytes were transduced with either MIG-WT Hhex, MIG-L23A, L24A Hhex, MIG-F32E Hhex, MIG-N187A Hhex or empty vector in the presence of cytokines. Every 7 days cells were analyzed for CD8 and CD4 positivity via flow cytometry. Cells transduced with retrovirus were gated on for GFP^+ cells and then analyzed for CD4 and CD8 expression.

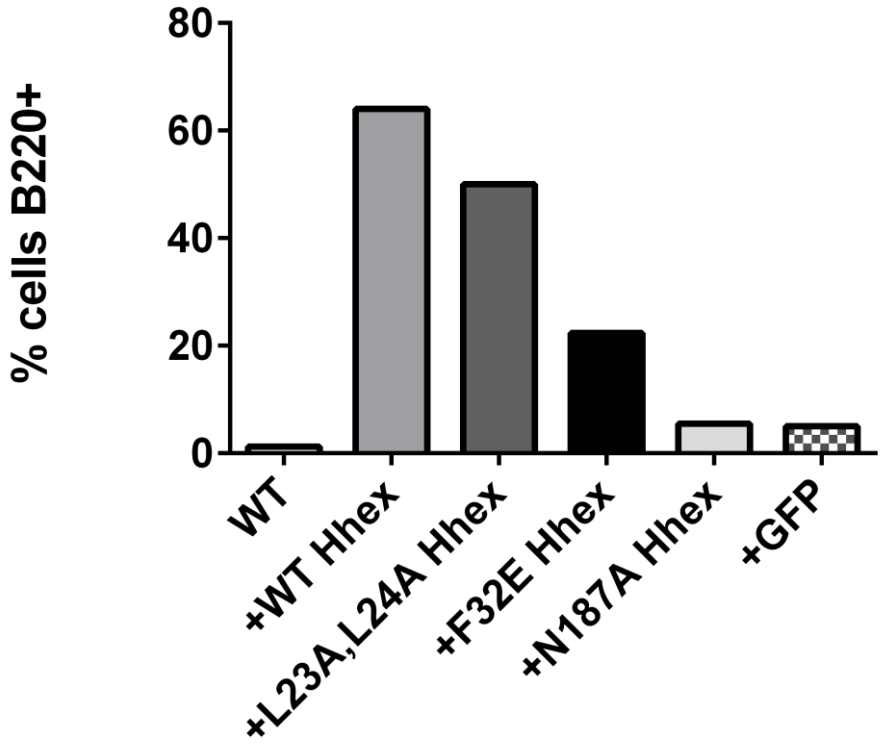

Figure 72. Loss of Hhex repression activity is important for B220 expression.

Double negative thymocytes were transduced with either MIG-WT Hhex, MIG-L23A, L24A Hhex, MIG-F32E Hhex, MIG-N187A Hhex or empty vector in the presence of cytokines. GFP^+ cells were assessed for B220 expression.

Hhex repression activity mutants are able to rescue Hhex defect in competitive repopulation bone marrow transplant

To assess the molecular determinants for Hhex in vivo, we performed a competitive repopulation bone marrow transplant assay. Hhex cKO bone marrow cells were retrovirally transduced with WT or mutant Hhex (Figure 69). Hhex cKO cells were mixed with B6.CD45.1 congenic bone marrow at a ratio of 6:1 CD45.2 to CD45.1. To assess the role of the various mutants in long-term hematopoiesis we assessed host and donor contributions in blood cells 16 weeks post-transplant. All mutant cells were able to contribute to the repopulation of the mononuclear cells of the bone marrow (Figure 73).

Since both transduced and untransduced CD45.2 donor cells were transplanted into lethally irradiated mice, GFP^+ and GFP^- cells were compared for their contributions to mature lineages. The GFP^+ mutant expressing cells contributed more to the B cells of the bone marrow and spleen compared to GFP^- cells (Figure 74). The proportion of myeloid cells was the same between GFP^+ and GFP^- cells in both bone marrow and spleen samples (Figure 75). Lastly, we observed an increase in the proportion of DN thymocytes expressing the L23A, L24A mutant (Figure 76). This result is similar to the results observed in the in vitro OP9-DL1 experiment.

Discussion

Our in vitro data suggests that DNA binding is critical for Hhex function. Expression of the N187A mutant in double negative thymocytes did not result in a T cell differentiation block. Both the F32E mutant and the L23A, L24A mutants

were able to induce similar differentiation blocks. In vivo analysis suggests Hhex can still function similar to WT Hhex. Further analysis will have to be done to fully elucidate the structure/function mechanism behind the role of Hhex in hematopoiesis.

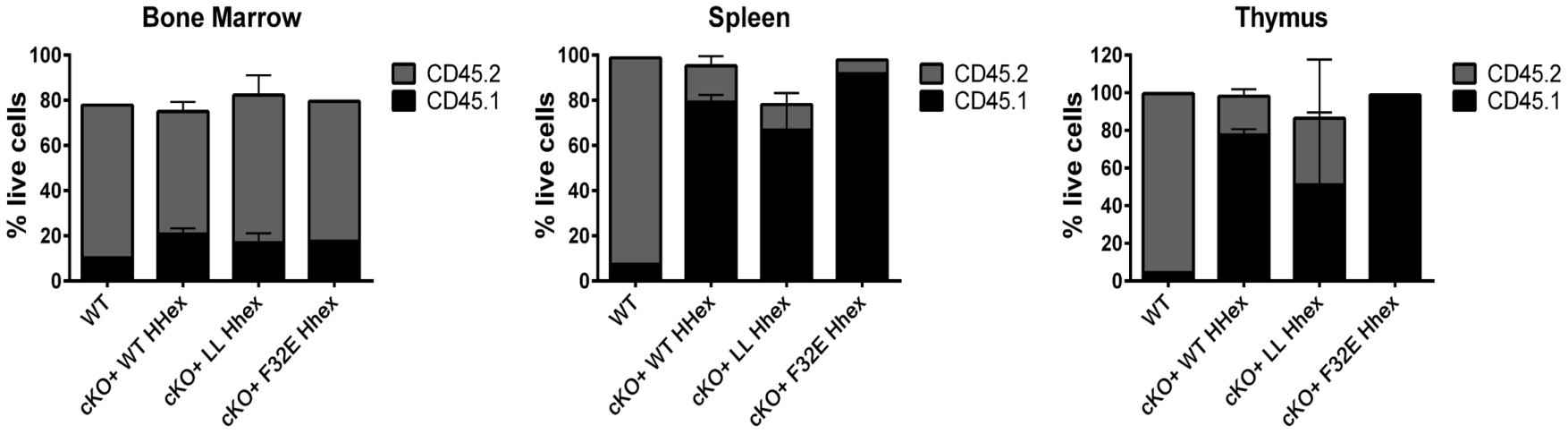

Figure 73. Hhex mutants contribute to the bone marrow of lethally irradiated host mice.

Sixteen weeks post-transplant mice were sacrificed and bone marrow, spleens and thymi were harvested and analyzed for CD45.1 and CD45.2 using flow cytometry.

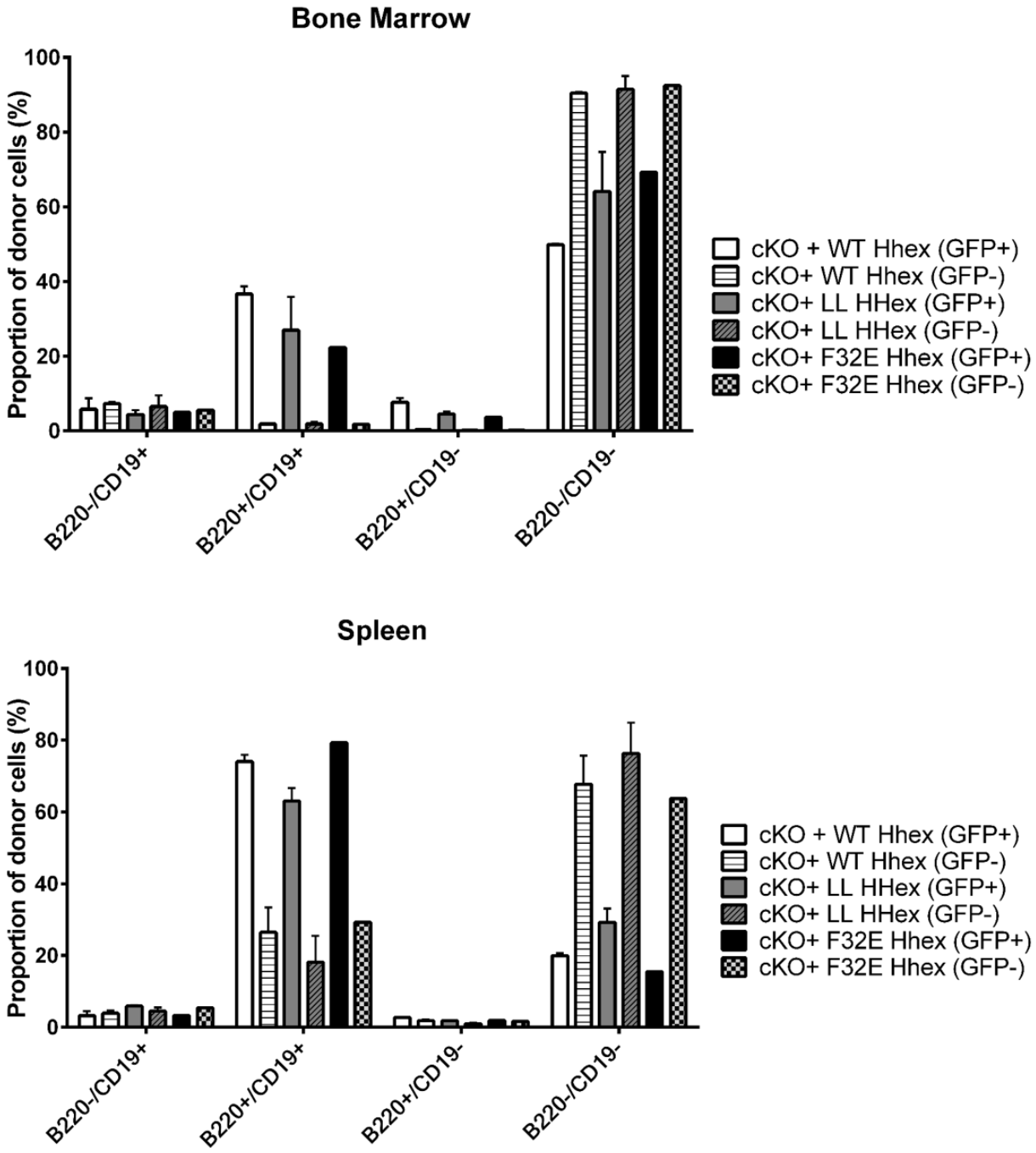

Figure 74. Hhex mutants are able to rescue B cell defect in Hhex cKO cells.

Proportion of donor B cells in the bone marrow and spleen of host mice 16 weeks after MIG-WT Hhex, MIG-L23A, L24A Hhex, or MIG-F32E Hhex, transduction and BMT are shown, gating on GFP^+ and GFP^- cells.

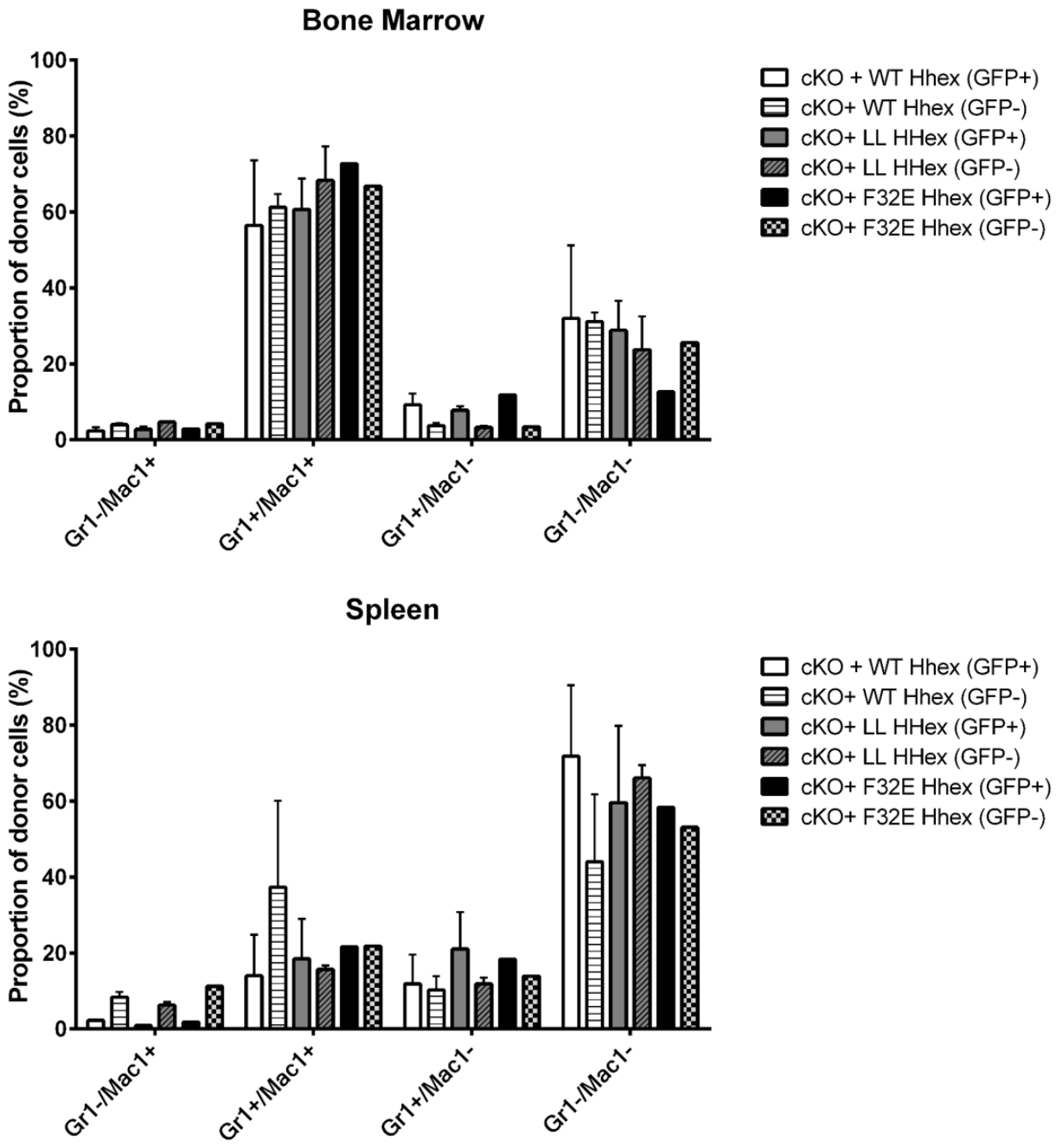

Figure 75. Hhex mutants have no effect on myeloid cells in BMT.

Proportion of donor myeloid cells in the bone marrow and spleen of host mice 16 weeks after MIG-WT Hhex, MIG-L23A, L24A Hhex, or MIG-F32E Hhex, transduction and BMT are shown, gating on GFP^+ and GFP^- cells.

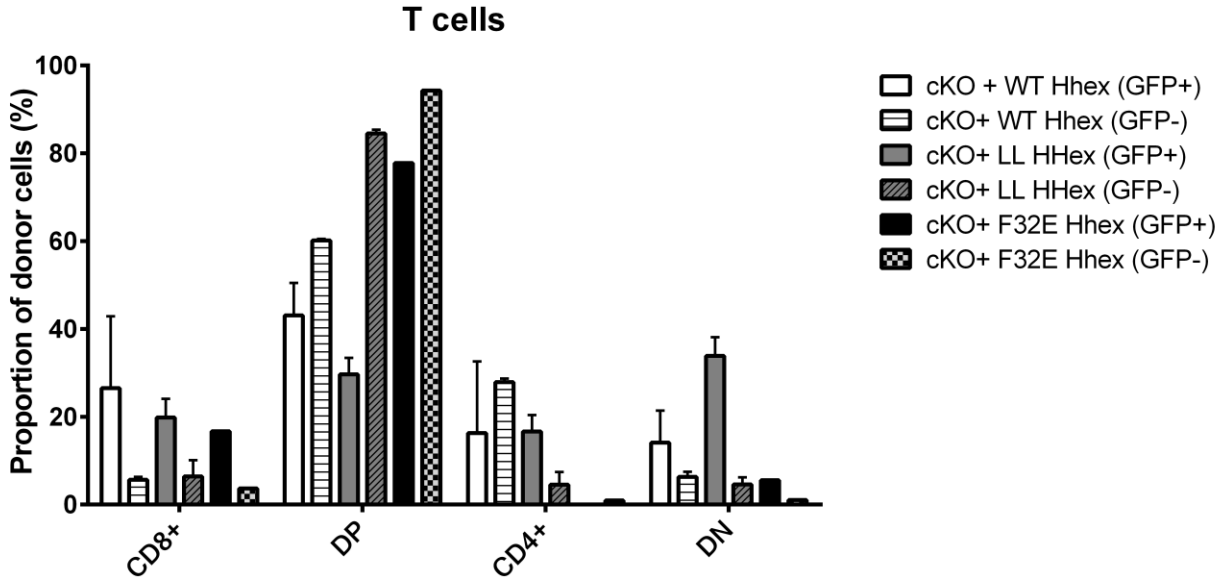

Figure 76. L23A, L24A mutant Hhex induced DN differentiation block in the thymus of lethally irradiated mice.

Proportion of donor T cells in the thymus of host mice 16 weeks after MIG-WT Hhex, MIG-L23A, L24A Hhex, or MIG-F32E Hhex, transduction and BMT are shown, gating on GFP^+ and GFP^- cells.

CHAPTER VIII

Summary and Future Directions

Summary

One of the most commonly mutated oncogenes in T-ALL is *LMO2*. Molecular studies and gene expression studies have led to two major mechanisms for Lmo2 induced T-ALL (Figure 4). One hypothesis is that Lmo2 and its binding partners create a functional deficiency of E2A proteins; which results in the inhibition of E2A target genes. The second hypothesis is that Lmo2-associated complexes can bind DNA and activate the Hhex gene; which plays a role in leukemogenesis. The primary goal of this work was to investigate both hypotheses to determine how Lmo2 induces T-ALL. This research also resulted in an understanding of the role of Hhex in normal adult hematopoiesis.

First we investigated whether Lmo2 induced T-ALLs require an E47 functional deficiency. CyQuant in vitro proliferation assay revealed that enforced E47 expression had no effect on Lmo2-induced T-ALL cell lines. However, two of the four Lmo2 induced T-ALL cell lines showed growth arrest upon enforced E47 homodimerization (Figure 8). Gene expression analysis of one sensitive and resistant cell line revealed striking differences in gene expression (Figure 17). One interesting finding was the lack of known Lmo2 binding partners in the sensitive lines, 020 and 080. Our data suggests that a functional defect of E47 is not a universal mechanism of Lmo2-inducing T-ALL.

To further investigate the development of Lmo2-induced T-ALL we looked at the role of Hhex in Lmo2-induced T-ALL development. We found that by

knocking out Hhex in an Lmo2 transgenic mouse model we were able to increase T-ALL latency in these mice, which spontaneously develop T-ALL (Figure 22). This information suggests that Hhex is important for T-ALL induction. While Hhex seemed to be a valuable target for T-ALL treatment, there was still more to learn about the role of Hhex in normal adult hematopoiesis.

To further understand the role of Hhex in adult hematopoiesis we characterized hematopoiesis in Hhex cKO mice induced by the vav-Cre transgene. While these mice appeared normal at birth, under closer inspection they exhibited three noteworthy phenotypes. At steady state, these mice showed severe absence of all B-cell subsets (Figure 34). Upon stressed hematopoiesis these mice showed a striking defect in stem and progenitor populations along with a T-cell deficiency that was not obvious at steady state (Figure 55, Figure 56, Figure 57, and Figure 58). Lastly, the Hhex cKO mice had significantly fewer long-term HSCs and increased cycling stem and progenitor cells when compared to WT mice (Figure 60 and Figure 64).

While Hhex may be a good target for T-ALL treatment, it may also play a significant role in adult hematopoiesis. Our Hhex cKO mouse model models various clinical situations; such as inadequate recovery of B- and T-cell immunity after incidences of stressed hematopoiesis such as post bone marrow transplantation, after chemotherapy, and after AIDS patients undergo highly active antiretroviral therapy (HAART). It would be interesting to determine whether variants within human *HHEX* or expression levels of this protein, influence this phenotype.

The loss of Hhex in *Hhex cKO* mice makes these cells unable to repopulate irradiated mice. Increased cycling of these cells may be exhausting the stem and progenitor populations in the *Hhex cKO* mice. It will be interesting to assess the ability of these cells to be serially transplanted. Since stem and progenitor cells in G1 phase of the cell cycle are unable to engraft compared to those in G0 phase. The increased cycling observed in *Hhex cKO* mice may be the reason for *Hhex cKO* cells being unable to compete with WT cells in competitive bone marrow transplant assays.

The loss of all B cell populations observed at steady state would suggest that Hhex is important for the transition from CLP to pro-B cells. On the other hand, the bone marrow transplant and sublethal irradiation experiments suggest that Hhex has a role in stem and progenitor differentiation as well. Transcription factors are active regulators of HSCs, then are downregulated in progenitors, then are upregulated again in lineage-specific gene regulation. We believe Hhex may be playing such a role in HSCs and also playing a separate role in B-cell development. Because *Hhex cKO* mice show defects in both myeloid and lymphoid development in sublethal irradiation experiments, we favor a role for Hhex in stem and progenitor differentiation.

Network analysis revealed an upregulation of the LPS and interferon beta 1 pathways, which may be driving the cycling and differentiation of HSCs. This may be also suggesting constitutive inflammatory stress in Hhex cKO stem and progenitor populations. It would be interesting to analyze these cells at steady state for markers of inflammatory stress.

Future Directions

Determine whether E2A proteins are important for the development of Lmo2-induced T-ALL

We will determine whether E2A proteins are important for the development of Lmo2-induced T-ALL. To determine whether E2A proteins are important for the development of Lmo2-induced T-ALL $Lmo2^{TG/+}$ mice that spontaneously develop T-ALL will be crossed with previously described $E2A^{ER/ER}$ mice[167]. Some mice will be treated with 4-hydroxytamoxifen, which will induce E2A protein expression and homodimerization. These mice will be aged to determine the onset of T-ALL. Upon development of T-ALL and we will treat mice with 4-hydroxytamoxifen to determine if E2A homodimerization is important for the development of T-ALL.

Assess Lmo2 and E47 binding partners in E47 resistant and sensitive lines

We propose to identify the binding partners of Lmo2 and E47 before and after enforced homodimerization in both sensitive and resistant cell lines. To identify binding partners, we will perform co-immunoprecipitations (co-IP) using antibodies against Lmo2 and E47. The identification of proteins interacting with these proteins will be identified using mass spectrometry. We can also identify complex sizes containing these proteins by performing HPLC analysis of the co-IP samples. This will give us preliminary insight into whether complexes are different between sensitive and resistant lines.

Identify direct targets of Hhex

Hhex has the ability to induce leukemia when overexpressed in T-cell lineages[168,169]. When expressed at elevated levels, Hhex also influences T-cell proliferation in transgenic mouse models[72]. It has also been shown that in the T-cell lineage Hhex functions as an oncogene[71]. Hhex is also upregulated in Lmo2 overexpressing T-cell acute lymphoblastic leukemia (T-ALL). Previous studies have shown Lmo2 and Hhex are coexpressed in an oncogenic gene signature[170].

We will identify genes that are directly regulated by Hhex in T-ALL induction. Unfortunately, current commercially available antibodies are inadequate to perform chromatin immunoprecipitations. However, we have found other methods for identifying Hhex target genes[171].

Timing has been shown to be an important criterion for identifying target genes. It has been shown that genes that are switched on shortly after the activation of a transcription factor are more likely to be activated by that transcription factor. Because there will not have been enough time for another gene to be activated and then activate the target gene[172-174].

We will transduce HSCs and T-cell progenitors taken from Hhex cKO mice with an inducible Hhex vector. Hhex expression will be induced in the presence of cyclohexamide. In the presence of cyclohexamide target genes cannot be translated so they cannot switch on further downstream genes as indirect targets.

We will also use the DNA adenine methyltransferase identification (DamID)[175-177] method to identify Hhex targets. Hhex will be fused to DNA methyltransferase. The binding of Hhex to DNA will localize the

methyltransferase in the region of the binding site. Adenosine methylation does not occur naturally in eukaryotes and therefore the presence of adenine methylation in any region can be concluded to have been caused by Hhex binding, which would imply that the region is located near a binding site.

References

1 Reya, T., Morrison, S. J., Clarke, M. F. & Weissman, I. L. Stem cells, cancer, and cancer stem cells. *Nature* **414**, 105-111, doi:10.1038/35102167 (2001).

2 Kondo, M., Weissman, I. L. & Akashi, K. Identification of clonogenic common lymphoid progenitors in mouse bone marrow. *Cell* **91**, 661-672 (1997).

3 Akashi, K., Traver, D., Miyamoto, T. & Weissman, I. L. A clonogenic common myeloid progenitor that gives rise to all myeloid lineages. *Nature* **404**, 193-197, doi:10.1038/35004599 (2000).

4 Adolfsson, J. *et al.* Identification of Flt3+ lympho-myeloid stem cells lacking erythro-megakaryocytic potential a revised road map for adult blood lineage commitment. *Cell* **121**, 295-306, doi:10.1016/j.cell.2005.02.013 (2005).

5 Till, J. E. & Mc, C. E. A direct measurement of the radiation sensitivity of normal mouse bone marrow cells. *Radiation research* **14**, 213-222 (1961).

6 Wognum, A. W., Eaves, A. C. & Thomas, T. E. Identification and isolation of hematopoietic stem cells. *Archives of medical research* **34**, 461-475, doi:10.1016/j.arcmed.2003.09.008 (2003).

7 Orford, K. W. & Scadden, D. T. Deconstructing stem cell self-renewal: genetic insights into cell-cycle regulation. *Nature reviews. Genetics* **9**, 115-128, doi:10.1038/nrg2269 (2008).

8 Osawa, M. *et al.* In vivo self-renewal of c-Kit+ Sca-1+ Lin(low/-) hemopoietic stem cells. *J Immunol* **156**, 3207-3214 (1996).

9 Purton, L. E. & Scadden, D. T. Limiting factors in murine hematopoietic stem cell assays. *Cell stem cell* **1**, 263-270, doi:10.1016/j.stem.2007.08.016 (2007).

10 Warr, M. R., Pietras, E. M. & Passegue, E. Mechanisms controlling hematopoietic stem cell functions during normal hematopoiesis and

hematological malignancies. *Wiley interdisciplinary reviews. Systems biology and medicine* **3**, 681-701, doi:10.1002/wsbm.145 (2011).

11 Bryder, D., Rossi, D. J. & Weissman, I. L. Hematopoietic stem cells: the paradigmatic tissue-specific stem cell. *The American journal of pathology* **169**, 338-346, doi:10.2353/ajpath.2006.060312 (2006).

12 Challen, G. A., Boles, N., Lin, K. K. & Goodell, M. A. Mouse hematopoietic stem cell identification and analysis. *Cytometry. Part A : the journal of the International Society for Analytical Cytology* **75**, 14-24, doi:10.1002/cyto.a.20674 (2009).

13 Adolfsson, J. *et al.* Upregulation of Flt3 expression within the bone marrow Lin(-)Sca1(+)c-kit(+) stem cell compartment is accompanied by loss of self-renewal capacity. *Immunity* **15**, 659-669 (2001).

14 Christensen, J. L. & Weissman, I. L. Flk-2 is a marker in hematopoietic stem cell differentiation: a simple method to isolate long-term stem cells. *Proceedings of the National Academy of Sciences of the United States of America* **98**, 14541-14546, doi:10.1073/pnas.261562798 (2001).

15 Kiel, M. J. *et al.* SLAM family receptors distinguish hematopoietic stem and progenitor cells and reveal endothelial niches for stem cells. *Cell* **121**, 1109-1121, doi:10.1016/j.cell.2005.05.026 (2005).

16 Osawa, M., Hanada, K., Hamada, H. & Nakauchi, H. Long-term lymphohematopoietic reconstitution by a single CD34-low/negative hematopoietic stem cell. *Science* **273**, 242-245 (1996).

17 Spangrude, G. J., Heimfeld, S. & Weissman, I. L. Purification and characterization of mouse hematopoietic stem cells. *Science* **241**, 58-62 (1988).

18 Wilson, A. *et al.* Hematopoietic Stem Cells Reversibly Switch from Dormancy to Self-Renewal during Homeostasis and Repair. *Cell* **135**, 1118-1129, doi:DOI 10.1016/j.cell.2008.10.048 (2008).

19 Denning-Kendall, P., Singha, S., Bradley, B. & Hows, J. Cobblestone area-forming cells in human cord blood are heterogeneous and differ from

long-term culture-initiating cells. *Stem Cells* **21**, 694-701, doi:10.1634/stemcells.21-6-694 (2003).

20 Pettengell, R. *et al.* Direct comparison by limiting dilution analysis of long-term culture-initiating cells in human bone marrow, umbilical cord blood, and blood stem cells. *Blood* **84**, 3653-3659 (1994).

21 Szilvassy, S. J., Humphries, R. K., Lansdorp, P. M., Eaves, A. C. & Eaves, C. J. Quantitative assay for totipotent reconstituting hematopoietic stem cells by a competitive repopulation strategy. *Proceedings of the National Academy of Sciences of the United States of America* **87**, 8736-8740 (1990).

22 Enver, T., Heyworth, C. M. & Dexter, T. M. Do stem cells play dice? *Blood* **92**, 348-351; discussion 352 (1998).

23 Muller-Sieburg, C. E., Cho, R. H., Thoman, M., Adkins, B. & Sieburg, H. B. Deterministic regulation of hematopoietic stem cell self-renewal and differentiation. *Blood* **100**, 1302-1309 (2002).

24 Wagers, A. J., Christensen, J. L. & Weissman, I. L. Cell fate determination from stem cells. *Gene therapy* **9**, 606-612, doi:10.1038/sj.gt.3301717 (2002).

25 Lajtha, L. G. On the Concept of the Cell Cycle. *Journal of cellular physiology* **62**, SUPPL1:143-145 (1963).

26 Drize, N. J., Keller, J. R. & Chertkov, J. L. Local clonal analysis of the hematopoietic system shows that multiple small short-living clones maintain life-long hematopoiesis in reconstituted mice. *Blood* **88**, 2927-2938 (1996).

27 Abkowitz, J. L. *et al.* Behavior of hematopoietic stem cells in a large animal. *Proceedings of the National Academy of Sciences of the United States of America* **92**, 2031-2035 (1995).

28 Jordan, C. T. & Lemischka, I. R. Clonal and systemic analysis of long-term hematopoiesis in the mouse. *Genes & development* **4**, 220-232 (1990).

29 McKenzie, J. L., Gan, O. I., Doedens, M., Wang, J. C. & Dick, J. E. Individual stem cells with highly variable proliferation and self-renewal properties comprise the human hematopoietic stem cell compartment. *Nature immunology* **7**, 1225-1233, doi:10.1038/ni1393 (2006).

30 Buza-Vidas, N. *et al.* Cytokines regulate postnatal hematopoietic stem cell expansion: opposing roles of thrombopoietin and LNK. *Genes & development* **20**, 2018-2023, doi:10.1101/gad.385606 (2006).

31 Ema, H. *et al.* Quantification of self-renewal capacity in single hematopoietic stem cells from normal and Lnk-deficient mice. *Developmental cell* **8**, 907-914, doi:10.1016/j.devcel.2005.03.019 (2005).

32 Lessard, J. & Sauvageau, G. Bmi-1 determines the proliferative capacity of normal and leukaemic stem cells. *Nature* **423**, 255-260, doi:10.1038/nature01572 (2003).

33 Park, I. K. *et al.* Bmi-1 is required for maintenance of adult self-renewing haematopoietic stem cells. *Nature* **423**, 302-305, doi:10.1038/nature01587 (2003).

34 Sauvageau, G. *et al.* Overexpression of HOXB4 in hematopoietic cells causes the selective expansion of more primitive populations in vitro and in vivo. *Genes & development* **9**, 1753-1765 (1995).

35 Bhardwaj, G. *et al.* Sonic hedgehog induces the proliferation of primitive human hematopoietic cells via BMP regulation. *Nature immunology* **2**, 172-180, doi:10.1038/84282 (2001).

36 Varnum-Finney, B. *et al.* Pluripotent, cytokine-dependent, hematopoietic stem cells are immortalized by constitutive Notch1 signaling. *Nature medicine* **6**, 1278-1281, doi:10.1038/81390 (2000).

37 Reya, T. *et al.* A role for Wnt signalling in self-renewal of haematopoietic stem cells. *Nature* **423**, 409-414, doi:10.1038/nature01593 (2003).

38 Jacobson, M. D., Weil, M. & Raff, M. C. Programmed cell death in animal development. *Cell* **88**, 347-354 (1997).

39 Domen, J. The role of apoptosis in regulating hematopoietic stem cell numbers. *Apoptosis : an international journal on programmed cell death* **6**, 239-252 (2001).

40 Domen, J., Cheshier, S. H. & Weissman, I. L. The role of apoptosis in the regulation of hematopoietic stem cells: Overexpression of Bcl-2 increases both their number and repopulation potential. *The Journal of experimental medicine* **191**, 253-264 (2000).

41 Orkin, S. H. & Zon, L. I. Hematopoiesis: an evolving paradigm for stem cell biology. *Cell* **132**, 631-644, doi:10.1016/j.cell.2008.01.025 (2008).

42 Orkin, S. H. Priming the hematopoietic pump. *Immunity* **19**, 633-634 (2003).

43 Enver, T. & Greaves, M. Loops, lineage, and leukemia. *Cell* **94**, 9-12 (1998).

44 Passegue, E., Jamieson, C. H., Ailles, L. E. & Weissman, I. L. Normal and leukemic hematopoiesis: are leukemias a stem cell disorder or a reacquisition of stem cell characteristics? *Proceedings of the National Academy of Sciences of the United States of America* **100 Suppl 1**, 11842-11849, doi:10.1073/pnas.2034201100 (2003).

45 Engel, I. & Murre, C. The function of E- and Id proteins in lymphocyte development. *Nature reviews. Immunology* **1**, 193-199, doi:10.1038/35105060 (2001).

46 Murre, C. Helix-loop-helix proteins and lymphocyte development. *Nature immunology* **6**, 1079-1086, doi:10.1038/ni1260 (2005).

47 Kee, B. L. E and ID proteins branch out. *Nature reviews. Immunology* **9**, 175-184, doi:10.1038/nri2507 (2009).

48 Murre, C., McCaw, P. S. & Baltimore, D. A new DNA binding and dimerization motif in immunoglobulin enhancer binding, daughterless, MyoD, and myc proteins. *Cell* **56**, 777-783 (1989).

49 Wang, D. *et al.* The basic helix-loop-helix transcription factor HEBAlt is expressed in pro-T cells and enhances the generation of T cell precursors. *J Immunol* **177**, 109-119 (2006).

50 Massari, M. E. & Murre, C. Helix-loop-helix proteins: regulators of transcription in eucaryotic organisms. *Molecular and cellular biology* **20**, 429-440 (2000).

51 Yan, W. *et al.* High incidence of T-cell tumors in E2A-null mice and E2A/Id1 double-knockout mice. *Molecular and cellular biology* **17**, 7317-7327 (1997).

52 Crompton, M. R. *et al.* Identification of a novel vertebrate homeobox gene expressed in haematopoietic cells. *Nucleic acids research* **20**, 5661-5667 (1992).

53 Soufi, A., Smith, C., Clarke, A. R., Gaston, K. & Jayaraman, P. S. Oligomerisation of the developmental regulator proline rich homeodomain (PRH/Hex) is mediated by a novel proline-rich dimerisation domain. *Journal of molecular biology* **358**, 943-962, doi:10.1016/j.jmb.2006.02.020 (2006).

54 Swingler, T. E., Bess, K. L., Yao, J., Stifani, S. & Jayaraman, P. S. The proline-rich homeodomain protein recruits members of the Groucho/Transducin-like enhancer of split protein family to co-repress transcription in hematopoietic cells. *The Journal of biological chemistry* **279**, 34938-34947, doi:10.1074/jbc.M404488200 (2004).

55 Topcu, Z., Mack, D. L., Hromas, R. A. & Borden, K. L. The promyelocytic leukemia protein PML interacts with the proline-rich homeodomain protein PRH: a RING may link hematopoiesis and growth control. *Oncogene* **18**, 7091-7100, doi:10.1038/sj.onc.1203201 (1999).

56 Denson, L. A., Karpen, S. J., Bogue, C. W. & Jacobs, H. C. Divergent homeobox gene hex regulates promoter of the Na(+)-dependent bile acid cotransporter. *American journal of physiology. Gastrointestinal and liver physiology* **279**, G347-355 (2000).

57 Kasamatsu, S. *et al.* Identification of the transactivating region of the homeodomain protein, hex. *Journal of biochemistry* **135**, 217-223 (2004).

58 Cong, R. *et al.* Hhex is a direct repressor of endothelial cell-specific molecule 1 (ESM-1). *Biochemical and biophysical research communications* **346**, 535-545, doi:10.1016/j.bbrc.2006.05.153 (2006).

59 Guiral, M., Bess, K., Goodwin, G. & Jayaraman, P. S. PRH represses transcription in hematopoietic cells by at least two independent mechanisms. *J Biol Chem* **276**, 2961-2970, doi:10.1074/jbc.M004948200 M004948200 [pii] (2001).

60 Hallaq, H. *et al.* A null mutation of Hhex results in abnormal cardiac development, defective vasculogenesis and elevated Vegfa levels. *Development* **131**, 5197-5209, doi:10.1242/dev.01393 (2004).

61 Manfioletti, G. *et al.* Differential expression of a novel proline-rich homeobox gene (Prh) in human hematolymphopoietic cells. *Blood* **85**, 1237-1245 (1995).

62 Noy, P., Williams, H., Sawasdichai, A., Gaston, K. & Jayaraman, P. S. PRH/Hhex controls cell survival through coordinate transcriptional regulation of vascular endothelial growth factor signaling. *Molecular and cellular biology* **30**, 2120-2134, doi:10.1128/MCB.01511-09 (2010).

63 Soufi, A., Gaston, K. & Jayaraman, P. S. Purification and characterisation of the PRH homeodomain: Removal of the N-terminal domain of PRH increases the PRH homeodomain-DNA interaction. *International journal of biological macromolecules* **39**, 45-50, doi:10.1016/j.ijbiomac.2006.01.004 (2006).

64 Soufi, A. & Jayaraman, P. S. PRH/Hex: an oligomeric transcription factor and multifunctional regulator of cell fate. *The Biochemical journal* **412**, 399-413, doi:10.1042/BJ20080035 (2008).

65 Soufi, A. *et al.* CK2 phosphorylation of the PRH/Hex homeodomain functions as a reversible switch for DNA binding. *Nucleic acids research* **37**, 3288-3300, doi:10.1093/nar/gkp197 (2009).

66 Tanaka, T. *et al.* cDNA cloning and expression of rat homeobox gene, Hex, and functional characterization of the protein. *The Biochemical journal* **339 (Pt 1)**, 111-117 (1999).

67 Bogue, C. W., Zhang, P. X., McGrath, J., Jacobs, H. C. & Fuleihan, R. L. Impaired B cell development and function in mice with a targeted disruption of the homeobox gene Hex. *Proceedings of the National Academy of Sciences of the United States of America* **100**, 556-561, doi:10.1073/pnas.0236979100 (2003).

68 Keng, V. W. *et al.* Homeobox gene Hex is essential for onset of mouse embryonic liver development and differentiation of the monocyte lineage. *Biochemical and biophysical research communications* **276**, 1155-1161, doi:10.1006/bbrc.2000.3548 (2000).

69 Ghosh, B. *et al.* Immunocytochemical characterization of murine Hex, a homeobox-containing protein. *Pediatric research* **48**, 634-638, doi:10.1203/00006450-200011000-00014 (2000).

70 Newman, C. S., Chia, F. & Krieg, P. A. The XHex homeobox gene is expressed during development of the vascular endothelium: overexpression leads to an increase in vascular endothelial cell number. *Mechanisms of development* **66**, 83-93 (1997).

71 George, A., Morse, H. C., 3rd & Justice, M. J. The homeobox gene Hex induces T-cell-derived lymphomas when overexpressed in hematopoietic precursor cells. *Oncogene* **22**, 6764-6773, doi:10.1038/sj.onc.1206822 (2003).

72 Mack, D. L. *et al.* Down-regulation of the myeloid homeobox protein Hex is essential for normal T-cell development. *Immunology* **107**, 444-451 (2002).

73 Topisirovic, I. *et al.* The proline-rich homeodomain protein, PRH, is a tissue-specific inhibitor of eIF4E-dependent cyclin D1 mRNA transport and growth. *The EMBO journal* **22**, 689-703, doi:10.1093/emboj/cdg069 (2003).

74 Lacroix, L. *et al.* HEX, PAX-8 and TTF-1 gene expression in human thyroid tissues: a comparative analysis with other genes involved in iodide metabolism. *Clinical endocrinology* **64**, 398-404, doi:10.1111/j.1365-2265.2006.02477.x (2006).

75 D'Elia, A. V. *et al.* Expression and localization of the homeodomain-containing protein HEX in human thyroid tumors. *The Journal of clinical*

endocrinology and metabolism **87**, 1376-1383, doi:10.1210/jcem.87.3.8344 (2002).

76 Topisirovic, I. *et al.* Aberrant eukaryotic translation initiation factor 4E-dependent mRNA transport impedes hematopoietic differentiation and contributes to leukemogenesis. *Molecular and cellular biology* **23**, 8992-9002 (2003).

77 Chiaretti, S. & Foa, R. T-cell acute lymphoblastic leukemia. *Haematologica* **94**, 160-162, doi:10.3324/haematol.2008.004150 (2009).

78 De Keersmaecker, K., Marynen, P. & Cools, J. Genetic insights in the pathogenesis of T-cell acute lymphoblastic leukemia. *Haematologica* **90**, 1116-1127 (2005).

79 Goldberg, J. M. *et al.* Childhood T-cell acute lymphoblastic leukemia: the Dana-Farber Cancer Institute acute lymphoblastic leukemia consortium experience. *Journal of clinical oncology : official journal of the American Society of Clinical Oncology* **21**, 3616-3622, doi:10.1200/JCO.2003.10.116 (2003).

80 Marks, D. I. *et al.* T-cell acute lymphoblastic leukemia in adults: clinical features, immunophenotype, cytogenetics, and outcome from the large randomized prospective trial (UKALL XII/ECOG 2993). *Blood* **114**, 5136-5145, doi:10.1182/blood-2009-08-231217 (2009).

81 Boehm, T., Foroni, L., Kaneko, Y., Perutz, M. F. & Rabbitts, T. H. The rhombotin family of cysteine-rich LIM-domain oncogenes: distinct members are involved in T-cell translocations to human chromosomes 11p15 and 11p13. *Proceedings of the National Academy of Sciences of the United States of America* **88**, 4367-4371 (1991).

82 McGuire, E. A. *et al.* The t(11;14)(p15;q11) in a T-cell acute lymphoblastic leukemia cell line activates multiple transcripts, including Ttg-1, a gene encoding a potential zinc finger protein. *Molecular and cellular biology* **9**, 2124-2132 (1989).

83 Royer-Pokora, B., Loos, U. & Ludwig, W. D. TTG-2, a new gene encoding a cysteine-rich protein with the LIM motif, is overexpressed in acute T-cell leukaemia with the t(11;14)(p13;q11). *Oncogene* **6**, 1887-1893 (1991).

84 Boehm, T. *et al.* The mechanism of chromosomal translocation t(11;14) involving the T-cell receptor C delta locus on human chromosome 14q11 and a transcribed region of chromosome 11p15. *The EMBO journal* **7**, 385-394 (1988).

85 Nam, C.-H. & Rabbitts, T. H. The role of LMO2 in development and in T cell leukemia after chromosomal translocation or retroviral insertion. *Molecular therapy : the journal of the American Society of Gene Therapy* **13**, 15-25 (2006).

86 Armstrong, S. A. & Look, A. T. Molecular genetics of acute lymphoblastic leukemia. *Journal of clinical oncology : official journal of the American Society of Clinical Oncology* **23**, 6306-6315, doi:10.1200/JCO.2005.05.047 (2005).

87 Look, A. T. Oncogenic transcription factors in the human acute leukemias. *Science* **278**, 1059-1064 (1997).

88 Boehm, T., Buluwela, L., Williams, D., White, L. & Rabbitts, T. H. A cluster of chromosome 11p13 translocations found via distinct D-D and D-D-J rearrangements of the human T cell receptor delta chain gene. *The EMBO journal* **7**, 2011-2017 (1988).

89 Hacein-Bey-Abina, S. *et al.* A serious adverse event after successful gene therapy for X-linked severe combined immunodeficiency. *The New England journal of medicine* **348**, 255-256, doi:10.1056/NEJM200301163480314 (2003).

90 Hacein-Bey-Abina, S. *et al.* LMO2-associated clonal T cell proliferation in two patients after gene therapy for SCID-X1. *Science* **302**, 415-419, doi:10.1126/science.1088547 (2003).

91 Schmidt, M. *et al.* Clonal evidence for the transduction of CD34+ cells with lymphomyeloid differentiation potential and self-renewal capacity in the SCID-X1 gene therapy trial. *Blood* **105**, 2699-2706, doi:10.1182/blood-2004-07-2648 (2005).

92 Nam, C. H. & Rabbitts, T. H. The role of LMO2 in development and in T cell leukemia after chromosomal translocation or retroviral insertion. *Molecular therapy : the journal of the American Society of Gene Therapy* **13**, 15-25, doi:10.1016/j.ymthe.2005.09.010 (2006).

93 Warren, A. J. *et al.* The oncogenic cysteine-rich LIM domain protein rbtn2 is essential for erythroid development. *Cell* **78**, 45-57 (1994).

94 Gering, M., Yamada, Y., Rabbitts, T. H. & Patient, R. K. Lmo2 and Scl/Tal1 convert non-axial mesoderm into haemangioblasts which differentiate into endothelial cells in the absence of Gata1. *Development* **130**, 6187-6199, doi:10.1242/dev.00875 (2003).

95 Mead, P. E., Deconinck, A. E., Huber, T. L., Orkin, S. H. & Zon, L. I. Primitive erythropoiesis in the Xenopus embryo: the synergistic role of LMO-2, SCL and GATA-binding proteins. *Development* **128**, 2301-2308 (2001).

96 Yamada, Y. *et al.* The T cell leukemia LIM protein Lmo2 is necessary for adult mouse hematopoiesis. *Proceedings of the National Academy of Sciences of the United States of America* **95**, 3890-3895 (1998).

97 Grutz, G. G. *et al.* The oncogenic T cell LIM-protein Lmo2 forms part of a DNA-binding complex specifically in immature T cells. *The EMBO journal* **17**, 4594-4605, doi:10.1093/emboj/17.16.4594 (1998).

98 Valge-Archer, V. E. *et al.* The LIM protein RBTN2 and the basic helix-loop-helix protein TAL1 are present in a complex in erythroid cells. *Proceedings of the National Academy of Sciences of the United States of America* **91**, 8617-8621 (1994).

99 Wadman, I. *et al.* Specific in vivo association between the bHLH and LIM proteins implicated in human T cell leukemia. *The EMBO journal* **13**, 4831-4839 (1994).

100 Wadman, I. A. *et al.* The LIM-only protein Lmo2 is a bridging molecule assembling an erythroid, DNA-binding complex which includes the TAL1, E47, GATA-1 and Ldb1/NLI proteins. *The EMBO journal* **16**, 3145-3157, doi:10.1093/emboj/16.11.3145 (1997).

101 El Omari, K. *et al.* Structural Basis for LMO2-Driven Recruitment of the SCL:E47bHLH Heterodimer to Hematopoietic-Specific Transcriptional Targets. *CellReports* **4**, 135-147, doi:10.1016/j.celrep.2013.06.008 (2013).

102 El Omari, K. *et al.* Structure of the leukemia oncogene LMO2: implications for the assembly of a hematopoietic transcription factor complex. *Blood* **117**, 2146-2156, doi:10.1182/blood-2010-07-293357 (2011).

103 Archer, V. E. *et al.* Cysteine-rich LIM domains of LIM-homeodomain and LIM-only proteins contain zinc but not iron. *Proceedings of the National Academy of Sciences of the United States of America* **91**, 316-320 (1994).

104 Smith, S. *et al.* LIM domain only-2 (LMO2) induces T-cell leukemia by two distinct pathways. *PloS one* **9**, e85883, doi:10.1371/journal.pone.0085883 (2014).

105 Ono, Y., Fukuhara, N. & Yoshie, O. TAL1 and LIM-only proteins synergistically induce retinaldehyde dehydrogenase 2 expression in T-cell acute lymphoblastic leukemia by acting as cofactors for GATA3. *Molecular and cellular biology* **18**, 6939-6950 (1998).

106 Ferrando, A. A. *et al.* Biallelic transcriptional activation of oncogenic transcription factors in T-cell acute lymphoblastic leukemia. *Blood* **103**, 1909-1911 (2004).

107 Ferrando, A. A. *et al.* Gene expression signatures define novel oncogenic pathways in T cell acute lymphoblastic leukemia. *Cancer Cell* **1**, 75-87 (2002).

108 Larson, R. C., Lavenir, I., Larson, T. A., Baer, R. & et.al. Priten dimerization between Lmo2(Rbtn2) and Tal1 alters thymocyte development and potentiates T cell tumorigenesis in transgenic mice. *EMBO J.* **15**, 1021-1027 (1996).

109 Tremblay, M. *et al.* Modeling T-cell acute lymphoblastic leukemia induced by the SCL and LMO1 oncogenes. *Genes & Development* **24**, 1093-1105.

110 Condorelli, G. L. *et al.* T-cell-directed TAL-1 expression induces T-cell malignancies in transgenic mice. *Cancer Res* **56**, 5113-5119 (1996).

111 Bain, G. *et al.* E2A deficiency leads to abnormalities in alphabeta T-cell development and to rapid development of T-cell lymphomas. *Molecular and cellular biology* **17**, 4782-4791 (1997).

112 Herblot, S., Steff, A. M., Hugo, P., Aplan, P. D. & Hoang, T. SCL and LMO1 alter thymocyte differentiation: inhibition of E2A-HEB function and pre-T alpha chain expression. *Nature immunology* **1**, 138-144, doi:10.1038/77819 (2000).

113 McCormack, M. P. *et al.* Requirement for Lyl1 in a model of Lmo2-driven early T-cell precursor ALL. *Blood* **122**, 2093-2103, doi:10.1182/blood-2012-09-458570 (2013).

114 Liu, P., Jenkins, N. A. & Copeland, N. G. A highly efficient recombineering-based method for generating conditional knockout mutations. *Genome research* **13**, 476-484, doi:10.1101/gr.749203 (2003).

115 Sayegh, C. E., Quong, M. W., Agata, Y. & Murre, C. E-proteins directly regulate expression of activation-induced deaminase in mature B cells. *Nature immunology* **4**, 586-593, doi:10.1038/ni923 (2003).

116 Sayegh, C. E., Quong, M. W., Agata, Y. & Murre, C. E-proteins directly regulate expression of activation-induced deaminase in mature B cells. *Nature immunology* **4**, 586-593 (2003).

117 Kinsella, T. M. & Nolan, G. P. Episomal vectors rapidly and stably produce high-titer recombinant retrovirus. *Human gene therapy* **7**, 1405-1413, doi:10.1089/hum.1996.7.12-1405 (1996).

118 Naviaux, R. K., Costanzi, E., Haas, M. & Verma, I. M. The pCL vector system: rapid production of helper-free, high-titer, recombinant retroviruses. *J Virol* **70**, 5701-5705 (1996).

119 Schmitt, T. M. & Zuniga-Pflucker, J. C. Induction of T cell development from hematopoietic progenitor cells by delta-like-1 in vitro. *Immunity* **17**, 749-756 (2002).

120 Yu, D. & Thomas-Tikhonenko, A. A non-transgenic mouse model for B-cell lymphoma: in vivo infection of p53-null bone marrow progenitors by a Myc retrovirus is sufficient for tumorigenesis. *Oncogene* **21**, 1922-1927, doi:10.1038/sj.onc.1205244 (2002).

121 Cleveland, S. M. *et al.* Lmo2 induces hematopoietic stem cell-like features in T-cell progenitor cells prior to leukemia. *Stem Cells* **31**, 882-894, doi:10.1002/stem.1345 (2013).

122 Guo, Y., Ye, F., Sheng, Q., Clark, T. & Samuels, D. C. Three-stage quality control strategies for DNA re-sequencing data. *Brief Bioinform*, doi:bbt069 [pii]
10.1093/bib/bbt069 (2013).

123 Guo, Y. *et al.* Multi-perspective quality control of Illumina exome sequencing data using QC3. *Genomics*, doi:S0888-7543(14)00035-4 [pii]
10.1016/j.ygeno.2014.03.006 (2014).

124 Guo, Y., Zhao, S., Ye, F., Sheng, Q. & Shyr, Y. MultiRankSeq: Multiperspective Approach for RNAseq Differential Expression Analysis and Quality Control. *BioMed Research International* **2014**, 8, doi:10.1155/2014/248090 (2014).

125 Kim, D. *et al.* TopHat2: accurate alignment of transcriptomes in the presence of insertions, deletions and gene fusions. *Genome Biol* **14**, R36, doi:gb-2013-14-4-r36 [pii]
10.1186/gb-2013-14-4-r36 (2013).

126 Trapnell, C. *et al.* Transcript assembly and quantification by RNA-Seq reveals unannotated transcripts and isoform switching during cell differentiation. *Nat Biotechnol* **28**, 511-515, doi:10.1038/nbt.1621
nbt.1621 [pii] (2010).

127 Consortium, E. P. *et al.* An integrated encyclopedia of DNA elements in the human genome. *Nature* **489**, 57-74, doi:10.1038/nature11247 (2012).

128 El Omari, K. *et al.* Structure of the leukemia oncogene LMO2: implications for the assembly of a hematopoietic transcription factor complex. *Blood* **117**, 2146-2156, doi:10.1182/blood-2010-07-293357 (2011).

129 El Omari, K. *et al.* Structural basis for LMO2-driven recruitment of the SCL:E47bHLH heterodimer to hematopoietic-specific transcriptional targets. *Cell reports* **4**, 135-147, doi:10.1016/j.celrep.2013.06.008 (2013).

130 Lecuyer, E. *et al.* The SCL complex regulates c-kit expression in hematopoietic cells through functional interaction with Sp1. *Blood* **100**, 2430-2440, doi:10.1182/blood-2002-02-0568 (2002).

131 Xu, Z., Huang, S., Chang, L. S., Agulnick, A. D. & Brandt, S. J. Identification of a TAL1 target gene reveals a positive role for the LIM domain-binding protein Ldb1 in erythroid gene expression and differentiation. *Molecular and cellular biology* **23**, 7585-7599 (2003).

132 Bain, G. *et al.* Both E12 and E47 allow commitment to the B cell lineage. *Immunity* **6**, 145-154 (1997).

133 Zhuang, Y., Barndt, R. J., Pan, L., Kelley, R. & Dai, M. Functional replacement of the mouse E2A gene with a human HEB cDNA. *Molecular and cellular biology* **18**, 3340-3349 (1998).

134 Cleveland, S. M. *et al.* LMO2 induces T-cell leukemia with epigenetic deregulation of CD4. *Experimental hematology* **42**, 581-593 e585, doi:10.1016/j.exphem.2014.04.010 (2014).

135 Akinleye, A., Avvaru, P., Furqan, M., Song, Y. & Liu, D. Phosphatidylinositol 3-kinase (PI3K) inhibitors as cancer therapeutics. *Journal of hematology & oncology* **6**, 88, doi:10.1186/1756-8722-6-88 (2013).

136 Crabbe, T. Exploring the potential of PI3K inhibitors for inflammation and cancer. *Biochemical Society transactions* **35**, 253-256, doi:10.1042/BST0350253 (2007).

137 Subramaniam, P. S. *et al.* Targeting nonclassical oncogenes for therapy in T-ALL. *Cancer cell* **21**, 459-472, doi:10.1016/j.ccr.2012.02.029 (2012).

138 Thorsteinsdottir, U., Sauvageau, G. & Humphries, R. K. Hox homeobox genes as regulators of normal and leukemic hematopoiesis. *Hematology/oncology clinics of North America* **11**, 1221-1237 (1997).

139 Sauvageau, G. *et al.* Overexpression of HOXB3 in hematopoietic cells causes defective lymphoid development and progressive myeloproliferation. *Immunity* **6**, 13-22 (1997).

140 Thorsteinsdottir, U. *et al.* Overexpression of HOXA10 in murine hematopoietic cells perturbs both myeloid and lymphoid differentiation and leads to acute myeloid leukemia. *Molecular and cellular biology* **17**, 495-505 (1997).

141 Owens, B. M. & Hawley, R. G. HOX and non-HOX homeobox genes in leukemic hematopoiesis. *Stem Cells* **20**, 364-379, doi:10.1634/stemcells.20-5-364 (2002).

142 Slape, C. *et al.* Retroviral insertional mutagenesis identifies genes that collaborate with NUP98-HOXD13 during leukemic transformation. *Cancer research* **67**, 5148-5155, doi:10.1158/0008-5472.CAN-07-0075 (2007).

143 Germain, R. N. T-cell development and the CD4-CD8 lineage decision. *Nature reviews. Immunology* **2**, 309-322, doi:10.1038/nri798 (2002).

144 de Boer, J. *et al.* Transgenic mice with hematopoietic and lymphoid specific expression of Cre. *European journal of immunology* **33**, 314-325, doi:10.1002/immu.200310005 (2003).

145 Ogilvy, S. *et al.* Promoter elements of vav drive transgene expression in vivo throughout the hematopoietic compartment. *Blood* **94**, 1855-1863 (1999).

146 Keller, G., Kennedy, M., Papayannopoulou, T. & Wiles, M. V. Hematopoietic commitment during embryonic stem cell differentiation in culture. *Molecular and cellular biology* **13**, 473-486 (1993).

147 Bustelo, X. R., Rubin, S. D., Suen, K. L., Carrasco, D. & Barbacid, M. Developmental expression of the vav protooncogene. *Cell growth & differentiation : the molecular biology journal of the American Association for Cancer Research* **4**, 297-308 (1993).

148 Jayaraman, P. S., Frampton, J. & Goodwin, G. The homeodomain protein PRH influences the differentiation of haematopoietic cells. *Leukemia research* **24**, 1023-1031 (2000).

149 Guo, Y. *et al.* The homeoprotein Hex is required for hemangioblast differentiation. *Blood* **102**, 2428-2435, doi:10.1182/blood-2003-02-0634 (2003).

150 Martinez-Barbera, J. P., Rodriguez, T. A. & Beddington, R. S. The homeobox gene Hesx1 is required in the anterior neural ectoderm for normal forebrain formation. *Developmental biology* **223**, 422-430, doi:10.1006/dbio.2000.9757 (2000).

151 Thomas, P. Q., Brown, A. & Beddington, R. S. Hex: a homeobox gene revealing peri-implantation asymmetry in the mouse embryo and an early transient marker of endothelial cell precursors. *Development* **125**, 85-94 (1998).

152 Brickman, J. M., Jones, C. M., Clements, M., Smith, J. C. & Beddington, R. S. Hex is a transcriptional repressor that contributes to anterior identity and suppresses Spemann organiser function. *Development* **127**, 2303-2315 (2000).

153 Bedford, F. K., Ashworth, A., Enver, T. & Wiedemann, L. M. HEX: a novel homeobox gene expressed during haematopoiesis and conserved between mouse and human. *Nucleic acids research* **21**, 1245-1249 (1993).

154 Kanji, S., Pompili, V. J. & Das, H. Plasticity and maintenance of hematopoietic stem cells during development. *Recent patents on biotechnology* **5**, 40-53 (2011).

155 Lawrence, H. J., Sauvageau, G., Humphries, R. K. & Largman, C. The role of HOX homeobox genes in normal and leukemic hematopoiesis. *Stem Cells* **14**, 281-291, doi:10.1002/stem.140281 (1996).

156 Thorsteinsdottir, U. *et al.* Overexpression of the myeloid leukemia-associated Hoxa9 gene in bone marrow cells induces stem cell expansion. *Blood* **99**, 121-129 (2002).

157 Wilson, A. *et al.* c-Myc controls the balance between hematopoietic stem cell self-renewal and differentiation. *Genes & development* **18**, 2747-2763, doi:10.1101/gad.313104 (2004).

158 Wilson, A. *et al.* Hematopoietic stem cells reversibly switch from dormancy to self-renewal during homeostasis and repair. *Cell* **135**, 1118-1129, doi:10.1016/j.cell.2008.10.048 (2008).

159 Hu, M. *et al.* Multilineage gene expression precedes commitment in the hemopoietic system. *Genes & development* **11**, 774-785 (1997).

160 Cheng, T. *et al.* Hematopoietic stem cell quiescence maintained by p21cip1/waf1. *Science* **287**, 1804-1808 (2000).

161 Desjobert, C. *et al.* The PRH/Hex repressor protein causes nuclear retention of Groucho/TLE co-repressors. *The Biochemical journal* **417**, 121-132, doi:10.1042/BJ20080872 (2009).

162 Soufi, A. & Jayaraman, P.-S. PRH/Hex: an oligomeric transcription factor and multifunctional regulator of cell fate. *The Biochemical journal* **412**, 399-413 (2008).

163 Topisirovic, I. *et al.* The proline-rich homeodomain protein, PRH, is a tissue-specific inhibitor of eIF4E-dependent cyclin D1 mRNA transport and growth. *The EMBO journal* **22**, 689-703 (2003).

164 Minami, T. *et al.* Interaction between hex and GATA transcription factors in vascular endothelial cells inhibits flk-1/KDR-mediated vascular endothelial growth factor signaling. *The Journal of biological chemistry* **279**, 20626-20635, doi:10.1074/jbc.M308730200 (2004).

165 Schaefer, L. K., Wang, S. & Schaefer, T. S. Functional interaction of Jun and homeodomain proteins. *The Journal of biological chemistry* **276**, 43074-43082, doi:10.1074/jbc.M102552200 (2001).

166 Sekiguchi, K. *et al.* Homeobox protein Hex induces SMemb/nonmuscle myosin heavy chain-B gene expression through the cAMP-responsive element. *Circulation research* **88**, 52-58 (2001).

167 Jones, M. E., Kondo, M. & Zhuang, Y. A tamoxifen inducible knock-in allele for investigation of E2A function. *BMC developmental biology* **9**, 51, doi:10.1186/1471-213X-9-51 (2009).

168 Hansen, G. M. & Justice, M. J. Activation of Hex and mEg5 by retroviral insertion may contribute to mouse B-cell leukemia. *Oncogene* **18**, 6531-6539, doi:10.1038/sj.onc.1203023 (1999).

169 Li, J. *et al.* Leukaemia disease genes: large-scale cloning and pathway predictions. *Nature genetics* **23**, 348-353, doi:10.1038/15531 (1999).

170 McCormack, M. P. *et al.* The Lmo2 oncogene initiates leukemia in mice by inducing thymocyte self-renewal. *Science* **327**, 879-883, doi:10.1126/science.1182378 (2010).

171 Taverner, N. V., Smith, J. C. & Wardle, F. C. Identifying transcriptional targets. *Genome biology* **5**, 210, doi:10.1186/gb-2004-5-3-210 (2004).

172 Rosa, F. M. Mix.1, a homeobox mRNA inducible by mesoderm inducers, is expressed mostly in the presumptive endodermal cells of Xenopus embryos. *Cell* **57**, 965-974 (1989).

173 McDonald, M. J. & Rosbash, M. Microarray analysis and organization of circadian gene expression in Drosophila. *Cell* **107**, 567-578 (2001).

174 Eilers, M., Picard, D., Yamamoto, K. R. & Bishop, J. M. Chimaeras of myc oncoprotein and steroid receptors cause hormone-dependent transformation of cells. *Nature* **340**, 66-68, doi:10.1038/340066a0 (1989).

175 Sun, L. V. *et al.* Protein-DNA interaction mapping using genomic tiling path microarrays in Drosophila. *Proceedings of the National Academy of Sciences of the United States of America* **100**, 9428-9433, doi:10.1073/pnas.1533393100 (2003).

176 van Steensel, B. & Henikoff, S. Identification of in vivo DNA targets of chromatin proteins using tethered dam methyltransferase. *Nature biotechnology* **18**, 424-428, doi:10.1038/74487 (2000).

177 Orian, A. *et al.* Genomic binding by the Drosophila Myc, Max, Mad/Mnt transcription factor network. *Genes & development* **17**, 1101-1114, doi:10.1101/gad.1066903 (2003).